



**NTNU – Trondheim**  
Norwegian University of  
Science and Technology

# Simulation of Surfactant EOR in a Mechanistic Model with Fracture and Ekofisk Properties

**Helene Skår**

Petroleum Geoscience and Engineering

Submission date: June 2014

Supervisor: Ole Torsæter, IPT

Co-supervisor: Ying Guo, Total

Norwegian University of Science and Technology

Department of Petroleum Engineering and Applied Geophysics



## Acknowledgement

I would like to thank Total Norway E&P and Ying Guo who gave me the opportunity to write this thesis and provided me with Ekofisk reservoir properties data. I would also like to thank fellow master students at NTNU who has helped me with Eclipse guidance.

Last, but most importantly, I would like to thank my supervisor Ole Torsæter for providing me with excellent guidance, valuable feedback, input, good technical discussions and support during the master thesis period.



## Abstract

Large amounts of oil are left in reservoirs after primary and secondary recovery. To recover as much of the remaining oil as possible, EOR techniques such as chemical flooding are considered. Naturally fractured carbonates have often large amounts of residual oil left in the reservoir after primary and secondary production periods. Carbonates are in general more complex reservoirs than sandstones, thus recovery methods must be tailored for the environment of the reservoir system. Chemical EOR has become more attractive after the financial crisis in 2008 because of the high oil prices.

Ekofisk is a naturally fractured chalk reservoir, and is the largest, oldest and longest producing reservoir on the Norwegian continental shelf. To improve the recovery, surfactant injection is considered as a possible EOR method. A mechanistic reservoir model with Ekofisk reservoir properties and a single fracture was made with the purpose to investigate the potential of surfactant injection in Ekofisk. Several parameters that affect the performance of surfactants were investigated and the recovery results were compared with a waterflood basecase. In addition, a mechanistic model with four fractures was made for further investigation of surfactant flow in a fracture network and for comparison of the performance of a surfactant flood with a surfactant-polymer flood.

The author's simulation results show that surfactant injection should be considered for the field, but more research with a more advanced reservoir model with respect to possible wettability alteration, a larger fracture network and heterogeneity should be done. The model shows poor sweep efficiency in layers far from the fracture in the model, thus should an eventual chemical flood in Ekofisk be considered done with polymers. Surfactant concentration in the injection solution affects the surfactant performance the most. For the single fracture model, the recovery increased with 2,8% when surfactants are injected, and NPV was increased with 8,31E+06 \$. For the 9-block model with four fractures, the recovery improved with 3% for the surfactant-polymer flood compared with a surfactant flood. Also the NPV was increased with 3,71E+06\$.



## Sammendrag

Store mengder residuell olje er igjen i reservoarene etter primær og sekundær utvinning. Ulike EOR teknikker blir vurdert for å utvinne så mye av den gjenværende oljen som mulig. Naturlig oppsprukne karbonat reservoar har ofte store mengder residuell olje etter første og andre produksjonsperiode. Karbonater er generelt mer komplekse reservoar enn sandsteiner, derfor må utvinningsteknikker skreddersys for det aktuelle reservoar systemet. Kjemisk EOR har blitt mer attraktivt etter finanskrisa i 2008 på grunn av de høye oljeprisene.

Ekofisk er et naturlig oppsprukket krittreservoar, og er det største, eldste og lengst produserende reservoaret på norsk kontinental sokkel. For å øke utvinningsgraden er surfaktantinjeksjon vurdert som en mulig EOR metode. En mekanistisk reservoarmodell med Ekofisk reservoar egenskaper har blitt laget med hensikt å undersøke potensialet for surfaktantinjeksjon i Ekofisk. Flere parametere som påvirker hvor god effekten av surfaktantene er, har blitt studert og resultatene er blitt sammenlignet med en vannflømming «basecase». I tillegg ble en mekanistisk modell med ni matriks blokker og fire sprekker bygget for videre studering av surfaktantstrømning i et sprekkenettverk og for å sammenligne oljeutvinningen for et tilfelle med surfaktantflømming med surfaktant-polymer flømming.

Simuleringsresultatene til forfatteren viser at surfaktantinjeksjon bør bli vurdert for feltet, men mer forskning og studering av en mer avansert reservoarmodell med hensyn på endringer av fuktegenskaper, et større sprekke nettverk og heterogenitet bør inkluderes. Modellen viser en dårlig fortrenningseffektivitet i lag langt fra sprekken i modellen og en eventuell kjemisk flømming i Ekofisk bør gjøres med polymer. Surfactantkonsentrasjon i injeksjonsløsning påvirker utvinningen mest. For modellen med en enkel sprekke ble utvinningsgraden økt med 2,8% når surfaktanter ble injisert, og NPV økte med 8,31E+06\$. For 9-blokk modellen med fire sprekker økte utvinningsgraden med 3% for surfaktant-polymer flømminga sammenlignet med surfaktant fløm, mens NPV økte med 3,71E+06 \$.





## Table of Content

|   |     |
|---|-----|
| Acknowledgement.....                                  | i   |
| Abstract .....  | iii |
| Sammendrag.....                                       | v   |
| List of figures .....                                 | xi  |
| List of Tables.....                                   | xv  |
| 1. Introduction.....                                  | 1   |
| 2. Reservoir Properties.....                          | 5   |
| 2.1 Porosity.....                                     | 5   |
| 2.1.1 Double porosity.....                            | 6   |
| 2.2 Permeability.....                                 | 7   |
| 2.2.1 Permeability in fractured reservoirs .....      | 8   |
| 2.2.2 Corey Equations for Relative Permeability ..... | 9   |
| 2.3 Saturation.....                                   | 10  |
| 2.4 Wettability .....                                 | 11  |
| 2.5 Interfacial tension .....                         | 13  |
| 2.6 Capillary Pressure.....                           | 15  |
| 2.6.1 Threshold Pressure.....                         | 16  |
| 3. Flow in porous media.....                          | 17  |
| 3.1 Darcy's law.....                                  | 17  |
| 3.2 Production mechanisms .....                       | 18  |
| 3.2.1 Imbibition.....                                 | 18  |
| 3.2.2 Drainage.....                                   | 19  |
| 3.3 Mobility .....                                    | 20  |
| 4. Naturally Fractured Reservoirs, NFR .....          | 21  |
| 4.1 NFR features.....                                 | 22  |
| 4.2 Characterisation of fractures.....                | 24  |
| 4.3 The Warren and Root model .....                   | 27  |
| 4.4 Matrix- Fracture Fluid Exchange .....             | 32  |
| 4.4.1 Imbibition.....                                 | 32  |
| 4.4.2 Gravity Drainage.....                           | 37  |
| 5. Recovery periods .....                             | 39  |
| 5.1 Primary recovery .....                            | 40  |
| 5.2 Secondary recovery .....                          | 41  |
| 5.3 Tertiary recovery .....                           | 42  |

|       |   |    |
|-------|---|----|
| 6.    | Surfactant flooding.....                                | 43 |
| 6.1   | Types of surfactants.....                               | 45 |
| 6.2   | Types of Microemulsions .....                           | 46 |
| 6.2.1 | Winsor type I.....                                      | 49 |
| 6.2.2 | Winsor type II .....                                    | 50 |
| 6.2.3 | Winsor type III.....                                    | 51 |
| 6.3   | Phase Behaviour and IFT .....                           | 52 |
| 6.4   | Parameters affecting phase behaviour .....              | 54 |
| 6.3.1 | Temperature .....                                       | 54 |
| 6.3.2 | Pressure .....  | 54 |
| 6.3.3 | Cosurfactants.....                                      | 55 |
| 6.3.4 | Oil .....   | 56 |
| 6.3.5 | Effect of divalent ions .....                           | 56 |
| 6.3.6 | Surfactant concentration and surfactant structure ..... | 56 |
| 6.5   | Capillary number .....                                  | 58 |
| 6.6   | Wettability Alteration .....                            | 59 |
| 6.7   | Surfactant-Polymer flooding .....                       | 61 |
| 7.    | Economics of Chemical EOR .....                         | 63 |
| 8.    | Numerical Simulation .....                              | 67 |
| 8.1   | Keywords for the surfactant model .....                 | 67 |
| 8.2   | The Basecase Model Input Data .....                     | 71 |
| 8.2.1 | PVT .....   | 73 |
| 8.2.2 | Matrix properties.....                                  | 73 |
| 8.2.3 | Fracture properties .....                               | 75 |
| 8.2.4 | Wells .....   | 76 |
| 8.3   | The Surfactant model input data.....                    | 77 |
| 8.4   | 9Block Model with Four Fractures.....                   | 79 |
| 8.5   | Polymer Input Data.....                                 | 80 |
| 9.    | Results and Discussion .....                            | 81 |
| 9.1   | Surfactant flow within the model .....                  | 82 |
| 9.2   | Saturation and relative permeability changes .....      | 84 |
| 9.3   | Recovery with and without surfactants .....             | 86 |
| 9.4   | Initial Capillary Pressure Sensitivity .....            | 88 |
| 9.5   | Fracture opening sensitivity.....                       | 91 |
| 9.6   | Surfactant Production .....                             | 93 |

|        |   |     |
|--------|---|-----|
| 9.7    | Surfactant Adsorption case study .....                          | 94  |
| 9.8    | Input Changes in Miscibility Index in the SURFCAPD keyword..... | 96  |
| 9.9    | Surfactant concentration in injected solution .....             | 98  |
| 9.10   | 9-block model with four fractures and surfactant injection..... | 101 |
| 9.11   | 9-block model with Surfactant-Polymer injection.....            | 102 |
| 9.12   | Economic Evaluation.....  | 105 |
| 9.12.1 | NPV-Results for Single Block Model.....                         | 106 |
| 9.12.2 | NPV-Results for Four-Fractures Model.....                       | 108 |
| 9.13   | Complete Evaluation of the Results .....                        | 110 |
| 9.13.1 | Single Fracture Model Evaluation .....                          | 110 |
| 9.13.2 | Nine-Block Model Evaluation .....                               | 114 |
| 10.    | Conclusion.....   | 117 |
| 11.    | Future Recommendations.....                                     | 119 |
|        | Nomenclature .....  | 120 |
|        | Bibliography.....   | 122 |



## List of figures

|   |    |
|---|----|
| Figure 2.1: Fracture porosity from structural geological data (Torsæter, 2014a). .....  | 6  |
| Figure 2.2: The figure to the left is relative permeability curves for oil and water in a typical water-wet system, while the figure to the right is the relative permeability curves for oil and water in a typical oil-wet system (Zolutukhin & Ursin, 2000). ..... | 8  |
| Figure 2.3: Relative permeability in fractures, vertical equilibrium (Torsæter, 2014a). .....   | 9  |
| Figure 2.4: A water droplet is placed on a smooth rock surface and is surrounded by oil, as the geometry show, the wetting angle is less than $90^\circ$ , the rock is water-wet (Torsæter & Abtahi, 2003). .....   | 12 |
| Figure 2.5: Capillary equilibrium of a spherical cap (Torsæter & Abtahi, 2003). .....   | 14 |
| Figure 2.6: Capillary rise of water surrounded by oil (Torsæter & Abtahi, 2003). .....  | 15 |
| Figure 3.1: Linear flow in a porous medium. ....  | 18 |
| Figure 3.2: Relative permeability curves and related capillary pressure curve for a typical imbibition process (Holter, 2012). .....  | 18 |
| Figure 3.3: Relative permeability curves and related capillary pressure curve for a typical drainage process (Holter, 2012). .....  | 19 |
| Figure 4.1: Pressure distribution around the wellbore for a) a fractured reservoir and b) a conventional reservoir (Torsæter, 2014a). .....   | 22 |
| Figure 4.2: Fracture orientation of a single fracture (Torsæter, 2014a). .....  | 24 |
| Figure 4.3: Idealized geometrical blocks (Torsæter, 2014a). .....   | 25 |
| Figure 4.4: The relationship between FINT and matrix block size (Torsæter, 2014a). .....  | 26 |
| Figure 4.5: Model of a real fractured reservoir to the left, and a model of an idealised fractured reservoir to the right (Chilingarian, et al., 1996). .....   | 27 |
| Figure 4.6: Fluid exchange between matrix and fractures during flow towards a well (Chilingarian, et al., 1996). .....  | 28 |
| Figure 4.7: Pressure drawdown behaviour in a producing well in a naturally fractured reservoir (Chilingarian, et al., 1996). .....  | 29 |
| Figure 4.8: Pressure build-up behaviour in a naturally fractured reservoir (Ghahfarokhi, 2012). .....   | 30 |
| Figure 4.9: Matrix block saturated with oil surrounded by fractures saturated by water (Torsæter, 2014c). .....   | 34 |
| Figure 4.10: The relationship between recovery, $Z_D$ , and dimensionless time, $t_D$ , for gravity dominated flow (Chilingarian, et al., 1996). .....  | 36 |
| Figure 4.11: The relationship between recovery, $Z_D$ , and dimensionless time, $t_D$ , for capillary dominated flow (Chilingarian, et al., 1996). .....  | 37 |
| Figure 4.12: Oil displacement by gas in a matrix block surrounded by fractures saturated with gas (Torsæter, 2014c). .....  | 38 |
| Figure 4.13: Oil produced from a matrix block surrounded by gas- saturated fractures, by examining the relative magnitude of gravity and capillary forces. (Chilingarian et. al. 1996)  | 38 |
| Figure 5.1: Recovery techniques for oil production (Torsæter, 2013). .....  | 39 |
| Figure 6.1: Relative permeability and capillary pressure alterations as a result of IFT reduction. ....   | 44 |
| Figure 6.2: a) Shows a micelle formed in an aqueous solvent that has captured oil within the core. b) Shows a micelle formed in an oil solvent that has captured the aqueous phase within the core (Lake, 1989). .....  | 46 |

|   |    |
|---|----|
| Figure 6.3: Lower-phase microemulsion, middle-phase microemulsion and upper-phase microemulsion in pipettes (Sheng, 2011).....  | 47 |
| Figure 6.4: Ternary presentation of Winsor type I system, the overall composition of surfactant (1), brine (2) and oil (3) (Lake, 1989). .....  | 49 |
| Figure 6.5: Ternary presentation of Winsor type II system, the overall composition of surfactant (1), brine (2) and oil (3) (Lake, 1989). .....   | 50 |
| Figure 6.6: Ternary presentation of Winsor type III system, the overall composition of surfactant (1), brine (2) and oil (3) (Lake, 1989). .....  | 51 |
| Figure 6.7: IFT between microemulsion and oil decreases as the salinity increase. While the IFT between microemulsion and water increases when the salinity increases. The optimal salinity is when the curves crosses, which here occurs at the approximate same salinity, and in a Winsor type III system (Lake, 1989)..... | 53 |
| Figure 6.8: Optimum pressure as a function of salinity. The numbers in each point refers to the solubilisation parameter (Skauge & Fotland, 1990).....  | 55 |
| Figure 6.9: Surfactant concentration as a function of interfacial tension (Schramm, 1992)....   | 57 |
| Figure 6.10: The relationship between capillary number and residual saturation. (Sheng, 2013).....  | 58 |
| Figure 6.11: Wettability alteration from oil-wet to water-wet mechanism. Large squares represent carboxylate groups ( $\text{COO}^-$ ), small squares represent polar components, and the circles represent cationic ammonium group ( $\text{N}^+(\text{CH}_3)_3$ ) (Austad & Standnes, 2003). .....                          | 59 |
| Figure 6.12: Formation of a water-wet bilayer. The squares represent carboxylates and the eclipses represents EO-sulfonates .....   | 60 |
| Figure 6.13: The relationship between surfactant concentration and IFT for the cases with a) without polymers, b) strong association between surfactants and polymers, c) low association between surfactant and polymers, d) no association between surfactants and polymers. (Austad & Standnes, 2003) .....                | 62 |
| Figure 7.1: Schematic of a typical deep-water chemical-EOR project (Raney, et al., 2012). .   | 64 |
| Figure 7.2: Historical crude oil and chemical costs (Wyatt, et al., 2008). .....  | 66 |
| Figure 8.1: Initial oil saturation in the model. ....   | 71 |
| Figure 8.2: Oil viscosity plotted against pressure. ....  | 72 |
| Figure 8.3: Relative permeability curves for water and oil in the matrix. ....  | 74 |
| Figure 8.4: Water-oil capillary pressure curve for the matrix. ....   | 74 |
| Figure 8.5: Relative permeability curves for water and oil in the fracture. ....  | 76 |
| Figure 8.6: Relative permeability curves for miscible (blue) and immiscible (orange) conditions. ....   | 78 |
| Figure 8.7: 9block Model with Four Fractures, initial Oil Saturation.....   | 79 |
| Figure 9.1: Surfactant concentration in six layers in various distances from the fracture at breakthrough, where blue is zero and red is $1 \text{ kg/Sm}^3$ . ....   | 82 |
| Figure 9.2: Average surfactant concentration for different layers in various distances from the fracture plotted along the length of the reservoir at breakthrough. ....  | 83 |
| Figure 9.3: Average relative permeability curves for matrix for the surfactant flooding case. The blue and orange curves represents the relative permeability for water and oil respectively, initially (dashed) and at breakthrough.....   | 84 |
| Figure 9.4: Average relative permeability curves for matrix for the waterflooding case. The blue and orange curves represents the relative permeability for water and oil respectively, initially (dashed) and at breakthrough.....   | 85 |

|   |     |
|---|-----|
| Figure 9.5: Recovery factor (FOE) and watercut (FWCT) for surfactant flood (blue) and water flood(green).....   | 87  |
| Figure 9.6: Average relative permeability for all matrix layers at surfactant breakthrough, for surfactant flood (orange) and waterflood (blue).....  | 87  |
| Figure 9.7: Three different capillary pressure curve for the Pc sensitivity case study. ....  | 88  |
| Figure 9.8: Recovery factor (FOE) for three cases of surfactant and waterflooding. Green, blue and red curves for basecase, high Pc and low Pc respectively.....  | 90  |
| Figure 9.9: Total production for the case with zero capillary pressure in the miscible zones (surfactantbasecase), and for the case where capillary pressure is not zero.....   | 90  |
| Figure 9.10: Recovery (FOE) of oil for water and oil at different fracture widths. The red, green and blue curves gives the recovery for 1mm, 1cm and 5cm width respectively.....   | 92  |
| Figure 9.11: Oil saturation, end of simulation in the bottom layer for the case with a wide layer (left) and for surfactant basecase (right).....   | 92  |
| Figure 9.12: Total amount of surfactants injected (FTITSUR), adsorbed (FTADSUR) and produced (FTPTSUR). ....  | 93  |
| Figure 9.13: Surfactant adsorption for the cases with low, intermediate and much adsorption. ....   | 95  |
| Figure 9.14: Recovery comparison of three cases with different surfactant adsorption by rock. ....  | 95  |
| Figure 9.15: Recovery (FOE) for case study with miscibility index alteration. Surfactant basecase, case 2 and case 3 are presented with green, blue and red curves respectively.....  | 97  |
| Figure 9.16: Plot of total oil production and watercut at breakthrough for the three different surfactant concentrations in the injection fluid. The green line is for the surfactantbasecase with a concentration of $1\text{kg}/\text{Sm}^3$ , the blue line is for high concentration, $30\text{kg}/\text{Sm}^3$ , and the red line is for low concentration, $0,1\text{kg}/\text{Sm}^3$ . The light blue line is for waterflood. ....   | 99  |
| Figure 9.17: IFT distribution in the reservoir model at breakthrough for the three cases with increasing surfactant concentration to the right. ....  | 99  |
| Figure 9.18: Recovery factor (FOE, solid lines) and total amount of surfactant injected (FTITSUR, dashed lines) for the three different surfactant concentrations in the injection fluid. The green line is for the surfactantbasecase with a concentration of $1\text{kg}/\text{Sm}^3$ , the blue line is for high concentration, $30\text{kg}/\text{Sm}^3$ , and the red line is for low concentration, $0,1\text{kg}/\text{Sm}^3$ . .... | 100 |
| Figure 9.19: Surfactant concentration in various layers. Layer 11 and layer 21 are fractures. ....  | 101 |
| Figure 9.20: Oil Saturation in various layers for the surfactant flood model.....   | 103 |
| Figure 9.21: Oil Saturation in various layers for the surfactant-polymer model. ....  | 103 |
| Figure 9.22: Recovery factor (FOE) for the SP- flood (green) and surfactantflood (blue. ....  | 104 |
| Figure 9.23: Oil recovery (FOE) for Surfactant injection (red), SP injection (blue) and polymer injection (green). ....   | 104 |





## List of Tables

|   |     |
|---|-----|
| Table 2.1: Wettability preferences of a water-oil system (Zolutukhin & Ursin, 2000).  | 11  |
| Table 4.1. Cases of drainage/imbibition displacement (Torsæter, 2014b).   | 33  |
| Table 7.1: Facility costs for a project size of 10.000MBBL PV.  | 65  |
| Table 7.2: Chemical costs.  | 65  |
| Table 8.1 Specific keywords for the ECLIPSE surfactant model (Schlumberger, 2011a) and (Schlumberger, 2011b).                               | 67  |
| Table 8.2: Fluid parameters   | 72  |
| Table 8.3: Matrix properties for the model  | 73  |
| Table 8.4: Fracture properties for the model.   | 75  |
| Table 8.5: Well properties.   | 76  |
| Table 8.6: Interfacial tension between oil and water at different surfactant concentrations...  | 77  |
| Table 8.7: Water viscosity at different surfactant concentrations.  | 77  |
| Table 8.8: Miscibility condition at different capillary numbers.  | 77  |
| Table 8.9: Surfactant adsorption at different surfactant concentrations.  | 77  |
| Table 8.10: Polymer Viscosity for the PLYVISC keyword.  | 80  |
| Table 8.11: Polymer-Rock Properties for PLYROCK keyword.  | 80  |
| Table 8.12: Polymer Adsorption data for the PLYADS keyword.   | 80  |
| Table 9.1 Overview of case studies.   | 81  |
| Table 9.2: Capillary pressure input data for the case study.  | 88  |
| Table 9.3: SURFADS keyword input data alteration for the surfactant adsorption case study.  | 94  |
| Table 9.4: Capillary number alterations for case study.   | 96  |
| Table 9.5: Oil and surfactant price.  | 105 |
| Table 9.6: Results NPV calculations, incremental revenue for the surfactant flood.  | 106 |
| Table 9.7: Results NPV calculations, incremental revenue for the surfactant flood with a surfactant concentration of 30kg/Sm <sup>3</sup> . | 107 |
| Table 9.8: Results NPV calculations, for the surfactant flood with low surfactant concentration.  | 107 |
| Table 9.9: Incremental NPV calculations for SP-flood compared with surfactant flood.  | 109 |
| Table 9.10: Incremental NPV calculation for polymer-flood compared with surfactant flood.   | 109 |



## 1. Introduction

60% of the world's oil reserves are in carbonate reservoirs. A large amount of the carbonates are naturally fractured. Naturally fractured reservoirs have a complex pore structure with heterogeneity and big differences in permeability in fractures and in matrix. The matrix has large storage capacity with high porosity, but has very low flow conductivity, while the fractures have only secondary porosity but high to very high permeability. A large amount of the carbonates are oil-wet or mixed-wet which makes waterflooding inefficient. Therefore is the recovery often less than 30% (Lu, et al., 2012).

The average oil recovery on Norwegian continental shelf was in 2008 as much as 46% (Norwegian Petroleum Department, 2008). Still, there are large amount of oil left to be produced. The Norwegian Petroleum Department's goal is to reach an average recovery factor of 50% in the North Sea. To reach this goal a lot of research investments have been done to find the best recovery techniques (Teigland & Kleppe, 2006).

The most successful recovery techniques in the North Sea has been hydrocarbon miscible gas injection (HC), water-alternating- gas (WAG) injection, simultaneous-water-and-gas (SWAG) injection, foam-assisted-WAG (FAWAG) and microbial EOR (MEOR). HC and WAG are mature technologies that have given great success in the North Sea (Teigland & Kleppe, 2006). To improve the recovery other technologies has to be considered. Chemical EOR as surfactant and polymer injection has become more attractive since the financial crisis in 2008 that lead to high oil prices (Hirasaki, et al., 2008; Teigland & Kleppe, 2006).

In chemical EOR are surfactant and polymers the most attractive alternatives. So far has no field in the North Sea been flooded by either surfactants or polymers. Research at universities (NTNU, UiS, UiB) and research institutions related to the universities (SINTEF, IRIS, CIPR) have since 2005 started many research project on chemical EOR potential in the North Sea.

So far has only surfactants been used in FAWAG processes in the North Sea (Teigland & Kleppe, 2006).

The first oil in Norway was discovered in 1969 in Ekofisk, the biggest field discovered on Norwegian Continental Shelf. Ekofisk is a naturally fractured chalk reservoir. Since it is a carbonate reservoir, the first predicted recovery factor was 17%. It was expected that the oil could only be produced by pressure depletion. Conveniently is Ekofisk water-wet, therefore has waterflooding been very successful and the expected recovery factor is now 50% (Norwegian Petroleum Departemet, 2011).

To improve the recovery of carbonate reservoir such as Ekofisk, is chemical EOR now carefully considered. Research, pilot tests and a few surfactant stimulation projects have been done in carbonates (Sheng, 2013). Manrique et.al presented in 2010 a paper of the current status of EOR and EOR opportunities in the future, as of the date in 2010, no chemical floods (expect polymers) had been done in carbonates. Today's technology for chemical floods with surfactants is only applicable in sandstones (Manrique, et al., 2010)

Research has shown that surfactants in carbonates have two main applications. It can be used to alter the wettability from oil or mixed-wet to water-wet, and it can be used to decrease the interfacial tension between oil and water ( (Sheng, 2013); (Lake, 1989); (Green & Willhite, 1998); (Levitt, et al., 2009)). A wettability alteration improves the imbibition process, while a reduction of interfacial tension may permit a gravity governed flow (Hirasaki & Zhang, 2004). Surfactants are easily adsorbed on the carbonate rock surface; this is a big challenge when surfactants are used with the purpose to lower interfacial tension. Surfactants are chemical components that are strongly affected by salinity, temperature and other chemical components. Surfactants should therefore be tailored for the surroundings to achieve the best possible effect (Levitt, et al., 2009).

Polymers are long chains of monomers that have the ability to increase the water viscosity. An increase in water viscosity will decrease the displacing fluid's mobility. Polymers are very suitable for injection in heterogeneous reservoirs with large permeability differences between layers. The polymers are injected to reduce the effective permeability of the displacing fluid in high permeable zones. With these features, are polymers able to obtain a mobility control of the displacing front, and decrease the displacing front's fingering of the oil and hence increase the sweep efficiency (Zolutukhin & Ursin, 2000; Sheng, 2011).

This thesis is written with the purpose to investigate the possibilities for injection of surfactants in a naturally fractured reservoir. A simplified reservoir model with Ekofisk data has been built in the Eclipse simulator. The model has been used to study the opportunity of surfactant injection in Ekofisk as a possible future enhanced recovery technique. The model was developed for further investigations of surfactants in a fracture network and to study the recovery performance for surfactants with and without polymers. A sensitivity study of several parameters that affect the performance of surfactants such as surfactant concentration, adsorption and initial capillary pressure has been done. Furthermore was the recovery performance for the surfactants compared with a waterflood for the first model, and with surfactant-polymer flood for the second model. In addition, an economical evaluation has been done for the chemical-flood cases.

A wide understanding of reservoir parameters, flow in porous media, features of naturally fractured reservoirs, fluid flow in fractured reservoirs and surfactants is necessary to be able to build a credible reservoir model and evaluate the simulation results. A literary theory background is therefore presented. Parts of the reservoir parameters and surfactants theory are taken from the author's semester project "Surfactants and Spinning Drop Interfacial Tension Measurements" (Skår, 2013).

Furthermore, a description of the building of the reservoir models is given; a list of the simulation runs is presented with results and discussion. Finally, conclusion and future recommendations are included.



## 2. Reservoir Properties

Knowledge of basic reservoir properties is fundamental for understanding reservoir and fluid behaviour in reservoir engineering. This chapter will give an introduction to the most important properties for the study.

### 2.1 Porosity

The porosity of a reservoir rock is a measurement of the storage capacity of the reservoir (Torsæter & Abtahi, 2003). This pore space can store fluids as hydrocarbons. The absolute porosity of a rock is defined as the total pore volume  $V_{ptot}$ , divided by the bulk volume  $V_b$ . The porosity of a reservoir rock is measured by a core sample in the laboratory.

(2.1)

$$\varphi^{def} = \frac{V_{ptot}}{V_b}$$

Effective porosity is a measurement of the connected pore volume  $V_p$ , divided by the rock's bulk volume.

For a fractured reservoir a double porosity situation appears where the total porosity for the rock is the sum of primary and secondary porosity. Primary porosity is the matrix porosity, while secondary porosity is also called fracture porosity.

Secondary porosity is developed in the rock in a later stage because of mechanical geological and/or chemical geological processes as dissolution, diagenesis etc. Compact brittle rocks of relatively low intergranular porosity such as limestones, shales, shaly sandstones etc. often have secondary porosity (Torsæter, 2014a). The secondary porosity of a rock is often reduced

with time because the fractures can be filled with minerals younger than the minerals that composed the matrix. In carbonate rocks as limestones and dolomites, the fractures are formed during weathering or burial in the sedimentary basin (Warren & Root, 1963).

### 2.1.1 Double porosity

For a fractured system, the total porosity is the sum of matrix and fracture porosity and is defined by formula (2.2) below. However, the fracture porosity is much less than the matrix porosity and can in many cases be neglected, hence is the total porosity often assumed equal to the matrix porosity.

(2.2)

$$\varphi_T = \varphi_m + \varphi_f$$

Fracture porosity is obtained from core measurements in the laboratory. If the average fracture opening and the volumetric fracture density can be obtained from core analysis, equation 2.3 can be used to find the fracture porosity (Warren & Root, 1963; Torsæter, 2014a).

(2.3)

$$\varphi_f = \frac{n_f b}{Z_{bl}}$$

Where,

- $n_f$  is the number of fractures
- $b$  is the fracture opening
- $Z_{bl}$  is the height of the fracture system.

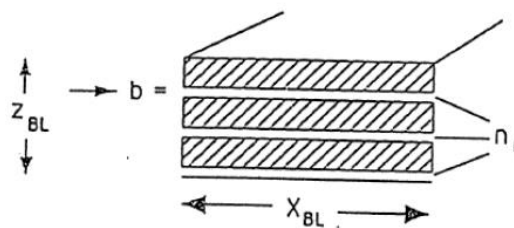


**Figure 2.1:** Fracture porosity from structural geological data (Torsæter, 2014a).



## 2.2 Permeability

Permeability is defined as the rocks ability to transport fluids in the pores and is measured in millidarcies or square meters. The *absolute permeability* of a rock is independent of the single phase or fluid type flowing through the porous medium and is constant (Zolutukhin & Ursin, 2000). By injecting a fluid of known viscosity into a core sample with known dimensions in the laboratory, the absolute permeability can be determined (Torsæter & Abtahi, 2003). The fluid is injected into the sample and fills even the smallest pores, hence the measurement will include all the pore channels and be an accurate average estimate of the bulk transmissibility in the pore network.

When there is more than one fluid present, the permeability depends on the relative saturation of the fluid in the rock. This is the *effective permeability* of the fluid and is given as the relative permeability times the absolute permeability of the rock (Schlumberger, 1998a).

The *relative permeability* is a dimensionless measure of the effective permeability of a phase in the rock (Zolutukhin & Ursin, 2000).

(2.4)

$$k_{ri} = \frac{k_i}{k}$$

Where

- $k_{ri}$  is the relative of the fluid i.
- $k_i$  is the effective permeability of the fluid i.
- $k$  is the absolute permeability.

Relative permeability is a function of fluid saturations, rock and fluid properties, reservoir conditions. When there are only two fluids present in a porous media, the relative permeability is usually plotted as a function of water saturation. The relative permeability for oil and water are strongly dependent on the wettability of the porous media. This can be seen from Figure 2.2.

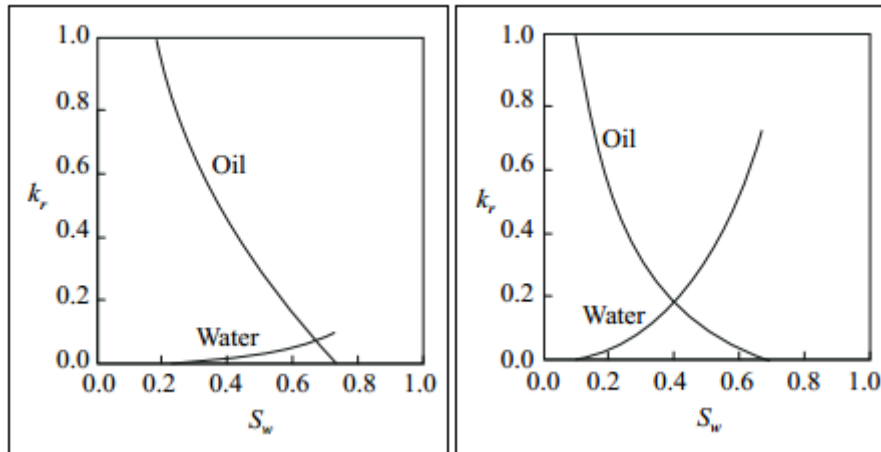


**Figure 2.2:** The figure to the left is relative permeability curves for oil and water in a typical water-wet system, while the figure to the right is the relative permeability curves for oil and water in a typical oil-wet system (Zolutukhin & Ursin, 2000).

### 2.2.1 Permeability in fractured reservoirs

In a fractured reservoir, the system contains *fracture permeability*, *matrix permeability* and *system permeability*. Fracture permeability is related to the secondary porosity, and tells how easily a fluid flows in the fracture (Schlumberger, 1998b).

For a single fracture system the flow in a fracture based on the “real flow cross- section” is given as equation 2.5. Where  $q_f$  equals the cross- sectional area times velocity.

(2.5)

$$q_f = ab \frac{b^2 l \Delta P}{12 \mu \Delta l}$$

For the flow in a porous media based on Darcy’s law, the same rate is expressed by equation 2.6.

(2.6)

$$q_f = ah \frac{k \Delta P}{\mu \Delta l}$$

Due to the large permeability differences between the matrix and in the fractures, the relative permeability for a fracture reservoir is evaluated for matrix and fracture separately. For the matrix, typical relative permeability curves are shown in Figure 2.2 above.

The intrinsic permeability in fractures is very high, and hence, mainly gravity forces will control multiphase flow in fractures. And because of gravity equilibrium, the relative permeability curves will be reduced to two straight lines as in Figure 2.3 (Torsæter, 2014a)

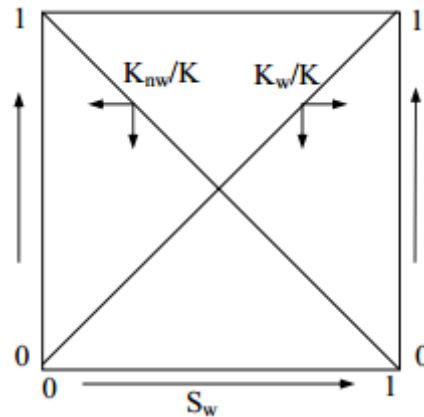


**Figure 2.3:** Relative permeability in fractures, vertical equilibrium (Torsæter, 2014a).

### 2.2.2 Corey Equations for Relative Permeability

To obtain the phase relative permeability the Corey equation can be used. The equation correlates relative permeability of oil and water to water saturation in a porous medium.

(2.7)

$$k_{rw}(S_w) = k_{rw}^0 S_{wn}(S_w)^n$$

(2.8)

$$k_{ro}(S_w) = k_{ro}^0 (1 - S_{wn}(S_w))^n$$

Where:

- $S_{wn}$  is the normalised water saturation
- $k_{ri}^0$  is the end-point relative permeability of phase  $i$ .
- $n$  is the Corey curve exponent

### 2.3 Saturation

The pore volume  $V_p$  can be filled by fluids. In a reservoir, those fluids are typically water, oil and gas. Therefore, the pore volume can be considered as the sum of oil, water and gas volume that fills the pores and  $V_p$  can be written as:

(2.9)

$$V_p = V_w + V_o + V_g$$

Saturation of a fluid in a rock is a measurement of how much of the rock's pore volume is occupied by a particular fluid.

(2.10)

$$S_i \stackrel{def}{=} \frac{V_i}{V_p} \quad i = 1, \dots, n$$

$n$ , is the total number of fluids present in the rock (Zolutukhin & Ursin, 2000).

## 2.4 Wettability

Electrostatic forces attracts the molecules within a fluid to each other, this attraction is referred to as *cohesion*. The extent of the attraction between the molecules in the fluid and an adjoining fluid in the same volume can be greater or less than the attraction within the single fluid. If the cohesion is greater than the attraction between the fluids, the fluids are *immiscible*, which is the case of a mixture of oil and water. In the opposite case when the attractions between the fluids are greater, the fluids are *miscible* (Zolutukhin & Ursin, 2000).

Fluids are also in some degree attracted to the molecules in an adjoining surface. This attraction comes from an electrostatic force, which is referred to as *adhesion*. If more than one fluid is present in the system, the fluid which is mostly attracted to the surface (where the adhesion is strongest), will stick to the surface. This fluid is the *wetting* fluid (Zolutukhin & Ursin, 2000).

The wettability of a rock is the tendency of a fluid to adhere to the surface of the rock, in a system with another immiscible fluid. Oil displacement is affected by the wettability of the reservoir rock (Torsæter & Abtahi, 2003).

Measurement of the contact angle between two phases, liquid-liquid or liquid-gas, in an immiscible blend on a rock surface can determine the wettability of the reservoir rock. The contact angle, generally referred to as the *wettability angle*  $\theta$ , is a measurement of equilibrium between the interfacial tension of the fluids and their adhesive attraction to the surface of the solid. The measurement is done in the laboratory with a very accurate micro-scale technique. The wettability angle is measured on the denser fluid's side of the interface. The measured angle gives the wettability preference of the system as given in Table 2.1. Figure 2.4 presents how the wettability angle is measured.

**Table 2.1:** Wettability preferences of a water-oil system (Zolutukhin & Ursin, 2000).

| Wetting angle (degree) | Wettability preference   |
|------------------------|--------------------------|
| 0 – 30                 | Strongly water-wet       |
| 30 – 90                | Preferentially water-wet |
| 90                     | Neutral wettability      |
| 90 – 150               | Preferentially oil-wet   |
| 150 – 180              | Strongly oil – wet       |

The presence of different minerals in the rock has a big impact of the wettability. Chamosite for example, is a diagenetic clay mineral whose presence in the reservoir rock and therefore the pore walls may result in an oil-wet system. In gas-water and oil-water system, rocks with quartz and calcite surfaces will most likely be water-wet.

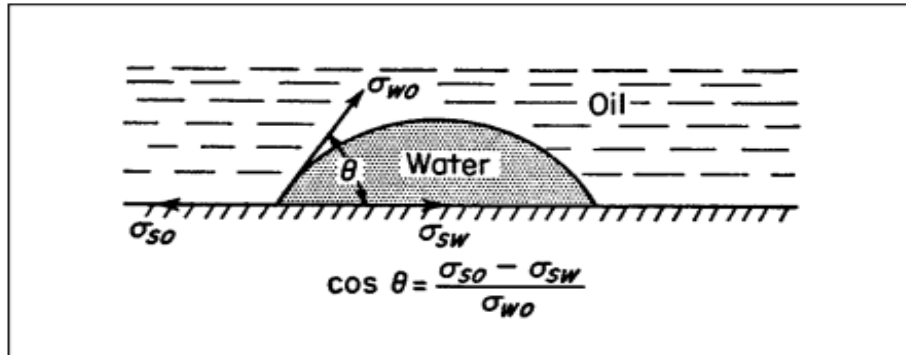


**Figure 2.4:** A water droplet is placed on a smooth rock surface and is surrounded by oil, as the geometry show, the wetting angle is less than  $90^\circ$ , the rock is water-wet (Torsæter & Abtahi, 2003).

The rocks preferential wettability is affected by several factors that either increase or decrease the wettability. The most important conditions are:

1. Reservoir pressure and temperature. An increase in temperature increases the wettability for water phase. A pressure decrease to below bubble point can cause precipitation of asphaltenes.
2. Oil composition. Certain hydrocarbon compounds reduce the water wettability.
3. Rock mineralogy. Some mineral with a degree of hydrophobia are more likely to be oil-wet. Talc-like silicates, pyrophyllites, sulphur, graphite, coal and sulphides are examples of such minerals (Torsæter, 2014a).

## 2.5 Interfacial tension

The interfacial tension (IFT) or the interfacial energy between two fluids in contact with each other is strictly dependent on the chemical composition of the fluids, and hence very sensitive for any composition changes. IFT is measured in dynes/cm or N/m, which will be the unit used in this thesis. The interfacial tension is the difference of the cohesive forces of two fluids in a mixture, and the magnitude is how much force needed to keep the two fluids apart in a pressure equilibrium state.

The *interfacial tension*,  $\sigma$ , between two fluids has different “sign” depending on the magnitude of the cohesive forces within the fluids own molecule and the cohesive forces between the molecules from the different fluids in a system.

- $\sigma > 0$ : The cohesive forces within the single fluid are stronger than the attraction forces between the molecules of the other fluid’s kind. The mixture is immiscible.
- $\sigma \approx 0$ : The molecules within the fluids are equally attracted to others of the same kind as to the molecule of the other fluid. The mixture will be more or less miscible.
- $\sigma < 0$ : The molecules prefer to blend with the molecules from the other fluid than the molecules of the same kind. The mixture will be miscible.

As Figure 2.4 of the water droplet shows, there is interfacial tension between the oil phase and the water phase, but also between the liquid and solid phase. The interfacial tensions to be considered are given below.

- $\sigma_{os}$ , surface tension between the oil phase and the rock surface.
- $\sigma_{ws}$ , surface tension between the water phase and the rock surface.
- $\sigma_{ow}$ , interfacial tension between the water phase and the oil phase.

The three interfacial tensions are not independent of each other, they depend of the wetting angle as showed in the Young-Dupré equation (2.11).

(2.11)

$$\frac{\sigma_{os} - \sigma_{ws}}{\sigma_{ow}} = \cos \theta$$

When two immiscible phases are collected in a container, the less dense fluid will form a droplet/bubble in the continuous denser fluid. The interfacial tension between the two phases, works to reduce the sphere of the droplet/bubble until it is mixed with denser fluid. However, due to pressure difference between the dense continuous fluid and within the bubble (Figure 2.5), the interfacial tension forces will not succeed. The relation between interfacial tension and differential pressure between the two phases is given by the Young-Laplace equation (2.12) for a spherical radius as:

(2.12)

$$p_2 - p_1 = \frac{2\sigma}{r}$$

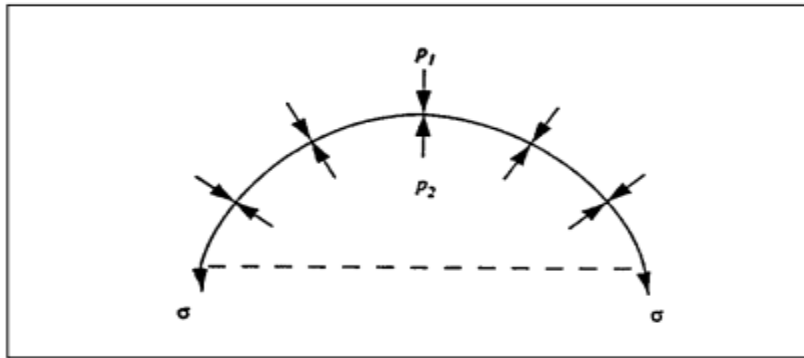


**Figure 2.5:** Capillary equilibrium of a spherical cap (Torsæter & Abtahi, 2003).



## 2.6 Capillary Pressure

If a capillary glass is placed in a vessel of two immiscible fluids, the fluid with the strongest adhesive forces will rise in the glass, and the interface between the two fluids will curve, as showed in Figure 2.6. The angle  $\theta$  between the convex part of the curve and the point where the meniscus connects with the glass wall is the wettability angle. The molecular pressure difference across the interfacial tension is the *capillary pressure*,  $P_c$ , between two fluids (Zolutukhin & Ursin, 2000).

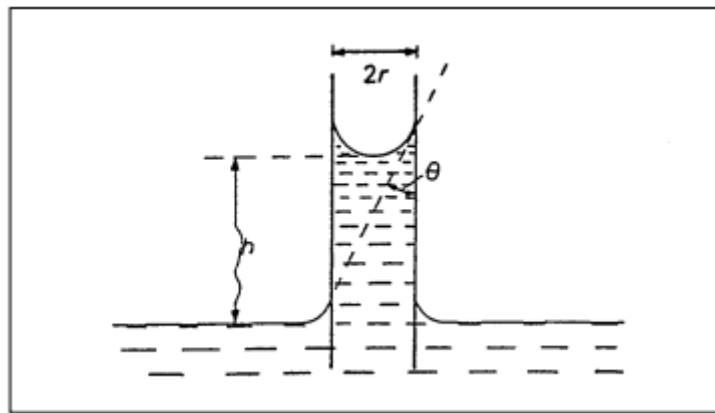


**Figure 2.6:** Capillary rise of water surrounded by oil (Torsæter & Abtahi, 2003).

In the case of a capillary glass in a vessel of oil and water, the water will rise due to cohesive and adhesive forces. Water is denser than oil and is more attracted to the surface than oil, hence the water will rise in the glass and displace the oil. The water will rise until equilibrium between the pressure differences and the fluid gravity is reached. The capillary pressure is the pressure difference between the wetting and the non-wetting phase.

### 2.6.1 Threshold Pressure

Threshold pressure is the non-wetting fluid pressure required to overcome the capillary resistance so that the fluid can enter a core. To overcome the threshold pressure, a pressure difference between the wetting and non-wetting fluid is required to make the fluids flow. The capillary pressure in a pore depends on the diameter. The smaller the diameter, the higher is the capillary pressure. The relation between diameter and capillary pressure can be seen from equation 2.13 (Torsæter & Abtahi, 2003). In an oil reservoir, this means that oil may be trapped in small pores. Due to high interfacial tension between oil and water, the capillary pressure is high and furthermore the threshold pressure is high, which result in high residual oil saturation. To be able to produce the trapped oil, enhanced oil recovery techniques can be applied to try to reduce the interfacial tension and furthermore the capillary pressure.

(2.13)

$$P_c = \frac{2\sigma_{ow} * \cos \theta}{r}$$

### 3. Flow in porous media

This chapter introduces the fundamentals of fluid flow in porous media. Reservoir properties as capillary pressure, saturation and permeability are already presented in chapter 2.

#### 3.1 Darcy's law

Darcy's law describes fluid flow in a porous medium by relating fluid velocity with viscosity, permeability and pressure drop over the medium. For linear flow of an incompressible fluid, Darcy's law can be expressed as:

$$\frac{q}{A} = v = \frac{k}{\mu} \frac{dP}{L} \quad (3.1)$$

Where:

- $q/A$  is the volumetric rate over the cross-sectional area for flow
- $v$  is the velocity
- $\mu$  is the viscosity
- $k$  is the absolute permeability
- $P$  is pressure
- $L$  is length

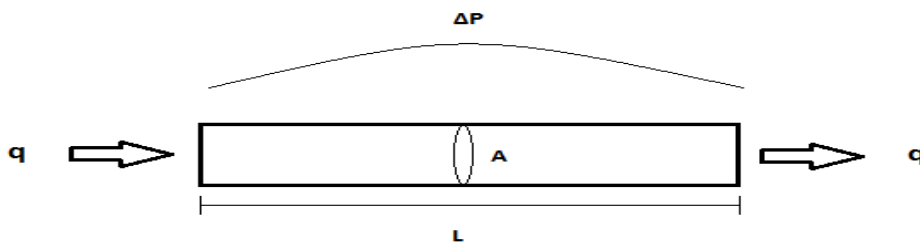


**Figure 3.1:** Linear flow in a porous medium.

### 3.2 Production mechanisms

For production of petroleum, the main production mechanisms are imbibition and drainage. The mechanisms depend on wettability of the rock and the phase of the displacing fluid.

#### 3.2.1 Imbibition

For the case when a wetting fluid is displacing a non-wetting fluid such that the saturation of the wetting phase increases, then the production mechanism is an imbibition. For waterflooding, the idealised condition is when the rock is water wet, because then the displacement of the non-wetting phase, oil, will be best. The rock prefers to be surrounded by water, and water can more easily enter the pores and displace oil. On the contrary when the rock is oil wet, the process will be drainage.

Figure 3.2 shows the relative permeability and capillary pressure curves for a typical imbibition process. The endpoints  $S_{wi}$  and  $1-S_{or}$  give the initial water saturation and residual oil saturation. The relative permeability endpoints can be used to obtain the mobility of the front.

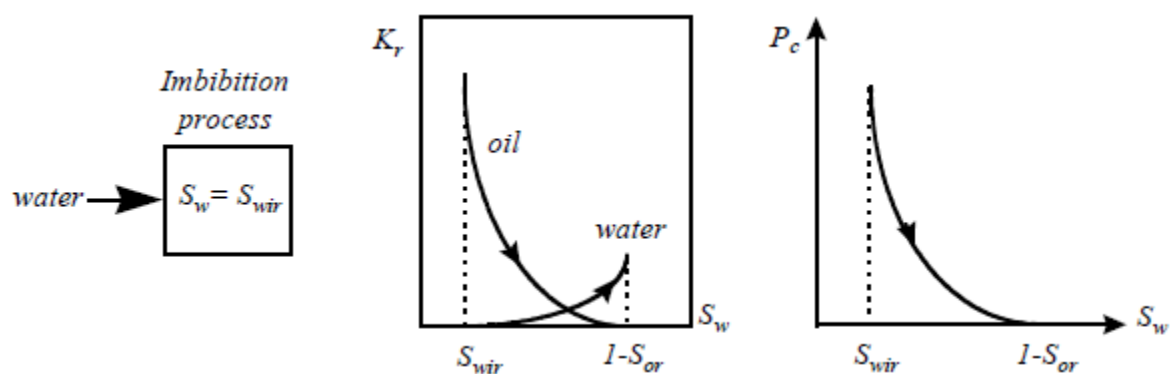


**Figure 3.2:** Relative permeability curves and related capillary pressure curve for a typical imbibition process (Holter, 2012).

## 3.2.2 Drainage

Drainage of fluids occurs when the saturation of the wetting phase decreases. This happens when a non-wetting fluid displaces a wetting fluid. For the case where gas displaces oil, the production mechanism is drainage. Many carbonates are oil-wet or mixed-wet. For waterflooding of such reservoirs, there may be large amount of residual oil left. This is because the rock prefers to be surrounded by oil, and the capillary forces will oppose the invasion of water. In some pores the capillary forces will resist the water to enter at all. Because of this, a water-wet reservoir is in many cases preferred. Some chemicals as surfactants are able to change the rock's preferred wettability by chemical reactions on the rocks surface. In a very successful surfactant flood, the wettability may change from oil-wet to water-wet and the original drainage process becomes an imbibition process in the case of water injection.

Figure 3.3 presents the relative permeability and capillary pressure curves for a typical drainage process.

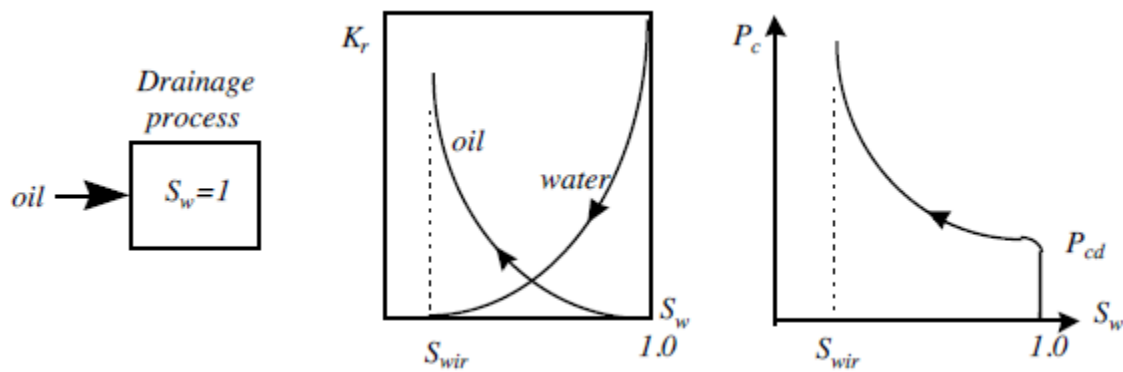


**Figure 3.3:** Relative permeability curves and related capillary pressure curve for a typical drainage process (Holter, 2012).

### 3.3 Mobility

The mobility of the fluid front in a displacement process is often presents as the *mobility ratio* of the mobility of the displacing fluid to the mobility of the displaced fluid (eq.(3.2)) (Schlumberger, 1998c).

(3.2)

$$M = \frac{M_w}{M_o} = \frac{k_{rw}/\mu_w}{k_{ro}/\mu_o} = \frac{k_{rw}\mu_o}{k_{ro}\mu_w}$$

Where:

- $k_{rw}$  is the relative permeability for water at  $1-S_{or}$ .
- $k_{ro}$  is the relative permeability for oil at  $S_{wi}$ .
- $M>1$ : Unfavorable mobility ratio
- $M=1$ : Unit mobility ratio
- $M<1$ : Favorable mobility ratio (Torsæter, 2011)

## 4. Naturally Fractured Reservoirs, NFR

A reservoir is defined as a naturally fractured reservoir when it contains a distribution of fractures of various degrees throughout the reservoir. Geological processes form the fractures naturally. Several factors that are observed initially as the field is discovered or throughout production of the field can identify that the reservoir of interest is fractured. Some of these features are (Chilingarian, et al., 1996):

- Significant mud losses during drilling
- Core examinations in the lab
- Observation on outcrops during the exploration phase.
- Use of a televiewer in the well during logging.
- Special behaviour of transient pressure analysis during well testing (the appearance of double slopes).

#### 4.1 NFR features

Natural fractured reservoirs have features that distinguish them from regular conventional reservoirs. In fractures, the equilibrium between two fluids is controlled by gravity and the capillary pressure can be neglected. This causes the fluid contact to be horizontal without any transition zone (Chilingarian, et al., 1996).

Because the flow toward the well only occurs within the fractures, the pressure drop around the well is very small, compared with a conventional reservoir. The high flow rate is assured by the high fracture permeability. The matrix will provide the fractures with fluids and therefore assure high flow rate and low pressure-drop. Figure 4.1 illustrates how much lower the pressure drop is around the wellbore in a naturally fractured reservoir.

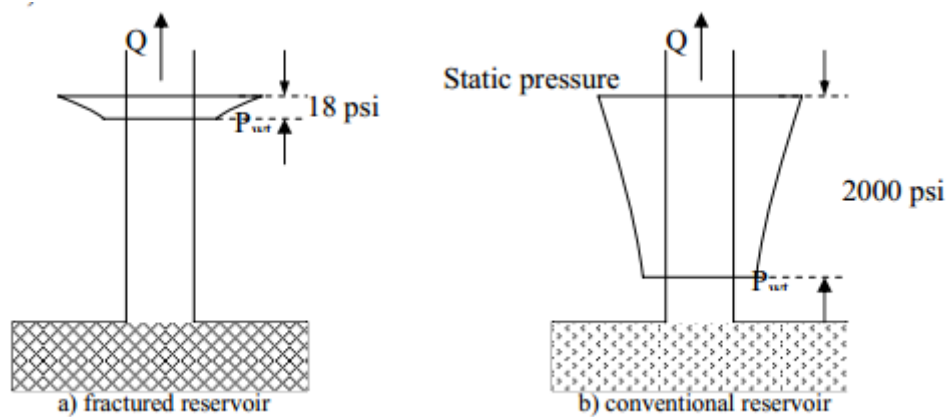


**Figure 4.1:** Pressure distribution around the wellbore for a) a fractured reservoir and b) a conventional reservoir (Torsæter, 2014a).

In fracture reservoirs with very low pressure gradients, a segregation of liberated gas will form a “fracture gas cap”. Because of the segregation the average density difference in the fractures (except in an area of 10m around wellbore) will be substantially higher than pressure gradients in fractures (Chilingarian, et al., 1996). In matrix with low permeability, a high pressure difference is required for flow to occur. The high pressure drop gives rise to viscous forces substantially higher than gravity forces, and thus the liberated gas will flow towards the well. Hence, the gas oil ratio for a conventional reservoir is often higher than for a fractured reservoir (Torsæter, 2011).



For a fractured reservoir, the water oil ratio is a function of the production rate. While for a non- fractured reservoir, the water oil ratio is a function of many variables, such as rock characteristic, displacement behaviour, in addition to production rate.

In a NFR reservoir, there is a possibility that the PVT properties remain constant. If there is a very good continuity both vertically and horizontally in the fracture network, a convection process may occur. As a result of fluid thermal expansion and gravitational compression a convection process in the fractures may take place. The convection may make the hydrocarbon composition uniform and hence bubble point pressure and other PVT properties may remain constant with depth (Torsæter, 2014a).

Because of different recovery mechanism in a fractured reservoir with double-porosity, an improvement in recovery due to a low pressure decline per unit oil produced can be expected compared to the same reservoir in absence of fractures. For the case of depletion below bubble point, an increase in recovery for a fractured reservoir compared to a non- fractured reservoir is a result of “gas- gravity drainage”. For the non- fractured reservoir, the same recovery can be achieved only by a reinjection of 80 per cent of produced gas (Chilingarian, et al., 1996).

## 4.2 Characterisation of fractures

A single fracture is characterised by width, size, orientation, etc. On the contrary is a group of fractures a combined description with matrix/fracture. A group of fractures can be divided in two categories, fracture system and fracture network. A fractured system is a set of several parallel fractures, while a fracture network is formed by several fractured system.

The intrinsic characteristic of a single fracture is width, size, nature of the fracture and orientation. The fracture width is often referred to as the fracture opening and is the distance between the fracture walls. The fracture opening varies, but is often in a range of 10-40 microns. However, in some cases the opening can be as large as 200 microns.

The orientation of a fracture characterise how the single fracture is connected to the environment. Figure 4.2 shows how the fracture plane can be defined by dip azimuth and dip angle (Torsæter, 2014a).

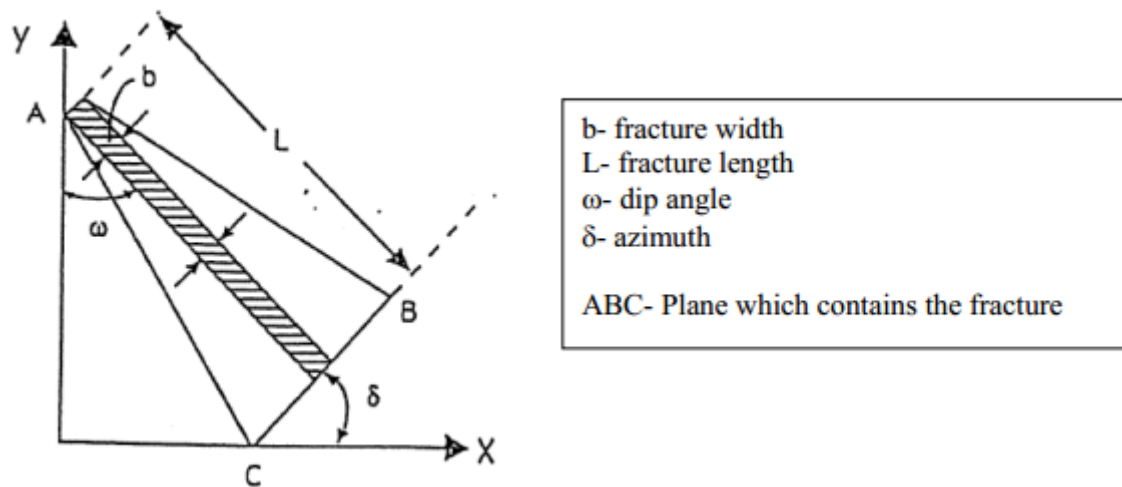


**Figure 4.2:** Fracture orientation of a single fracture (Torsæter, 2014a).

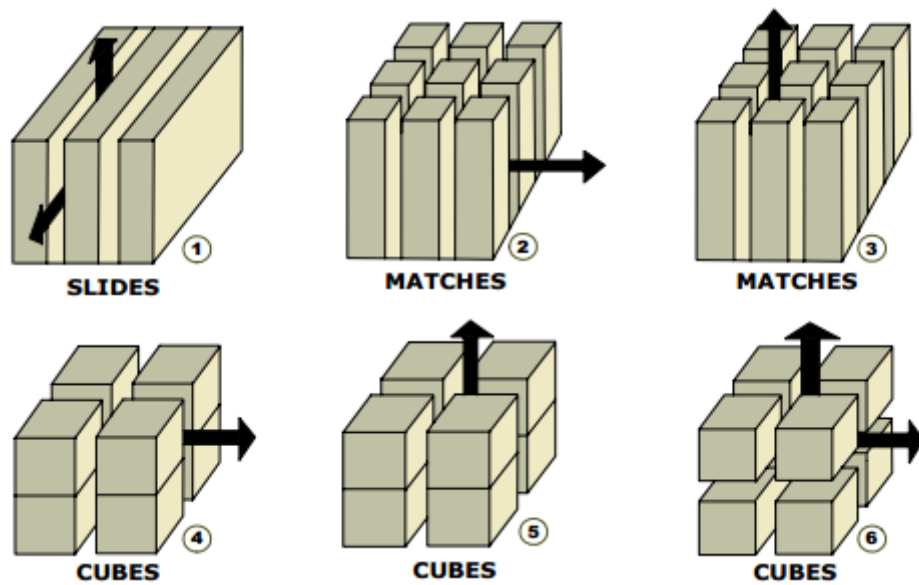
For a group of fractures the characterisation parameters refer to fracture arrangement (geometry) which generates the matrix block. The geometry describes the frequency of fractures along a given direction and the extension of matrix limited by surrounding fractures. For a system with several orthogonal fracture systems, the intersection between them will result in single matrix blocks of different sizes and shapes (Chilingarian, et al., 1996).

The linear fracture density (LFD) is defined as the number of fractures divided by block length along a certain direction.

(4.1)

$$[LFD]_x = \frac{n_f}{L_x}$$

A set of simplified idealized block shapes based on this approach is carried out from various distributions of fractures in an orthogonal fracture network. As Figure 4.3 presents, the blocks can be structures as elongated slides or matches with only one permeability direction or as cubes with one (number 4 and 5) or two (number 6) flowing directions.

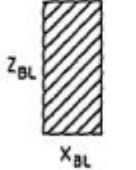
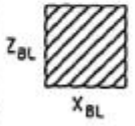
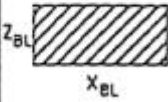


**Figure 4.3:** Idealized geometrical blocks (Torsæter, 2014a).

For a large pay zone with both vertical and horizontal fractures, the notion fracture intensity (FINT) is introduced and is defined as the ratio between vertical fracture density and horizontal fracture density. The relationship between FINT and matrix block size is presented in Figure 4.4.

(4.2)

$$FINT = \frac{LFDV}{LFDH}$$

| CASE 1  | CASE 2  | CASE 3   |
|---|---|--|
| Vertical Density > Horizontal Density   | Vertical Density = Horizontal Density   | Vertical Density < Horizontal Density  |
| LFDZ > LFDX   | LFDZ = LFDX   | LFDZ < LFDX  |
| FINT > 1  | FINT = 1  | FINT < 1   |
| $\frac{z_{BL}}{x_{BL}} > 1$   | $\frac{z_{BL}}{x_{BL}} = 1$   | $\frac{z_{BL}}{x_{BL}} < 1$  |
|  <p>VERTICALLY<br/>ELONGATED<br/>MATCH</p> |  <p>CUBE</p> |  <p>ELONGATED<br/>SLAB</p> |

**Figure 4.4:** The relationship between FINT and matrix block size (Torsæter, 2014a).

### 4.3 The Warren and Root model

A conventional reservoir is studied under the simplified assumption that it is homogenous, and reservoir properties as permeability and porosity are overall certain trends in the field (Chilingarian, et al., 1996). In a naturally fracture reservoir there are several discontinuities throughout the reservoir which results in a double porosity situation. The matrix has high storage capacity but very low permeability and hence low flowing conductivity, while the fractures have low storage capacity but high to very high permeability and flowing conductivity. With such contrasting conditions within the reservoir, a different model than those used in conventional intergranular reservoir is required to approach reservoir physical data. Warren and Root presented in 1963 a method that is still considered to be the most representative approach for a naturally fractured reservoir.

The method Warren and Root was developed for studying the characteristic behaviour of a permeable medium that contains regions that contribute significantly to the pore volume of the system, but contribute negligibly to the flow capacity (Warren & Root, 1963). The model uses a simplified representation of an idealised fractured reservoir system, where single matrix blocks are identical rectangular parallelepipeds separated by an orthogonal network of fractures (Chilingarian, et al., 1996). In the model, the flow towards the wellbore is considered to only occur in the fractures, and the matrix feeds the fractures with fluids as a result of the pressure depletion in the fracture network. A schematic presentation of the model is shown in Figure 4.5 and Figure 4.6.

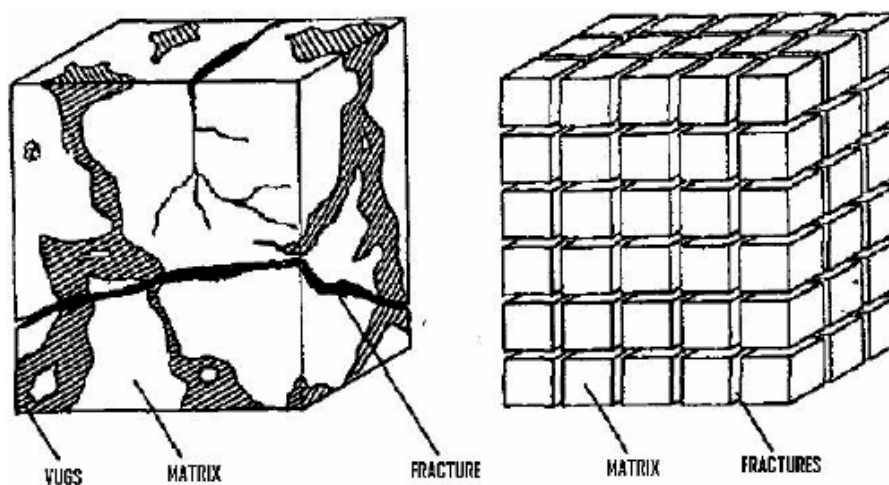


**Figure 4.5:** Model of a real fractured reservoir to the left, and a model of an idealised fractured reservoir to the right (Chilingarian, et al., 1996).

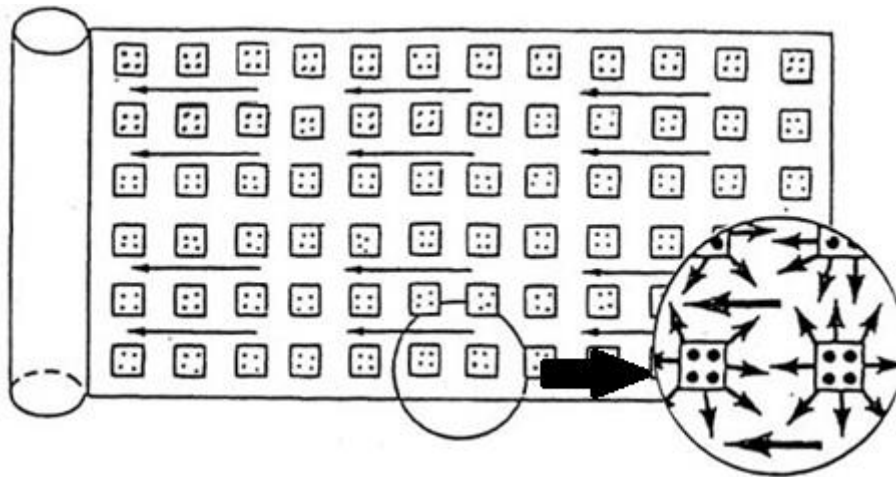


**Figure 4.6:** Fluid exchange between matrix and fractures during flow towards a well (Chilingarian, et al., 1996).

The Warren and Root procedure is based on a similar processing approach that is used in a conventional reservoir. As for a conventional approach, its well data is plotted as delta pressure versus log time for either pressure drawdown or pressure build up. In a conventional “one-porosity” reservoir, all transient behaviour analysis gives a straight line in the semi log plot of pressure vs. time, both drawdown and build-up. For “double-porosity” fractured reservoirs, the semilog plot of pressure vs time, a double-slope over three stages will appear, for both cases, build-up and drawdown (Chilingarian, et al., 1996).

The three stages have different behaviour and are divided into early stage, intermediate or transition stage and late stage behaviour. Each stage reflects the fluid exchange between matrix and the fracture network.

The early stage reflects the start of the production with a constant rate  $Q$  in a well. The well pressure decreases because of the small fracture pore volume, and the fluid exchange from the matrix has not yet started. Figure 4.7 below shows a pressure drawdown semi log plot, the early stage is presented as the first slope and reflects the flowing capacity of the fractured network.

A continuous production with the constant rate  $Q$  will induce a continually pressure decline in the fractures  $p_f$ . A pressure difference between the matrix and fractures ( $p_m - p_f$ ) will develop and induce a fluid supply from matrix to the fracture network. The result of such fluid supply from matrix to fracture is similar to a fluid injection in fractures, the well pressure decline is

reduced. On Figure 4.7, number 2 marks the start of this transition stage,  $t_{ti}$ , which is the point where the fluid supply from the matrix reaches the fractures and compensates for the production rate. The pressure decline reduction continues to point 3 ( $t_{\phi}$ ) where the pressure decline becomes practically zero and the pressure drop ( $\Delta p_{\lambda}$ ) is constant for a short period. After a time  $t_{tf}$ , the fluid pressure decline will start to increase again. The start of the decline is marked by point 4 in Figure 4.7 and represents the end of the transition stage (Chilingarian, et al., 1996).

In the late stage, the production rate is still constant and the matrix cannot supply the fracture network with sufficiently fluids to maintain the pressure. Therefore, the pressure decline will increase. The difference between the production rate and the fluid- supply rate will practically become constant, and from point 4 to 5 in Figure 4.7 a straight line appears in the semi log plot representing a “quasi- steady- state” well pressure decline.

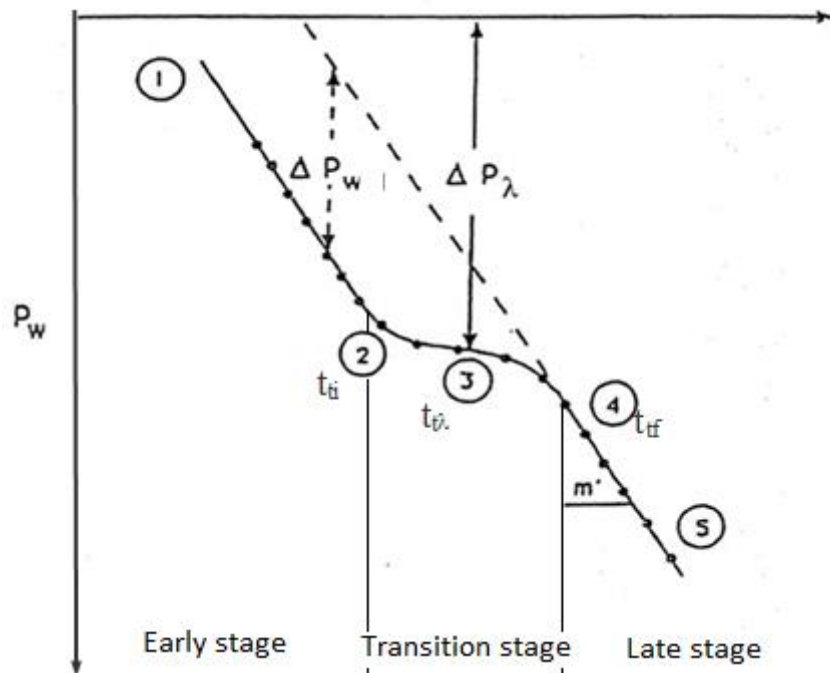


**Figure 4.7:** Pressure drawdown behaviour in a producing well in a naturally fractured reservoir (Chilingarian, et al., 1996).

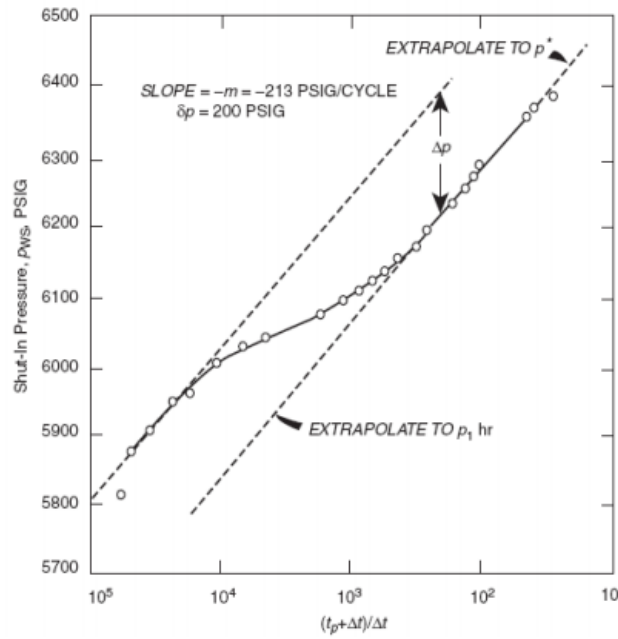


**Figure 4.8:** Pressure build-up behaviour in a naturally fractured reservoir (Ghahfarokhi, 2012).

### Warren and Root parameters

Warren and Root uses the following parameters to obtain fracture permeability, fracture porosity and matrix- block size.

- $k$ : permeability, [md]
- $\omega$ : dimensionless fracture storage capacity.
- $\lambda$ : dimensionless fracture- matrix interflow capacity.

To obtain these parameters the following set of parameters, an evaluation of a semi log plot such as Figure 4.7, has to be done (Chilingarian, et al., 1996).

The pressure difference ( $\Delta p_w$ ) between the early and late stage straight-line separation (Figure 4.7) is associated with the fracture storage capacity and evaluated through equation (4.3).

(4.3)

$$\omega = \frac{\varphi_f * C_f}{\varphi_m * C_m}$$

(4.4)



$$\omega = \frac{1}{e^{2.3 * \Delta p_{\omega} / m'}}$$

In the transition stage of the pressure from the early to late stage, straight- line will be a function of the fracture- matrix interflow capacity  $\lambda$ , which can be evaluated from equation (4.5) at time  $t_{\lambda}$  from the pressure drop  $\Delta p_{\lambda}$ .

(4.5)

$$\lambda = \frac{(1 - \omega)}{1.78 * e^{2.3 * \Delta p_{\lambda} / m'}}$$

From equation (4.6) the matrix- fracture contact surface,  $\alpha$ , can be obtained through the matrix fluids flows toward the fractures.

(4.6)

$$\lambda = \alpha \frac{k_m}{k_f} r_w^2$$

The matrix- fracture contact surface,  $\alpha$ , depends on matrix block size, L. The square of block size, L equals number of flowing directions,  $\psi$ , divided by the matrix- fracture contact surface as expressed in equation (4.7).

(4.7)

$$L^2 = \frac{\psi}{\alpha}$$

Where,

(4.8)

$$\psi = 4n(n + 2)$$

The fracture permeability is a function of the slope,  $m'$ , of the two parallel straight lines. From the slope between point 4 and 5 in the final stage in the semi log plot of pressure vs. time (Figure 4.7), the permeability of the fracture network can be obtained by applying equation (4.9) (Chilingarian, et al., 1996).

(4.9)

$$k_f = \frac{1.15q\mu}{2\pi h m'}$$

#### 4.4 Matrix- Fracture Fluid Exchange

For the evaluation of fluid exchange between matrix and fractures, is Warren and Root's simplified model applied (Figure 4.6). The matrix blocks are assumed to be surrounded only by fractures without any direct contact with other matrix blocks. The matrix- fracture fluid exchange will depend on rock and fluid characterisation, such as wettability and fluid saturation in matrix and fractures. With different fluid saturation in fractures and matrix, a drainage or imbibition fluid displacement will take place.

There are two different displacement scenarios that will be discussed in this subchapter. For the first case, the fractures are partially or fully saturated with water while the matrix block is saturated with oil. In the second case, the matrix block is saturated with oil, while the fractures are partially or fully saturated by gas.

For the case where the matrix is surrounded by gas, a gas invasion into the matrix will occur at the top of the matrix block displacing the oil downwards, due to the specific weight difference between gas and oil that will drive the heavier oil downwards by gravity forces. The capillary forces will oppose the invasion of non-wetting gas phase. This displacement process is called "gravity drainage".

For the scenario where water is saturating the fractures and oil is saturating the matrix, a water invasion from water injection or expansion of an aquifer will cause a water- oil contact rise in the matrix. The denser water will provoke an upward movement of the oil in the matrix. In this case, both capillary forces and gravity forces work in the favour of an oil displacement. This process is called an imbibition displacement (Chilingarian, et al., 1996).

##### 4.4.1 Imbibition

Chilingarian et. al (1996) state that experimental studies have shown the importance of the wettability of the rock in the determination of occurrence of drainage/imbibition. In the case of drainage: if the contact angle is below  $49^\circ$ , the capillary pressure and hence the threshold pressure will remain constant. While for an imbibition process, the magnitude of the contact angle can say something about how easily the imbibition displacement will go.

- When  $\theta < 49^\circ$ , a spontaneous imbibition is observed.
- When  $49^\circ < \theta < 73^\circ$ , limited imbibition is observed.
- When  $\theta > 73^\circ$ , no imbibition is observed.

As mention in chapter 3, the displacement process is strongly related to the wettability of the rock and the fluid saturation. Table 3 present an overview of displacement types and respective displacement history. An imbibition displacement process will take place when the matrix is saturated by a non-wetting fluid (oil, gas) and the fractures are saturated by a wetting fluid (water).

**Table 4.1.** Cases of drainage/imbibition displacement (Torsæter, 2014b).

| Case | Matrix block saturation | Fracture network saturation | Wetting phase in matrix | Oil displacement Process | Displacement history |
|------|-------------------------|-----------------------------|-------------------------|--------------------------|----------------------|
| 1    | Oil                     | Water                       | Water                   | Imbibition               | Reservoir Production |
| 2    | Oil                     | Water                       | Oil                     | Drainage                 | Reservoir Production |
| 3    | Oil                     | Gas                         | Oil                     | Drainage                 | Reservoir Production |
| 4    | Gas                     | Water                       | Water                   | Imbibition               | Reservoir Production |
| 5    | Water                   | Oil                         | Water                   | Drainage                 | Reservoir Migration  |
| 6    | Water                   | Gas                         | Water                   | Drainage                 | Reservoir Migration  |

In an evaluation of the imbibition process, the objective is to obtain for a given matrix block, the relationship between

- 1) recovery vs. time,
- 2) single matrix block rate vs. recovery and,
- 3) single matrix block rate decline vs. time.

In the evaluation, it is assumed that the matrix block is a parallelepiped of height  $h$ , where the pores in the matrix contain oil and irreducible water (Figure 4.9). Another objective of the evaluation is to estimate the role of the gravity and capillary forces that control the imbibition process.

The evaluation of the imbibition process has to be considered for three different cases, since the displacement process can be governed by either capillary or gravity forces or both.

Figure 4.9 is used to explain the simplified model for evaluation of recovery of a matrix-fracture reservoir system. It is assumed that the lateral walls are coated and therefore will the fluid exchange between matrix and fractures only happen through the upper and lower face of the block.  $H_w$  is the water – oil contact height in the fractures which corresponds to the fracture oil height  $H_o$ , hence the total block height can be expressed as  $H = H_w + H_o$ . Within the matrix the water advancement front is referred to as  $Z$ , and thus the oil column in the matrix is expressed as  $H - Z$ .

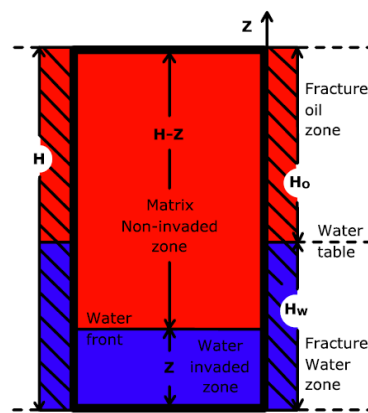


**Figure 4.9:** Matrix block saturated with oil surrounded by fractures saturated by water (Torsæter, 2014c).

### Recovery formulation for the simplified model.

A full derivation of the formulation for recovery is given in Chilingarian et. al. 1996, “Carbonate Reservoir Characterizations: a geological – engineering analysis, part II, page 755”.

(4.10)

$$Recovery = A * Z * \varphi_{eff} = A * Z * \varphi_{eff} * \Delta S_o = A * Z * \varphi * (1 - S_{wi} - S_{or,imb})$$

The recovery is directly proportional to the displacement front distance  $Z$  (Chilingarian, et al., 1996).

Capillary and gravity forces are governing the flow.

(4.11)

$$p_{tot} = p_c + G = h_c(\rho_w - \rho_o)g + (H_w - Z)(\rho_w - \rho_o)g$$

By introducing Darcy's law where  $\Delta p = \Delta p_w + \Delta p_o$ , the displacement front velocity solution can be obtained:

(4.12)

$$u = \frac{(H_w - Z)((\rho_w - \rho_o)g + p_c)}{\frac{\mu_w Z}{k_w} + \frac{\mu_o(1 - Z)}{k_o}}$$

In the case of total immersion,  $H=H_w$  the displacement front velocity will become:

(4.13)

$$u = \frac{\left[ (1 - Z_D) + \frac{h_c}{H} \right] (\rho_w - \rho_o)g \frac{k_w}{\mu_w}}{Z_D + M(1 - Z_D)}$$

Where;

the dimensionless front position  $Z_D = Z/H$ ,

the mobility ratio,  $M = \frac{k_w \mu_o}{\mu_w k_o}$ ,

and;  $p_c = (\rho_w - \rho_o)gh_c$

### **Time vs. recovery general formulation for matrix block.**

To obtain the formulation, Darcy velocity for one-dimensional flow in a porous media has to be introduced together with the intrinsic velocity in the pore system.

Darcy velocity,  $u = -\frac{k}{\mu} \frac{dp}{dz}$

Intrinsic velocity,  $\frac{dz}{dt} = \frac{u}{\varphi_{eff}} = \frac{u}{\varphi_m(1 - S_{wi} - S_{or})}$

Resulting in the general formulation for recovery vs. time for a totally immersed matrix block for one- dimensional flow.

(4.14)

$$dt = \frac{\varphi_{eff} H [Z_D + M(1 - Z_D)]}{\left[ (1 - Z_D) + \frac{h_c}{H} \right] (\rho_w - \rho_o) g \frac{k_w}{\mu_w}} dz_D$$

Equation (4.14) includes both capillary and gravity forces and can be solved for both cases. For gravity dominated flow,  $H \gg h_c$  and hence  $h_c/H$  becomes negligible and equation (4.14) can be solved for gravity dominated flow.

In the case of capillary dominated flow  $h_c \gg H$  and then  $h_c/H \gg (1 - Z_D)$  so that;

$$\frac{h_c}{H} + (1 - Z_D) = \frac{h_c}{H}$$

Then equation (4.14), can be solved to count for capillary dominated flow.

Figure 4.10 and Figure 4.11 present the relationship between recovery,  $Z_D$ , and dimensionless time,  $t_D$ , for gravity dominated flow and capillary dominated flow respectively.

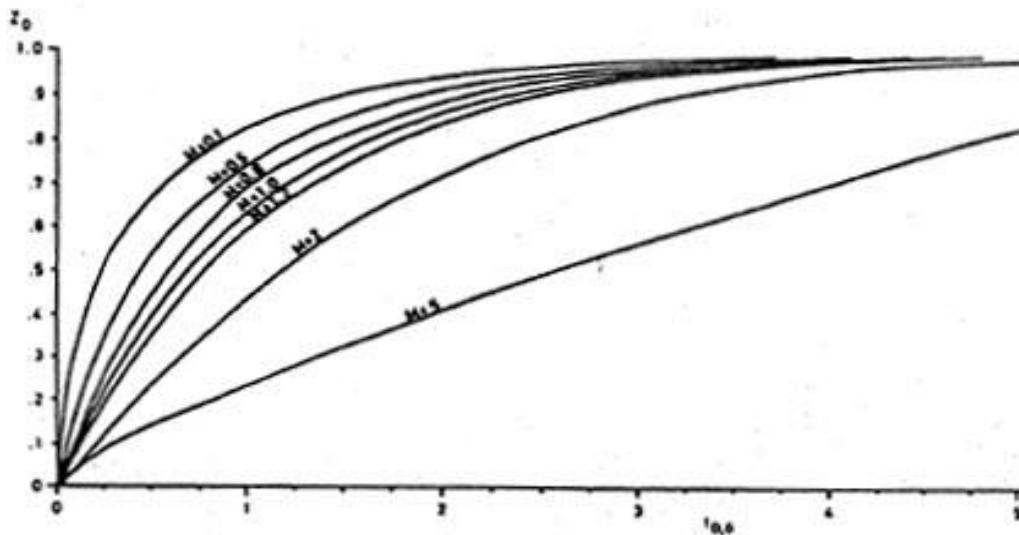


**Figure 4.10:** The relationship between recovery,  $Z_D$ , and dimensionless time,  $t_D$ , for gravity dominated flow (Chilingarian, et al., 1996).

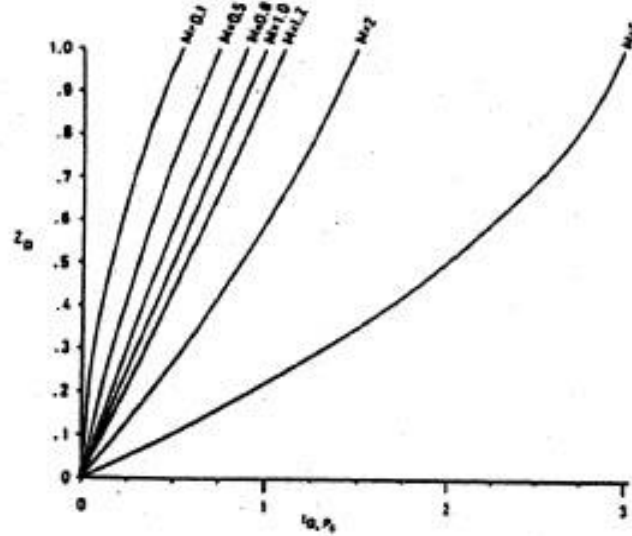


**Figure 4.11:** The relationship between recovery,  $Z_D$ , and dimensionless time,  $t_D$ , for capillary dominated flow (Chilingarian, et al., 1996).

#### 4.4.2 Gravity Drainage

When a non-wetting phase displaces a wetting phase, the process is drainage. In fractured reservoirs, the most common drainage processes occurs when a non-wetting gas saturated in the fracture network, displaces the wetting oil saturating the matrix. This fracture invasion occurs when a gas cap expands. The free gas may be liberated from oil because of depletion, which has segregated in fractures and formed a fracture gas-cap as discussed in chapter 4.1, or external gas injected into the reservoir. The gas in fracture advancement and the density difference between matrix oil and the gas in the fracture network, provide energy for the gas-gravity-drainage process. As long as the field gravity- drainage rate is equal to the production rate, there will not be a pressure decline in the field (Chilingarian, et al., 1996).

A classic drainage process can be explained by Figure 4.12. There is only fluid exchange on the top and bottom of the matrix block. Oil is drained by gas and move downwards while the gas enters the top of the matrix block and replaces the produced oil. The initial condition is at  $Z= 0$  (Figure 4.12), while the production stops when  $Z= H - h_{th}$ , which is at the threshold level.

Flow is assured when the gravity forces is higher than the capillary forces. This is presented in Figure 4.13: **Oil produced from a matrix block surrounded by gas- saturated fractures, by examining the relative magnitude of gravity and capillary forces. (Chilingarian et. al. 1996)**Figure 4.13. When the capillary forces remain constant while the gravity forces increases by depth, the block bottom flow is assured by the much larger gravity forces. For the second case the block bottom flow is assured since the gravity forces are still larger than the capillary forces. While for the third case, the capillary forces are equal to the gravity forces and the flow stops. The remaining oil in the matrix is called the “oil hold-up zone”.

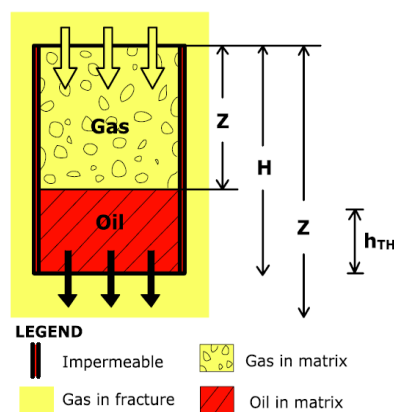


**Figure 4.12:** Oil displacement by gas in a matrix block surrounded by fractures saturated with gas (Torsæter, 2014c).

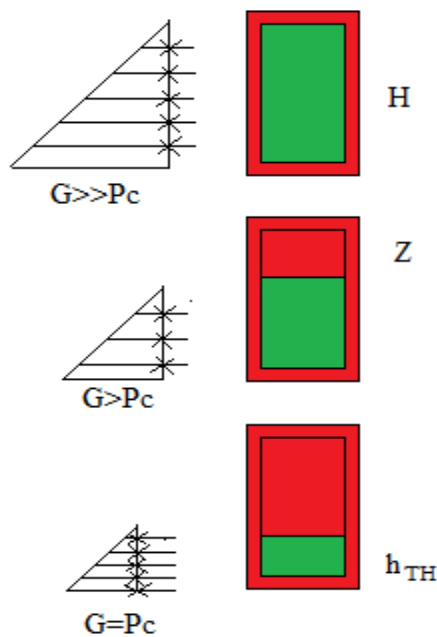


**Figure 4.13:** Oil produced from a matrix block surrounded by gas- saturated fractures, by examining the relative magnitude of gravity and capillary forces. (Chilingarian et. al. 1996)



## 5. Recovery periods

The production lifetime of a reservoir is often divided into three stages, primary, secondary and tertiary recovery periods. Figure 5.1 below shows typical recovery techniques for the three production stages.

|                                      | Primary Recovery  | Secondary Recovery  | Tertiary Recovery  |
|--------------------------------------|---|---|--|
| Conventional Oil Recovery Techniques | <ul style="list-style-type: none"> <li>• Natural Flow</li> <li>• Artificial Lift</li> </ul>   | <ul style="list-style-type: none"> <li>• Water Flood</li> <li>• Pressure Maintenance</li> </ul> | <ul style="list-style-type: none"> <li>• Thermal</li> <li>• Gas Flood</li> <li>• Chemical Flood</li> </ul>   |
| Oil Sands Applications               | <ul style="list-style-type: none"> <li>• Cold Heavy Oil Production with Sand (CHOPS)</li> <li>• Multi-Lateral Horizontal Wells</li> </ul> | <ul style="list-style-type: none"> <li>• Water Flood</li> <li>• Polymer Flood</li> </ul>        | <ul style="list-style-type: none"> <li>• Steam <ul style="list-style-type: none"> <li>▪ CSS</li> <li>▪ SAGD</li> </ul> </li> <li>• Solvent <ul style="list-style-type: none"> <li>▪ VAPEX</li> <li>▪ Thermal Solvent</li> </ul> </li> <li>• Hybrid/ Co-injection</li> <li>• Combustion <ul style="list-style-type: none"> <li>▪ THAI™</li> </ul> </li> </ul> |
| Application                          | > 100 kb/d  | Limited   | Extensive  |

**Figure 5.1:** Recovery techniques for oil production (Torsæter, 2013).

### 5.1 Primary recovery

During first stage of the production period, oil is recovered from pressure differences between the reservoir and the bottom hole wellbore pressure. The oil is displaced from natural gasdrive, waterdrive or gravity drainage. Due to production, the reservoir pressure will decrease. To maintain the differential pressure, an artificial lift system must be installed. Eventually the reservoir pressure will drop so low that the production flow will not be economical, or the water oil ratio and/or gas oil ratio will be too high. After primary production, about 10% of the oil in place can be produced (Schlumberger, 1998d).

### 5.2 Secondary recovery

In conventional hydrocarbon production, waterflooding and gas injection are the most common methods to enhance the oil recovery. Water is injected into the production zone to displace the oil, while gas is injected into the gas cap. The purpose of these injections is to maintain the reservoir pressure, so more oil can flow toward the production wells. The secondary recovery will continue until the water cut or the gas production is so high that the production is no longer conventional. A recovery factor of 15-40% can be obtained by secondary recovery techniques (Schlumberger, 1998e).

### 5.3 Tertiary recovery

The third stage in oil production is any enhanced oil recovery (EOR) techniques applied after the second stage of the production (Schlumberger, 1998f). In tertiary recovery, the purpose is to enhance the production even more by changing the properties of the injection fluid or change the chemical properties between the displacing fluid and the displaced fluid. The most common method is gasflooding, but thermal injection methods and chemical injection are also often used in addition to water injection (Lake, 1989).

Gas injection is one of the earliest enhanced oil recovery techniques applied in addition oil production. It was first applied in the early 1960s by injecting slugs of liquefied petroleum gas (LPG) and then displacing the LPG with a dry “chase” gas. Both miscible and immiscible gasflooding is applied. Two fluids are miscible when they mix together in all proportions in a single-phase. Most of the miscible fluids that are used in EOR processes are only partly miscible with the crude oil itself. Thus, miscible gas injection is often referred to as solvent flooding. The main function of solvent flooding is to extract, dissolve, vaporise, condensate and solubilise the crude. The solvents that are used for extraction is primary CO<sub>2</sub>, CH<sub>4</sub> and N<sub>2</sub>, but other fluids as LPG, LNG and air for example are also used (Lake, 1989).

Thermal injection is mainly done by in-situ combustion, steam applied gravity drainage (SAGD) and steam injection. The purpose is to increase the heat in the reservoir, so that light oil components in the crude will vaporize and the crude will become more mobile due to lower viscosity (Torsæter, 2013).

In chemical recovery, polymers and surfactants are the two most common agents. Polymers are injected to improve the mobility ratio, which results in a better sweep efficiency (Statoil, 2008). Surfactants’ main task is to decrease the interfacial tension between the oil and brine, so that the capillary trapped oil becomes mobile. Polymers are most widely used and is therefore the most important chemical recovery method. However, due to high oil prices, there is a growing use of surfactants in EOR (Hirasaki, et al., 2008).

## 6. Surfactant flooding

The purpose of surfactant flooding as an enhanced oil recovery method is to recover the capillary-trapped residual oil after waterflooding. In order to produce the trapped oil in flooded zones, the pressure drop across the trapped oil has to overcome the capillary forces that trap the oil. By injection of surfactant solution, the interfacial tension between oil and water may be strongly reduced and the residual oil can be mobilised. By decreasing the IFT, also the capillary pressure will be reduced. It is the capillary forces that oppose the invasion in pores, as explained in chapter 2.6.1 “threshold pressure”. A reduction in capillary forces will have an impact of the relative permeability curves. A lower capillary pressure will allow fluid flow to occur at other saturations than originally. The endpoints in the relative permeability vs. saturation plot will change. Figure 6.1 presents how the capillary and relative permeability curves and saturation endpoint may change as a result of IFT reduction and hence capillary pressure reduction. An efficient surfactant solution can reduce the IFT by a factor of about  $10^4$  (Zolutukhin & Ursin, 2000).

The technological efficiency of surfactant flooding is far less in the field than measured in the laboratory. There are several factors affecting the performance of surfactant flooding. The most important are:

- Salinity and hardness of brine are those factors that affect the surfactants ability to reduce IFT in the reservoir the most (Zolutukhin & Ursin, 2000).
- High absorption of surfactants by reservoir rock affects the efficiency of the surfactant injected. Often a larger amount of the surfactant is absorbed by the porous media in a reservoir rock, than the amount measured in a laboratory test (Zolutukhin & Ursin, 2000).

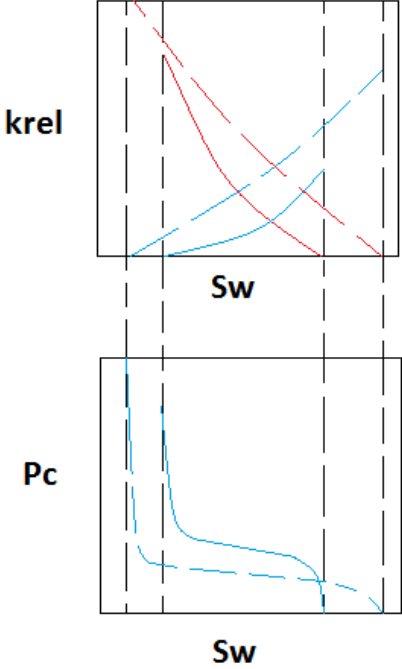


**Figure 6.1:** Relative permeability and capillary pressure alterations as a result of IFT reduction.

### 6.1 Types of surfactants

Surfactants are a blend of surface acting agents. They are organic compounds that are amphiphile, meaning that they are composed of a hydrocarbon chain, lipophilic (fat-loving) component and a hydrophilic (water-loving) component (Zolutukhin & Ursin, 2000). The lipophilic part is the tail and the polar hydrophilic part is the head. Surfactants concentrate or absorb at the surface and in a fluid/fluid interface and alter the surface properties. Accordingly, they reduce the surface tension between fluid and surface or they reduce the interfacial tension between two fluids (Sheng, 2011). There are different kinds of surfactants with different range of application. The surfactants are classified into four main groups.

- *Anionic*: Most used in chemical enhanced oil recovery since they are soluble in aqueous phase, stable and not expensive. Relative low absorption on sandstone (negatively charged surface) (Sheng, 2011).
- *Cationic*: Strongly absorbed in sandstone by the interstitial clay's anionic surfaces. Used in carbonate reservoir to change the wettability from oil-wet to water-wet (Sheng, 2011).
- *Nonionic*: Do not bind ionic when they are dissolved in water. Nonionic surfactants serve as cosurfactants to improve system phase behaviour. They cannot reduce IFT as much as anionics, but they are more tolerant to salinity and is often used in a mixture with anionic surfactants to tackle high salinity environments (Sheng, 2011).
- *Zwitterionic*: These surfactants contain two active groups. They can be nonionic-anionic, nonionic- cationic, anionic – cationic. The zwitterionic surfactants are very tolerant to temperature and salinity, but they are also expensive (Sheng, 2011). Due to the costs, zwitterionic surfactants have not yet been used in EOR projects (Green & Willhite, 1998).

## 6.2 Types of Microemulsions

When a very low concentration of surfactant is added to a solvent, the dissolved surfactant molecules will be spread as monomers. As more surfactant is added to the solvent, the concentration will after sometime reach the critical micelle concentration, CMC. Any further addition of surfactants will form micelles in the solution. Depending on which solvent the surfactants are added, the surfactants will form micelles where the tail (hydrophobic) is pointing toward the core of the micelle, while the head (hydrophilic) is pointing out, or opposite (Figure 5.1). In the scenario where the solvent is an aqueous phase, the tail will point against the core, while the head will be pointing out. Within the core, oil can be captured and solubilized, conversely for the scenario with an oil-phase solvent (Green & Willhite, 1998).

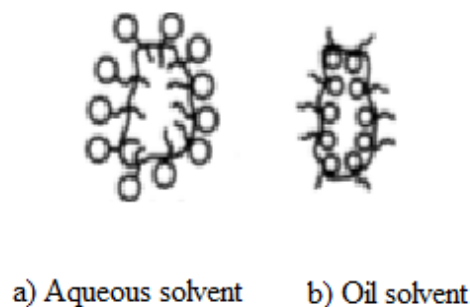


**Figure 6.2:** a) Shows a micelle formed in an aqueous solvent that has captured oil within the core. b) Shows a micelle formed in an oil solvent that has captured the aqueous phase within the core (Lake, 1989).

The phase behaviour of surfactant, oil, brine systems are strongly affected by the salinity of brine. An increase in the brine salinity will reduce the solubility of the surfactant in brine. Measurements of the solubility of surfactants in brine can very easily be done in laboratories. Therefore is phase behaviour often presented as a function of salinity (Sheng, 2011).

Green and Willhite defined in 1998 microemulsion in enhanced oil recovery processes as

“a stable, translucent micelle solution of oil and water that may contain electrolytes and one or more amphiphilic compounds.”



Microemulsion is more generally when there are two immiscible phases present in a system, and are made soluble within micelles. The micelles are made of amphiphilic compounds as surfactants, and the continuous phase will capture the excess phase in the core of the micelles.

Microemulsion system can be used to create ultralow IFT between oil and water in EOR processes (Green & Willhite, 1998). These systems are thermodynamically stable mixtures of oil and water, and are clear and transparent. However, due to aggregates of micelles, or if the oil in the system is dark and viscous, the mixture may not be clear (Sheng, 2011).

As mentioned earlier, the surfactant solubility in water decreases as salinity of water increases. When the salinity of water is low, there will form a microemulsion in the aqueous phase, and since water is denser than oil, the microemulsion will reside below the oil phase and is therefore called a lower-phase microemulsion. In a high salinity environment, the surfactant will easier solve in oil. The microemulsion will form in the oil phase, which will reside above the water phase and is therefore called an upper-phase microemulsion. In an intermediate salinity environment, the microemulsion will form in between the two phases and form a three-phase system containing an excess oil-phase, an excess water-phase and a middle-phase microemulsion in between. These three salinity systems are shown in Figure 6.3.

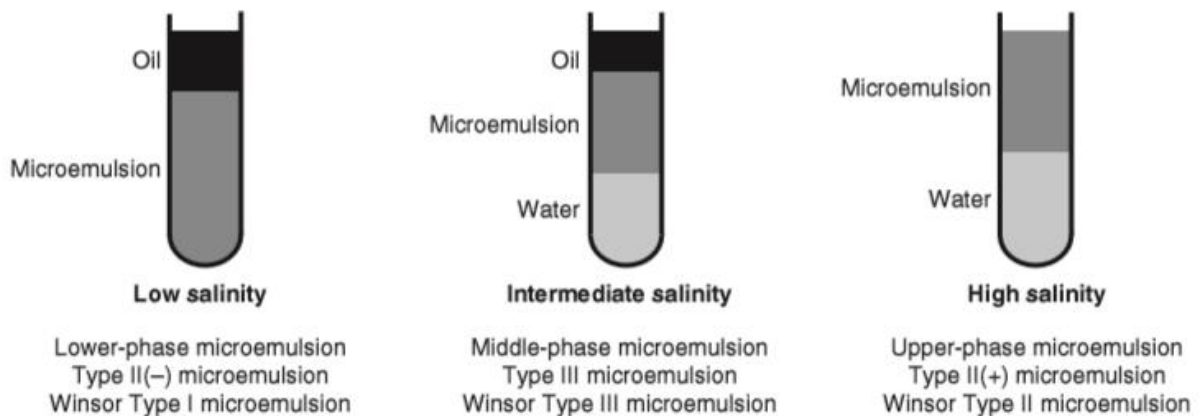


**Figure 6.3:** Lower-phase microemulsion, middle-phase microemulsion and upper-phase microemulsion in pipettes (Sheng, 2011).

To describe phase behaviour of oil, water, surfactant system, a ternary diagram is often used. The top of the triangle represent surfactant concentration, the lower left water concentration and the lower right oil concentration. The tie lines within the ternary representing a lower-phase microemulsion system will be negative. This will be a type II (-) environment, because there are two phases present and the tie lines are negative. A typically high salinity, upper-phase microemulsion system will be type II and a typically intermediate salinity, middle-phase microemulsion will be type III (Sheng, 2011).

The terminologies were originally given by Winsor (1954) and are presented in Figure 6.3. For anionic surfactants in a mixture with increasing salinity, the system will move from a Winsor type I  $\rightarrow$  type III  $\rightarrow$  type II. (Sheng, 2011).

Figure 6.4-6.6 present the typical three Winsor ternary systems used to represent type II(-), type II(+) and type III phase behaviour. In further discussion about surfactant phase behaviour, the Winsor terminology will be used

6.2.1 Winsor type I

Surfactants solve easily in water/brine with low salinity. There will be some oil solubilized within the micelles formed by a water-external microemulsion (Sheng, 2011). Thus an overall composition close to the boundary between oil and brine of the ternary will divide into two phases. The two phases will be one of an excess more or less pure oil-phase, and a (water external) microemulsion-phase with a mixture of brine and surfactant, and some solubilized oil (Lake, 1989). Winsor type 1, or “*underoptimum salinity*”, as it is often referred to, is described schematically in Figure 6.4 below.

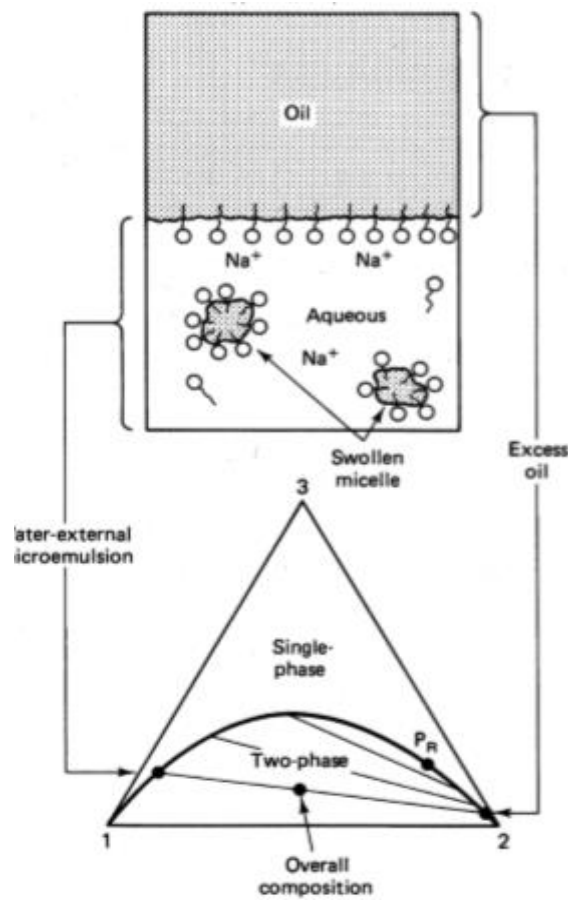


**Figure 6.4:** Ternary presentation of Winsor type I system, the overall composition of surfactant (1), brine (2) and oil (3) (Lake, 1989).

### 6.2.2 Winsor type II

The surfactants solubility in high salinity brines strongly decreases, due to electrostatic forces. The composition will now be divided into an excess aqueous-phase and a microemulsion-phase of surfactant, oil and some brine captured in the cores of the micelles (Lake, 1989). This is a Winsor type II system, often referred to as an «*over optimum salinity*» system and is presented in Figure 6.5.

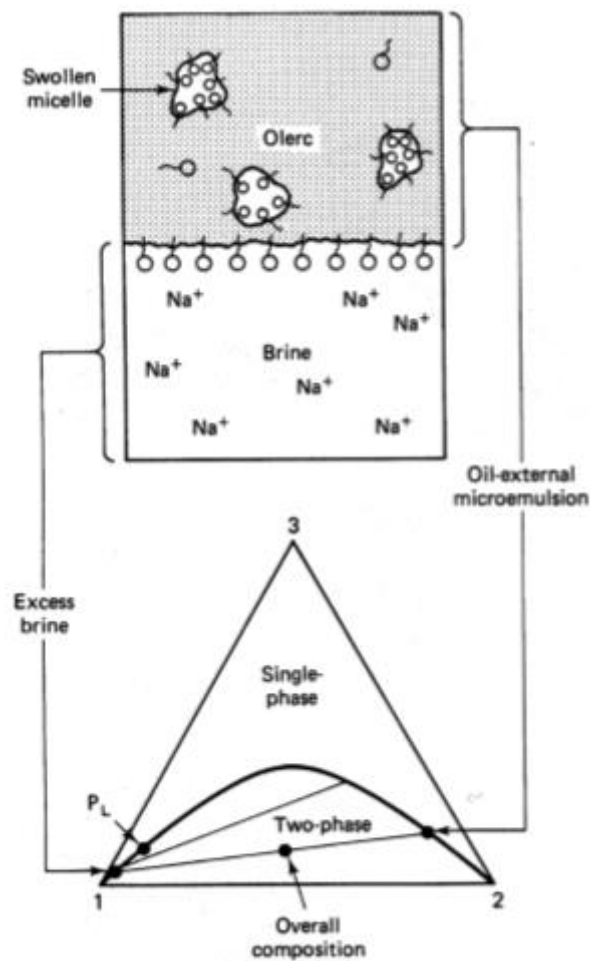


**Figure 6.5:** Ternary presentation of Winsor type II system, the overall composition of surfactant (1), brine (2) and oil (3) (Lake, 1989).

6.2.3 Winsor type III

Winsor type I and II are two extreme cases, where there is only a two phase system. But there are grades of salinity in between which will result in a three-phase system with an oil-phase, a aqueous-phase and a microemulsion phase in between. Winsor type III system is often referred to as an “*optimal salinity*” system where an equal amount of water and oil is solved by surfactants and form a microemulsion-phase. (Lake, 1989). Figure 6.6 presents the system.

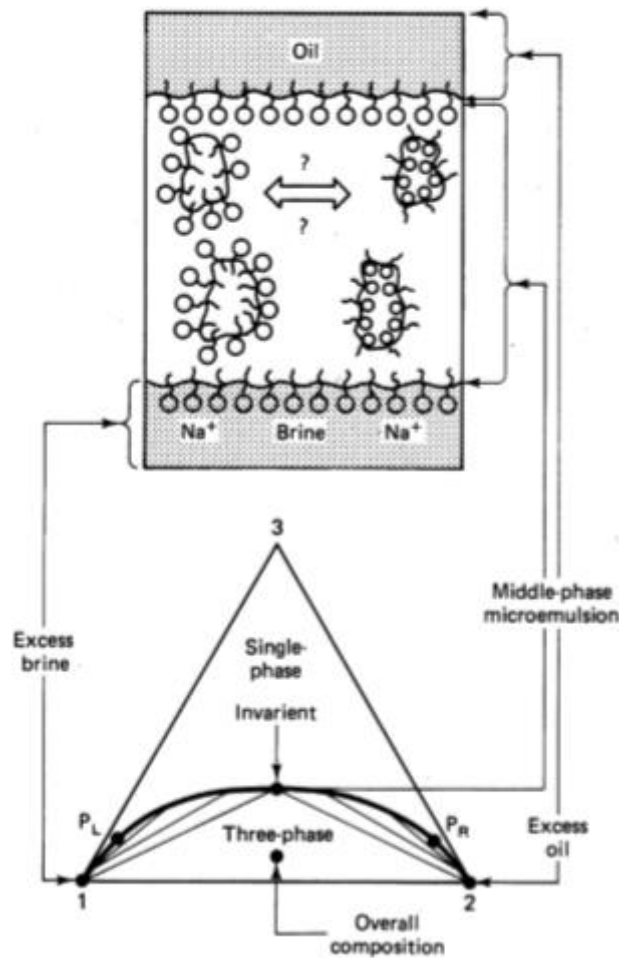


**Figure 6.6:** Ternary presentation of Winsor type III system, the overall composition of surfactant (1), brine (2) and oil (3) (Lake, 1989).

### 6.3 Phase Behaviour and IFT

The correlation between phase behaviour and interfacial tension was theoretically discussed by Huh in 1979 and was later verified experimentally (Huh, 1979). The optimal salinity to get an ultra-low IFT between water and oil and water in the microemulsion-phase is very close the optimal salinity obtained in phase behaviour tests (Green & Willhite, 1998). This correlation gives great advantages for prediction of the effect of surfactant as an EOR method in oil production. Since IFT is difficult to measure and time absorbing, the correlation is often used as an estimate in measurements of the IFT. This is done by calculations of the solubilisation parameters for oil and water. The solubilisation parameters will be referred to as  $SP_o$  and  $SP_w$  for oil and water respectively and was defined by Green and Willhite as:

(6.1)

$$\bullet \quad SP_o = \frac{V_o}{V_s} = \frac{\text{Volume of oil in the microemulsion phase}}{\text{Volume of surfactant in the microemulsion phase}}$$

(6.2)

$$\bullet \quad SP_w = \frac{V_w}{V_s} = \frac{\text{Volume of water in the microemulsion phase}}{\text{Volume of surfactant in the microemulsion phase}}$$

IFT depends on the types and concentration of surfactant in the system, cosurfactant, the electrolyte, the oil and temperature (Lake, 1989). At optimal salinity, the IFT between oil and microemulsion,  $\sigma_{mo}$  and the IFT between water and microemulsion  $\sigma_{mw}$ , will be ultra-low. The optimal salinity is obtained when  $SP_o=SP_w$ , and this value is more or less equal to the salinity obtained when  $\sigma_{mo}=\sigma_{mw}$ . This correlation can be seen from Figure 6.7. Huh used this to obtain a formula for estimation of the IFT by only using phase behaviour test. (Huh, 1979)

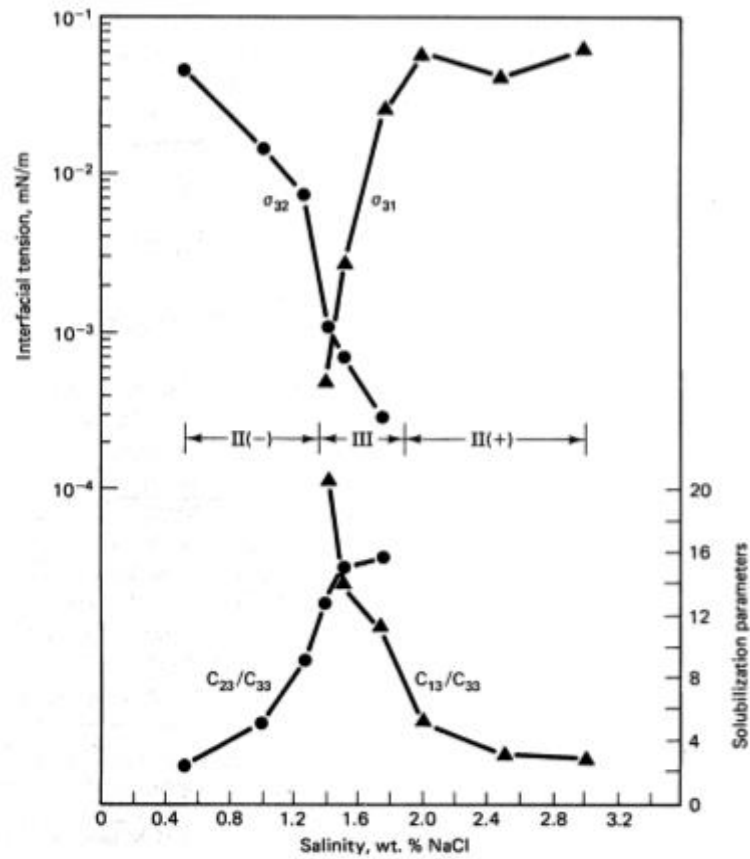


**Figure 6.7:** IFT between microemulsion and oil decreases as the salinity increase. While the IFT between microemulsion and water increases when the salinity increases. The optimal salinity is when the curves cross, which here occurs at the approximate same salinity, and in a Winsor type III system (Lake, 1989).

The correlation between the solubilisation parameter and IFT that Huh established, is valid and a good approximation at optimal salinity. The correlation says that the interfacial tension is inverse proportional to the square of the solubilisation parameter:

(6.3)

$$\sigma^* = \frac{C}{(SP^*)^2}$$

Where  $C$  is an empirical constant which is often assumed to be 0,3 mN/m (Fuseni, et al., 2013). At optimal salinity the solubilisation factor is above 10 (Lake, 1989).

### 6.4 Parameters affecting phase behaviour

Salinity of the aqueous phase is the most important parameter that affects the phase behaviour of water, oil, surfactant system. The solubility of surfactant in water decreases as the salinity increases, and an ultra-low IFT between oil and brine can easier be obtained when the optimal salinity for the surfactant is found. However, there are other parameters that have an impact of the phase behaviour to the system; they are listed in the following subchapters.

#### 6.3.1 Temperature

A change in temperature will affect the solubilisation parameters and therefore also the IFT between oil and brine. An increase in temperature leads to a reduction of the solubilisation parameters for oil and water. This results in an increase in the interfacial tension and a shift in the optimal salinity window (Sheng, 2011). The optimal salinity for the surfactant increases. In a test conducted by (Green & Willhite, 1998), an increase in temperature from 23°C to 65°C resulted in an increase in optimal salinity from 1,6wt% to 2,1wt% and a decrease in the optimal solubilisation parameter from 14,5 to 7,5. Roshanfekar & Johns (2011), confirm the negative effect of a temperature increase.

#### 6.3.2 Pressure

The phase behaviour of the all-liquid system is insensitive to a pressure change. Nelson found that there was a change in the phase behaviour due to pressure changes in gassy crudes. The oil-phase volume increased as the pressure decreased (Lake, 1989). During pressure changes, the water-oil ratio changes because of the difference in the compressibility between oil and water. Even if there are no changes in the phase-volume, the phase behaviour is changed. And further, the solubilisation parameter for water will increase with increasing pressure, while the oil solubilisation parameter will decrease. Thus, phase-behaviour is shifted towards lower-phase microemulsion (Skauge & Fotland, 1990).



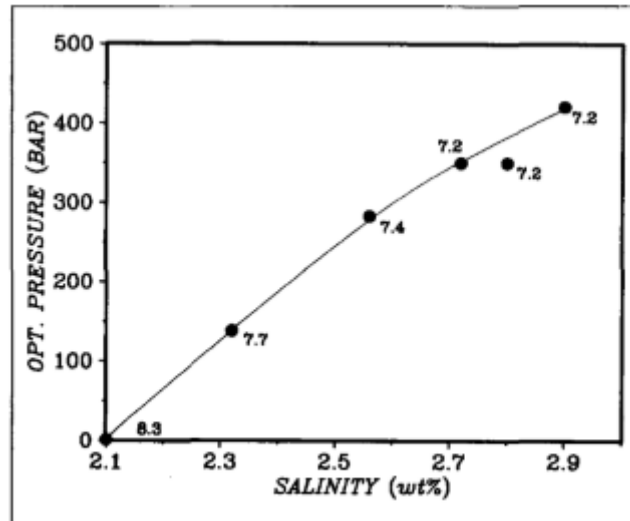


**Figure 6.8:** Optimum pressure as a function of salinity. The numbers in each point refers to the solubilisation parameter (Skauge & Fotland, 1990).

### 6.3.3 Cosurfactants

Cosurfactants are added to minimize the formation of gels, liquid crystals, emulsion of polymer-rich phase separating from the surfactant solution, to lower the equilibrium time and to reduce microemulsion viscosity (Sheng, 2011). They also adjust the surfactant pseudocomponent so make sure that the change of a Winsor type I to a Winsor type II microemulsion occurs at different salinities (Lake, 1989). However, the addition of a cosurfactant reduces the effect of the surfactant.

By adding a water-soluble surfactant as a tertiary amyl alcohol, a second petroleum sulphate, n-butanol or other light molecular weight alcohols will make the surfactant more water-soluble. While an addition of higher molecular weight alcohols increases the surfactant's oil solubility (Lake, 1989).

Larry Britton stated in 2008 that alcohols alone cannot function as surfactants. Short-tailed alcohols with only a few carbon atoms cannot form micelles because they are too short. The alcohols should have at least eight to ten carbons. However, even with long chains of carbons, the OH group is not polar enough to be a good hydrophilic group (Sheng, 2011).

### 6.3.4 Oil

The oil composition affects how good oil is as a solvent for the surfactant. If the oil is made more polar, it will act as a better solvent and make the transition from Winsor type I to Winsor type II occur faster. The specific gravity also affects the surfactant oil solubility. The high specific gravity crudes have a high content of organic acids that lowers the solubility (Lake, 1989).

To find the best surfactant for the specific crude oil, time-consuming test of different surfactants in the refined oil has to be done. Cayias et. al found a relating between the alkane carbon number (ACN) in refined oils with the equivalent alkane carbon number (EACN) for crudes (Cayias, et al., 1977). By testing different surfactants with the synthetic oil, the surfactant that gives the lowest IFT will also be the best surfactant for the crude (Sheng, 2011).

### 6.3.5 Effect of divalent ions

Interaction between divalent ions and surfactants changes the optimal salinity for the surfactant (Hirasaki, et al., 1983). According to Sheng, found Pope and Baviere in 1991 in a test with surfactant, oil, brine that with a NaCl brine, the electrolyte is partially excluded from the micelle. They observed the opposite trend with CaCl<sub>2</sub> brine (Sheng, 2011). Because of the strong connection of anionic surfactant and divalent ions, the surfactant concentration will decrease due to the surfactants will mix with the brine. A decrease in the surfactant concentration reduces the interaction between the interfacial region and the brine, and the optimal salinity decreases (Sheng, 2010).

### 6.3.6 Surfactant concentration and surfactant structure

Until the critical micelle concentration, an increase in the surfactant concentration leads to a decrease in the interfacial tension. A further addition of surfactant will not affect the IFT (Sheng, 2011). The surfactants will just form more micelles as Figure 6.9 shows. In surfactant flooding, where the purpose is to lower the IFT and/or alter the wettability by microemulsion or micellar flooding, a high concentration of surfactant is applied. The surfactant concentration is normally between 1wt% to 10wt% (Al-Yousef, et al., 2013).

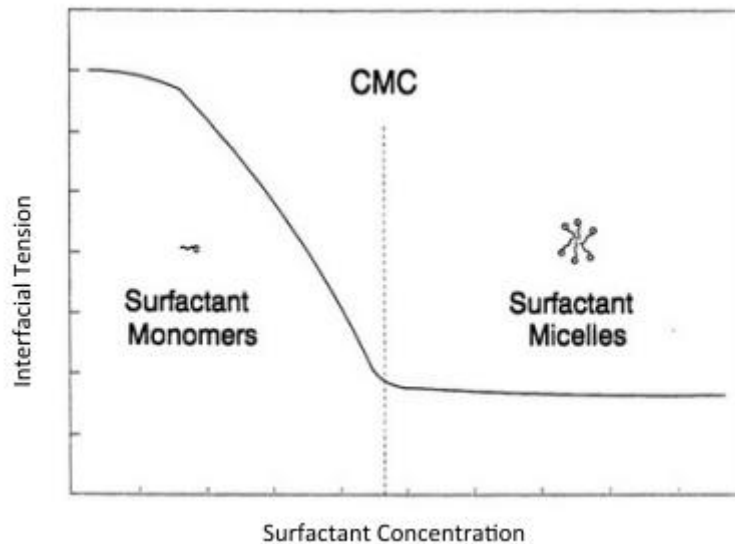


**Figure 6.9:** Surfactant concentration as a function of interfacial tension (Schramm, 1992).

The selection of a surfactant is based upon the desirable surfactant structure. Levitt et. al stated in 2009 that recent advances in the research and development of surfactants as the understanding the relationship between structure and performance, have made it possible to quickly identify promising high-performance surfactants for EOR. Several tests are conducted to obtain the favourable surfactant. A phase behaviour-screening test will quickly identify a favourable surfactant formulation. A salinity scan can revile equilibrium time, viscosity of the microemulsion, solubilisation parameters, and IFT. To tailor the surfactants for the particular case, cosurfactants and cosolvent are added (Levitt, et al., 2009).

Extensive research on surfactants points out a clear relationship between surfactant structure, fluid properties and EOR related performance (Levitt, et al., 2009). An increasing hydrophobic length of the surfactant's tail causes the solubilisation parameters to increase, while the optimal salinity decreases. Weakly hydrophobic functional groups as propylene oxide (PO) have interface affinity and can wider the ultra-low IFT region. PO decreases the optimal salinity and the surfactant becomes more calcium-tolerant. Because of these properties PO and also ethylene oxide (EO), which has similar effects, can be added to tailor the surfactant to the crude oil, temperature and the salinity. PO and EO are inexpensive chemicals and are practical to use in improving the performance (Sheng, 2011).

## 6.5 Capillary number

The capillary number is a ratio of the viscous force to capillary force (Sheng, 2013):

$$N_c = \frac{\mu v}{\sigma} \quad (6.4)$$

Where:

$\mu$  is the displacing fluid viscosity,

$v$  is the Darcy velocity of the displacing fluid,

$\sigma$  is the IFT between the displacing fluid and displaced fluid.

From equation 6.4 it can easily be seen that a high capillary number implies low IFT. When surfactants are injected in a reservoir, the purpose is to lower the interfacial tension between the immiscible fluids oil and water by making a microemulsion where oil and water are bound together with the surface acting agents. Hence the IFT is reduced and accordingly also the capillary pressure is reduced. Then more residual oil can be produced. Figure 6.10 shows an example on how an increase capillary number gives a lower residual saturation.

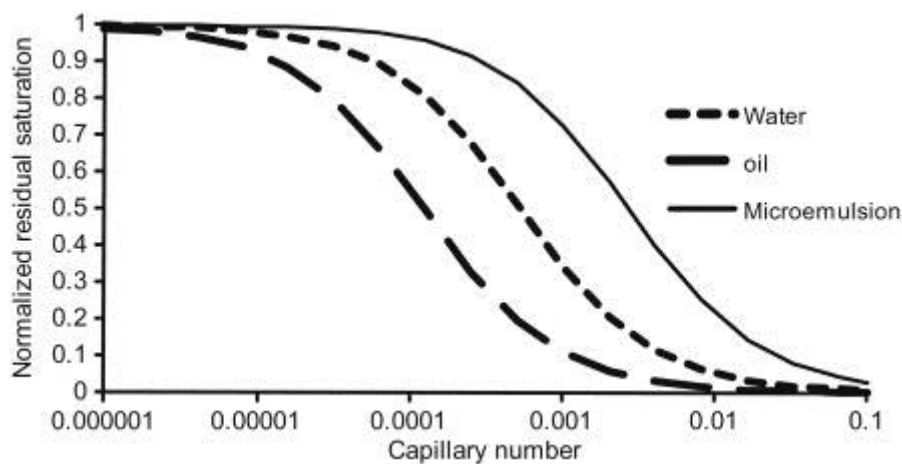


**Figure 6.10:** The relationship between capillary number and residual saturation (Sheng, 2013).

## 6.6 Wettability Alteration

Most carbonates are oil-wet or mixed wet (Hirasaki & Zhang, 2004). Surfactants can be used to alter the wettability to more favourable wetting condition for spontaneous imbibition. Cationic and non-ionic are mostly used for this purpose, but Hirasaki and Zhang presented in 2004 promising results for injection of anionic surfactants with salts.

In carbonates are often organic carboxylates from the crude oil adsorbed on the rock surface. The cationics are injected into the reservoir to form ion-pairs with the adsorbed organic carboxylates and stabilise them into the crude oil and alter the wettability to water-wet. A schematic presentation of the process is given in Figure 6.11. The cations ( $R-N^+(CH_3)_3$ ) desorb the organic carboxylates ( $-COO^-$ ) from the carbonate surface by formation of ion-pairs. Since the hydrophilic part is used in ion-pair formation with the carboxylates, is only the hydrophobic part of the surfactant free, and therefore is the ion-pair complex only soluble in miscelles and in oil (Sheng, 2013).

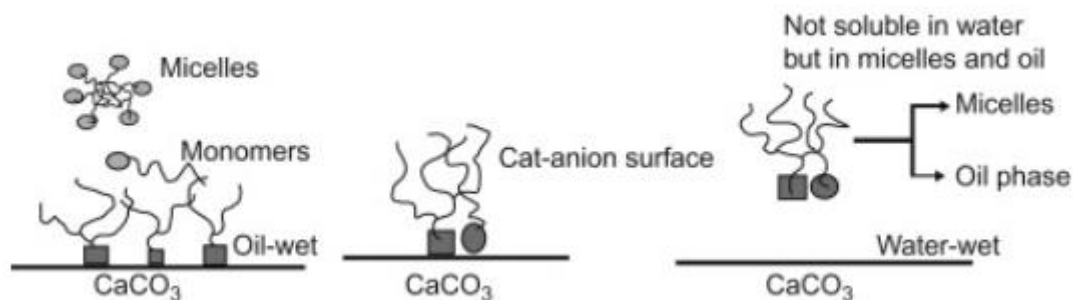


**Figure 6.11:** Wettability alteration from oil-wet to water-wet mechanism. Large squares represent carboxylate groups ( $COO^-$ ), small squares represent polar components, and the circles represent cationic ammonium group ( $N^+(CH_3)_3$ ) (Austad & Standnes, 2003).

Anionic surfactants are not able to desorb organic carboxylates and form ion-pairs as the cationics. However, when an Ethoxylated sulfonate with high EO number is used, the anionic surfactant may form a water-wet bilayer between the oil-wet chalk surface and the oil. The EO part of the surfactant is adsorbed on the rock surface with the hydrophobic tail, while the hydrophilic head makes a film of a water-wet layer on top of the rock surface. This way a weak capillary force is created during imbibition (Sheng, 2013). These EO-anionic surfactants are not able to form a permanent alteration of the wettability, because the bonds between the hydrophobic rock surface and the hydrophobic tail of the surfactant is probably fully reversible.

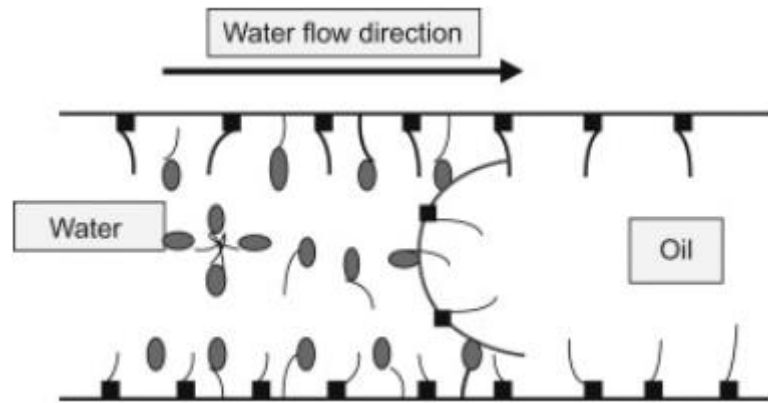


**Figure 6.12:** Formation of a water-wet bilayer. The squares represent carboxylates and the eclipses represents EO-sulfonates (Austad & Standnes, 2003).

Hirasaki and Zheng injected in 2004  $\text{Na}_2\text{CO}_2$  with the surfactants with the purpose to reduce the anionic surfactant adsorption on carbonate rock surface. The  $\text{CO}_3^{2-}$  and  $\text{HCO}_3^-$  components from the salt alter the rock surface to be negatively charge, and hence less of the anionic surfactants are adsorbed. This maintains the surfactant concentration, and the surfactants can react on the interface between oil and water and reduce the IFT. This way is the capillary forces reduced and the gravity force is increased and is the main oil recovery mechanism in the drainage. It is important for the surfactant to reduce the IFT so that the gravity forces overcome the capillary forces and can invade small pores and displace the oil upwards in the matrix.

## 6.7 Surfactant-Polymer flooding

Polymers are often injected with surfactants in order to reduce costs, reduce surfactant adsorption, and increase the surfactants performance. The following injection pattern is conventionally used:

- Preflush, to form the best effective IFT reduction condition for the surfactant
- Surfactant Slug injection, to reduce IFT and recovery residual oil.
- Polymer Slug Injection, to improve sweep efficiency in the reservoir.
- Taper- injection of polymer slug with decreasing polymer concentration from front to back to mitigate the effect of adverse mobility ratio between polymer slug and the chase water.
- Chase water is injected with the purpose to move the SP composition deep into the reservoir (Zolutukhin & Ursin, 2000).

Polymer flooding is the only chemical- EOR technique that is well-established for use in fields. Polymers are injected with to increase the water viscosity with the purpose to decrease the displacing fluid's mobility (Zolutukhin & Ursin, 2000). An increase in the mobility (relative permeability and/or viscosity) of the displaced fluid, oil, is not feasible expect with heat, therefore are polymers injected for mobility control of the flowing fluid fronts (Sheng, 2011).

Polymers are very suitable for injection in heterogeneous reservoirs with large permeability differences between layers. The polymers are injected to reduce the effective permeability of the displacing fluid in high permeable zones (Zolutukhin & Ursin, 2000).

Polymers are formed by long chains of monomers bounded by covalent bonds. There are several factors affecting their performance. The most important factors are concentration of polymers, salinity and surfactant and alkaline concentration in SP and ASP floods. Polymers can as surfactants, become adsorbed by the rock surface, and hence reduce the polymer concentration. Mechanical entrapment in pores and local accumulation of polymer molecules are other retention mechanism that affects the polymerflood performance.

Entrapment of polymers leads to a dilution of the polymer solution, and the mobility control can be drastically reduced or destroyed. The adsorption of polymers on the rock surface may decrease the rock permeability which contributes to a further reduction of mobility of the

polymer front and the chase water which may lead to better sweep (Zolutukhin & Ursin, 2000).

Surfactant-polymer flooding has advantages compared to a single surfactant flood. As explained in chapter 6.3.6, the surfactant concentration in the flood, should be the critical miscelle concentration. At CMC the concentration of monomers are large enough to reduce IFT as much as possible by microemulsion. An addition of polymers can reduce the point of CMC, therefore less expensive surfactants are required for an effective IFT reduction (Austad, et al., 1994). The reduction of surfactant concentration required can be by a factor of 10, or even higher. Polymers bind the water, so that surfactant monomers are free to be more active in the IFT reduction (Zolutukhin & Ursin, 2000).

The polymers and surfactant chosen for injection must be compatible and should be carefully chosen. If there are strong chemical associations between the polymers and surfactants, they can form chemical interaction and reduce the performance (Figure 6.13).

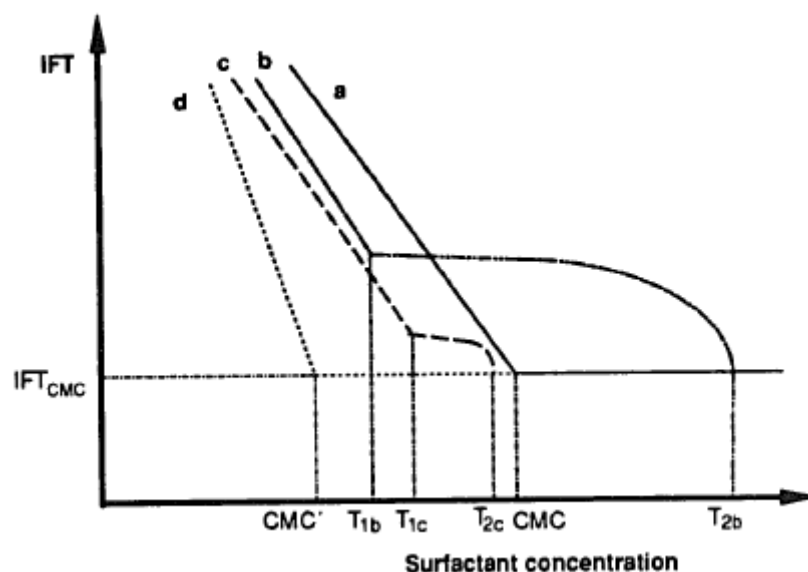


Figure 6.13: The relationship between surfactant concentration and IFT for the cases with a) without polymers, b) strong association between surfactants and polymers, c) low association between surfactant and polymers, d) no association between surfactants and polymers. (Austad & Standnes, 2003)



## 7. Economics of Chemical EOR

With chemical EOR come a lot of extra costs. Some of the chemicals are very expensive, some even unconventional, but the extra costs related to facility requirement, transportation of chemicals and environmental demands, are just as important to include. For an offshore field the expenses can soon overcome the conventional limit. Some of the challenges that stand out for offshore field are listed below.

- Remote locations
- Poor weather
- Expensive wells and large well spacing
- Space and weight limitation on the deck
- Seawater as the only available injection-water source
- Limited disposal options. (Raney, et al., 2012).

Offshore fields have different facility challenges depending on how far they are from shore. For near-shore field, will the extra costs related to chemical EOR not be as extensive as for deep-water projects. Those advantages are related to well costs, disposal costs and storage costs (Raney, et al., 2012); (Wyatt, et al., 2008). Figure 7.1 presents an overview of typical deep-water chemical EOR facilities.

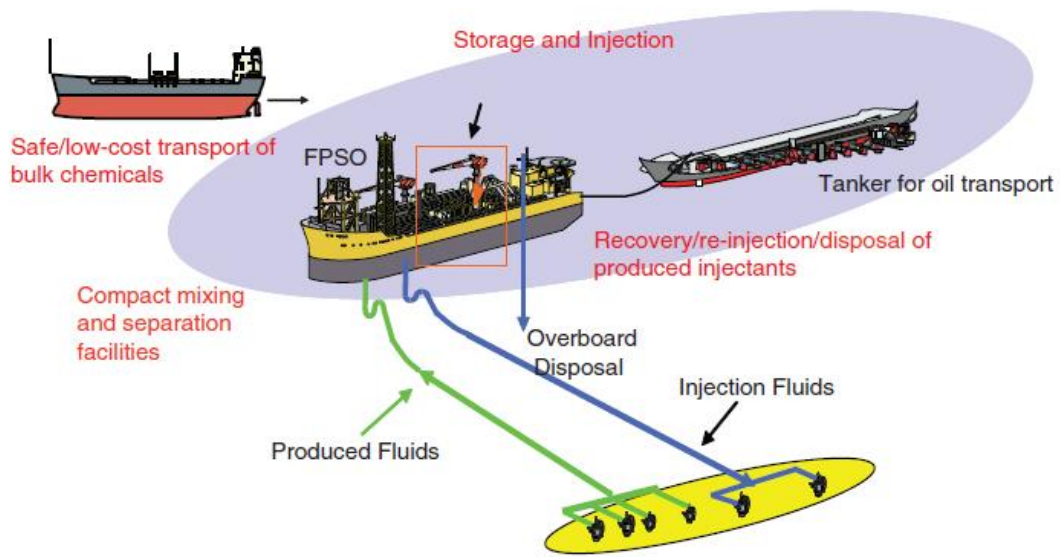


**Figure 7.1:** Schematic of a typical deep-water chemical-EOR project (Raney, et al., 2012).

The effects of the challenges listed on the previous page are subsurface efficiency, logistics, injection, production and environmental. Since saltwater is the only available injection fluid, must the chemicals be able to handle the salinity. As explained in chapter 6 are surfactants strongly affected by salinity. To get an effective surfactant flood, a desalinating may be done with nanofiltration and reverse osmosis (Raney, et al., 2012). Alternatively salinity tolerant surfactant may be used.

The biggest problems related to offshore chemical EOR projects are the logistics. Logistics is related to the implementation of the project. The costs are linked to available surfactants for the offshore environment, the large storage requirements, and the special equipment required storing high-active chemicals, separating oil and water from the microemulsion phase, recycle and disposal of chemicals and the distribution of the chemical solution over long distances. The large storage capacity requirement is related to the importance of maintain the surfactant concentration in the reservoir. Therefore must there always be a sufficient amount of chemicals available. In offshore fields, the supply from onshore may be delayed because of the weather. Because of these risks, it is normal to store chemicals for 21 days in case of a supply stop. For a field with a surfactant injection rate of  $30\,000\text{m}^3/\text{day}$ , a storage capacity of 10500tonnes for 21 days is required (Raney, et al., 2012).

Wyatt et.al presented in 2008 a paper with estimations of costs related to different chemical EOR projects. The costs include chemical costs and a total facility costs estimation for different process. Figure 7.2 gives the historical costs for some chemicals included surfactants, and crude oil from 1985 to 2007. The facility cost Wyatt et. al presents are listed in Table 7.1 below. An overview of chemical costs is given in Table 7.2. The facility costs are estimated for a project size of 10.000MBBL PV with a run for 10 years with a water injection rate of 5000bbl/day.

**Table 7.1:** Facility costs for a project size of 10.000MBBL PV.

| <b>Chemical EOR process</b>                | <b>Facility costs \$</b> |
|--|--------------------------|
| Micellar- Polymer                          | 5.500.000                |
| Surfactant- Polymer                        | 1.500.000                |
| Alkaline-Polymer, fresh water              | 2.800.000                |
| Alkaline- Polymer, brine                   | 3.200.000                |
| Alkaline- Surfactant- Polymer, fresh water | 3.000.000                |
| Alkaline- Surfactant- Polymer, brine       | 3.400.000                |

**Table 7.2:** Chemical costs.

| <b>Chemical</b> | <b>Costs \$/kg</b> |
|-----------------|--------------------|
| Surfactant      | 4,08               |
| Co-surfactant   | 1,54               |
| Polymer         | 2,65               |
| Caustic soda    | 1,01               |
| Soda ash        | 0,24               |

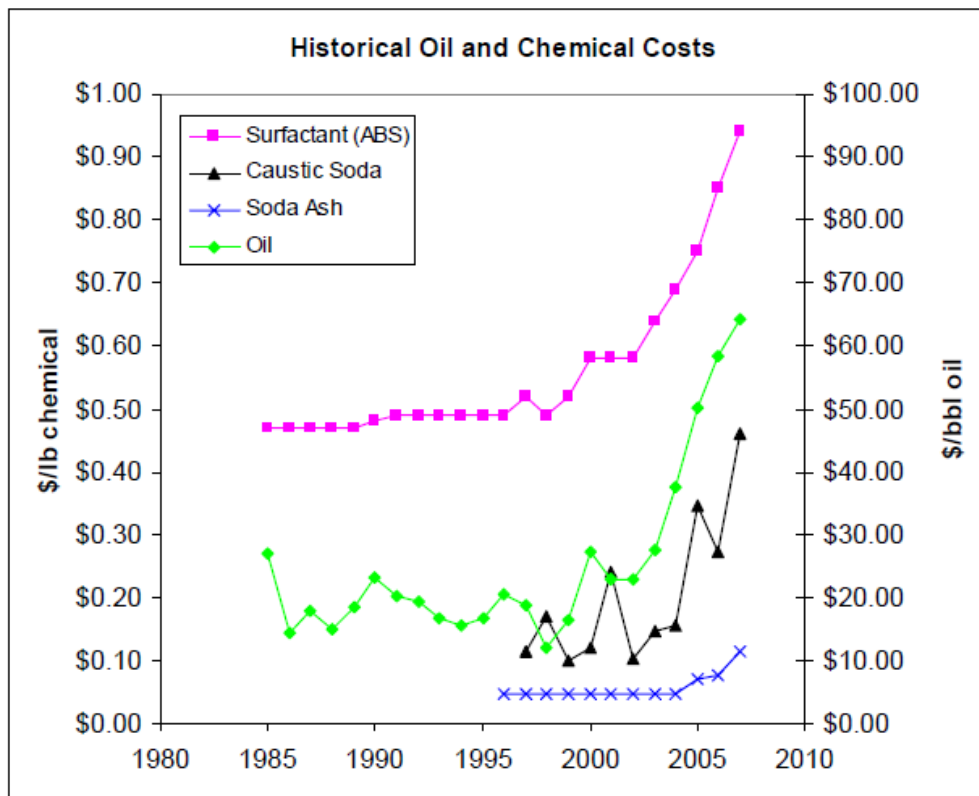


Figure 7.2: Historical crude oil and chemical costs (Wyatt, et al., 2008).

## 8. Numerical Simulation

This chapter gives an insight in the keywords used in the surfactant model (Table 8.1), and an overview of input data, assumptions and the model building process.

### 8.1 Keywords for the surfactant model

**Table 8.1** Specific keywords for the ECLIPSE surfactant model (Schlumberger, 2011a) and (Schlumberger, 2011b).

| <b>Keyword</b> | <b>Description</b>                | <b>Notes</b>                    |
|----------------|-----------------------------------|---------------------------------|
| SURFACT        | Model initialisation              | Obligatory                      |
| SURFST         | IFT data                          | Obligatory                      |
| SURFVISC       | Viscosity modifier                | Obligatory                      |
| SURFCAPD       | Capillary de-saturation           | Obligatory                      |
| SURFADS        | Surfactant adsorption             | Optional                        |
| SURFROCK       | Rock properties                   | Obligatory when SURFADS is used |
| SURFNUM        | Grid region specification         | Obligatory                      |
| WSURFACT       | Injected surfactant concentration | Optional                        |

## **SURFACT**

This keyword starts the surfactant model in ECLIPSE and is listed in the start of the RUNSPEC section.

## **SURFST**

Water/oil surface tension versus surfactant concentration. This keyword gives the IFT between oil and water as a function of surfactant concentration. The keyword is supplied with two tables; the first is for surfactant concentration in  $\text{kg/m}^3$  and the other for corresponding water-oil surface tension in N/m.

## **SURFVISC**

This keyword calculates the water-surfactant solution viscosity,  $\mu_{ws}$  by applying equation (8.1).

(8.1)

$$\mu_{ws}(C_{surf}, P) = \mu_w(P) \frac{\mu_s(C_{surf})}{\mu_w(P_{ref})}$$

## **SURFCAPD**

This keyword gives the capillary de-saturation function that describes the transition between immiscible condition and miscible condition for surfactant concentrations above the critical micelle concentration. The keyword contains two columns of data, where the first column is the logarithmic value of the capillary number and the second column is the miscibility factor,  $m$ . The miscibility factor ranges from 0 to 1, where 0 is immiscible conditions and 1 is fully miscible conditions.

## **SURFADS**

The SURFADS keyword gives the quantity of how much surfactant is adsorbed by the rock. The adsorption is a function of the surrounding surfactant concentration and the rock density and is calculated by equation (8.2).

(8.2)

$$\text{Mass of adsorbed surfactant} = PORV * \frac{1 - \phi}{\phi} * MD * CA(C_{surf})$$

PORV = Pore volume of the cell

$\phi$  = porosity

MD = Mass density of rock

CA( $C_{surf}$ ) = adsorption isotherm as a function of local surfactant concentration in solution.

## **SURFROCK**

This keyword specifies the surfactant-rock properties. When surfactant is adsorbed at the rock surface, some of the adsorbed surfactant can go back into the solution, this mechanism is called desorption. SURFROCK contains two items, where the first item is the adsorption index which states if the surfactant adsorbed can be desorbed or not. If value 1 is selected adsorbed surfactants can go back into the solution. If value 2 is selected, no surfactant desorption may occur. The second item of the keyword is the mass density of rock in kg/m<sup>3</sup>. The properties tabulated in this keyword are used in the different grid regions defined in keyword SURFNUM.

## **SURFNUM**

This keyword specifies in which region a full miscibility between water and oil may occur. In the RUNSPEC section is TABDIMS applied to control the number of tabulated data that is inserted to the model. The first item in TABDIMS determines how many saturation tables the model will apply. The SATNUM keyword is used to specify the immiscible saturation functions.

## **WSURFACT**

This keyword specifies which wells are injecting surfactants, and the surfactant concentration in the injected solution. The first item of the input data is the name of the well selected for surfactant injection. The well is chosen from the wells defined in WELSPECS and COMPDATA keywords. The second item is the surfactant concentration in the injection steam given in  $\text{kg}/\text{Sm}^3$ . If the surfactant injection is not to start before n-timestep of production, the keyword should be entered after the first timestep keyword in the SCHEDULE section.



### 8.2 The Basecase Model Input Data

The simulation model is built as a single block with the grid dimensions 20x20x30 in ECLIPSE. The 15<sup>th</sup> layer in z-direction is a fracture. The model is a black oil model solved with IMPES and contains one producer and one injector that are placed on the boundaries at each side of the model (Figure 8.1). The model is simulated for pressures above bubble point pressure for the oil and includes two fluid phases, oil and water. Fracture and matrix are induced with different permeability and porosity properties and the model act as a dual porosity/dual permeability model. All the properties used in the model are presented in the following subchapters.

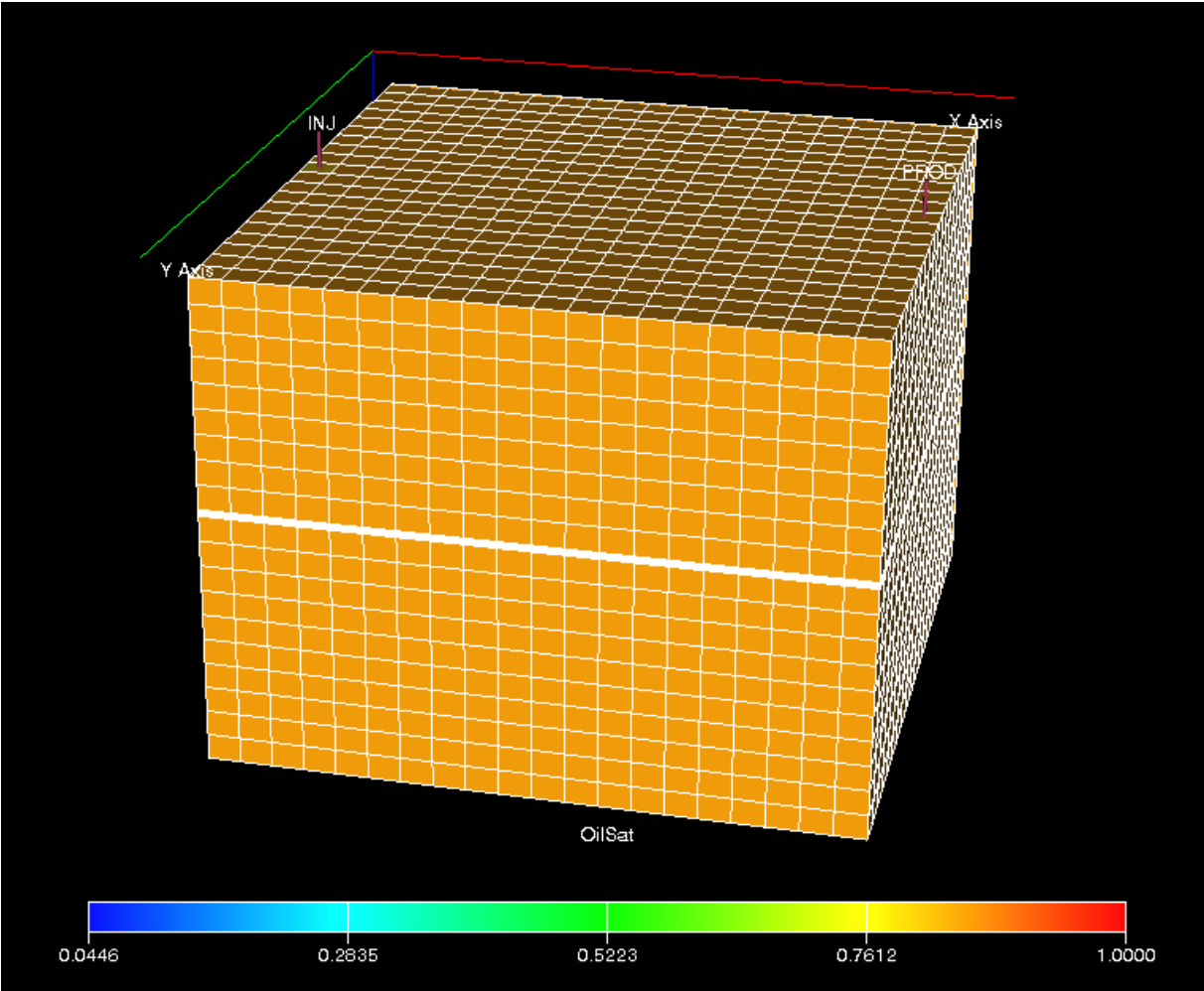


Figure 8.1: Initial oil saturation in the model.

Fluid parameters used in the model are listed in table 8.2.

**Table 8.2:** Fluid parameters

| Fluid parameters |                          |
|------------------|--------------------------|
| $S_{w,i}$        | 0,15                     |
| $\rho_{w,s,c}$   | 997,35 kg/m <sup>3</sup> |
| $\rho_{o,s,c}$   | 722,2 kg/m <sup>3</sup>  |
| $\mu_{w,ref}$    | 0,61cp                   |
| Pref             | 1,014bar                 |

The fluid viscosity changes with pressure. The oil viscosity changes are presented in Figure 8.2.

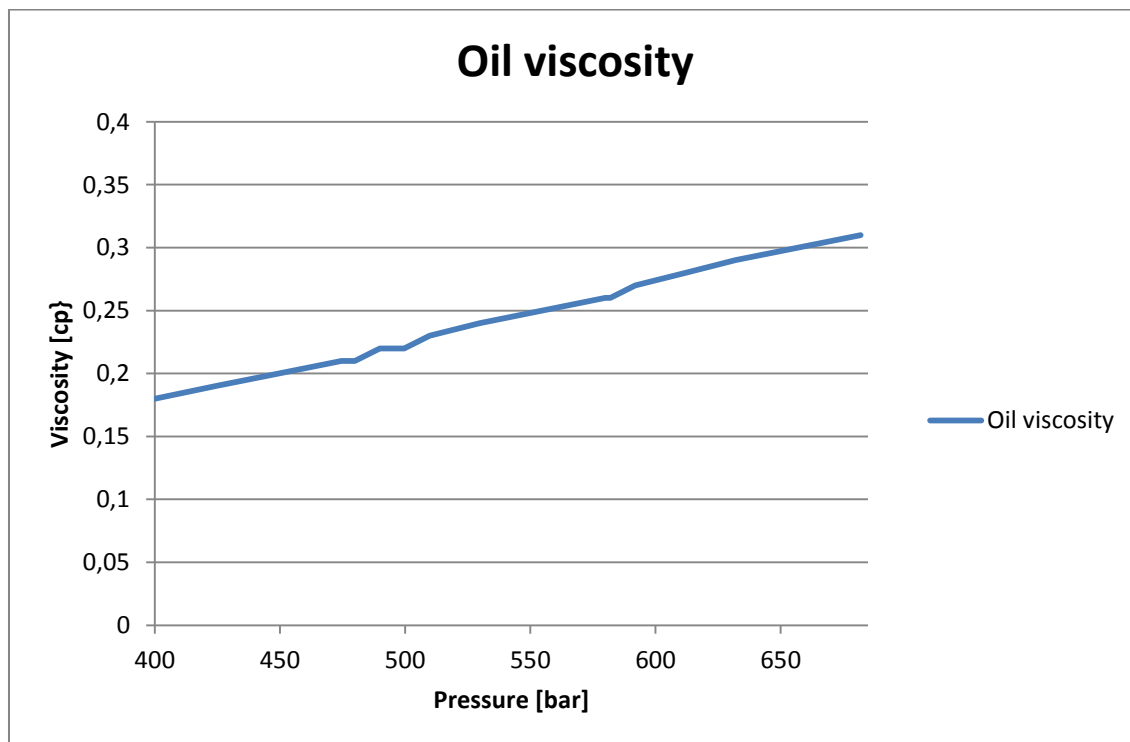


**Figure 8.2:** Oil viscosity plotted against pressure.

### 8.2.1 PVT

Total E&P Norway provided PVT data for the model. The PVT data is for live-oil. However, since the model shall only be a two-phase system is only the PVT data above bubblepoint pressure is included in the model. To avoid gas segregation and three phase flow, a minimum bottomhole pressure equal to bubblepoint pressure was set as restriction in the producing well in the model. The initial reservoir pressure given in Total's dataset is below bubblepoint pressure. To overcome the producer restriction, was initial reservoir pressure and reference depth chosen from Linda Riise's master thesis 2005 (Riise, 2005). The thesis is an evaluation of the secondary depletion in the Ekofisk field. Three case studies were conducted, where the first case was a single block fracture model, similar to the case in this study.

### 8.2.2 Matrix properties

The matrix properties are taken from Linda Riis' master thesis 2005 (Riise, 2005) and presented in Table 8.3.

**Table 8.3:** Matrix properties for the model

| <b>Property</b>                    | <b>Value</b>  |
|------------------------------------|---------------|
| Initial pressure (z=3133m)         | 489,73 [bars] |
| Porosity                           | 0,4           |
| Horizontal permeability, $k_x=k_y$ | 1mD           |
| Vertical permeability, $k_z$       | 1mD           |
| Initial water saturation           | 0,15          |
| Initial oil saturation             | 0,85          |

The oil-water relative permeability curve for the matrix is presented in Figure 8.3.

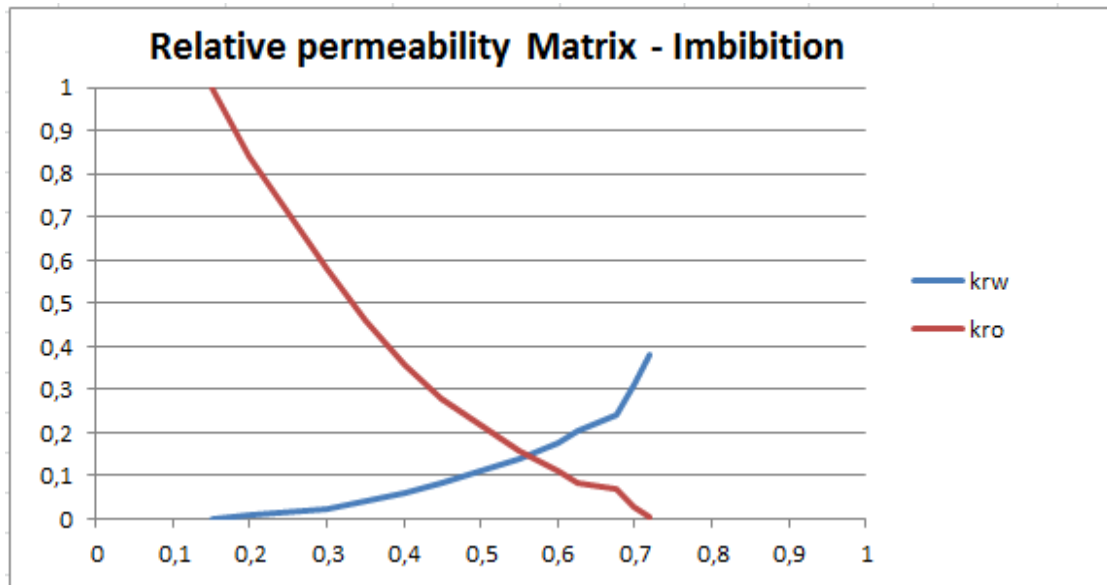


**Figure 8.3:** Relative permeability curves for water and oil in the matrix.

Figure 8.4 presents the corresponding water-oil capillary pressure curve. As the curve illustrates, the spontaneous imbibition will stop at  $S_w=0,6$ . However, with forced imbibition the saturation can increase to 0.75.

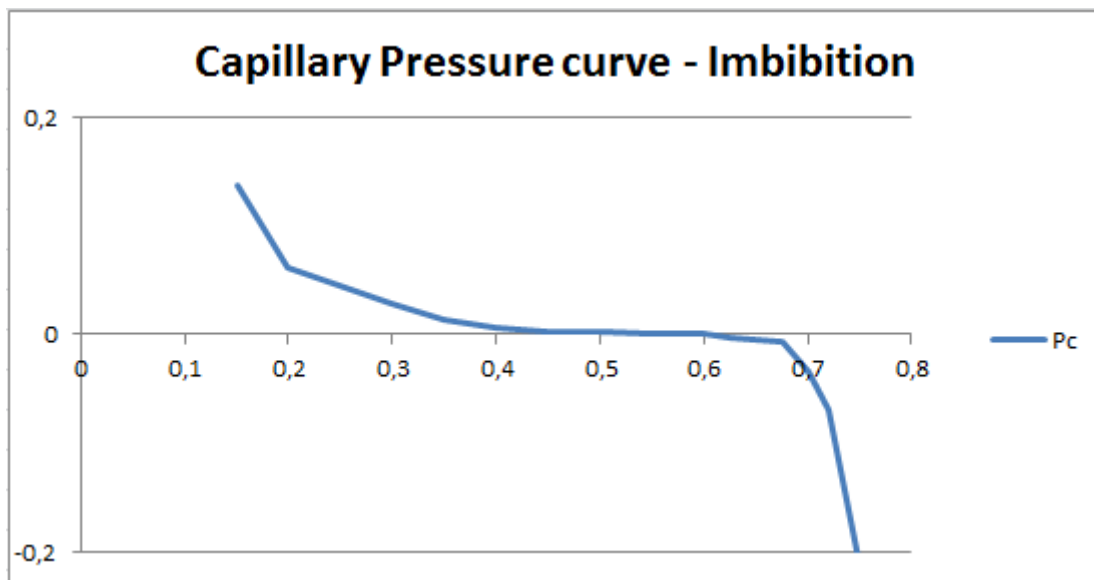


**Figure 8.4:** Water-oil capillary pressure curve for the matrix.

### 8.2.3 Fracture properties

The fracture properties are listed in Table 8.4 and the relative permeability curves for oil and water are presented in Figure 8.5.

**Table 8.4:** Fracture properties for the model.

| Property                           | Value         |
|------------------------------------|---------------|
| Initial pressure (z=3133.34)       | 489,73 [bars] |
| Porosity                           | 1,0           |
| Porosity in surfactant model       | 0,95          |
| Horizontal permeability, $k_x=k_y$ | 90mD          |
| Vertical permeability, $k_z$       | 90mD          |
| Initial oil saturation             | 1,0           |
| Irreducible water saturation       | 0,0           |

For the case with only water injection is the porosity set to be 1,0 in the fracture. ECLIPSE demands that the porosity must be reduced to less than 1,0 for the case with surfactant injection, and is therefore set to be 0,95.

Actual fracture permeability is much larger than 90mD which is used in the model. The fracture permeability is approximately 1000mD, but a much lower permeability is used to avoid unstable simulation runs. The conductivity for the fracture is maintained with the wide fracture. The fracture width is set to be 1cm. A realistic fracture width is 10-50microns (Chilingarian, et al., 1996).

The fracture is considered to act as a very large pore, and there is accordingly no capillary pressure between water and oil.

The relative permeability curves for oil and gas are linear in the fracture.

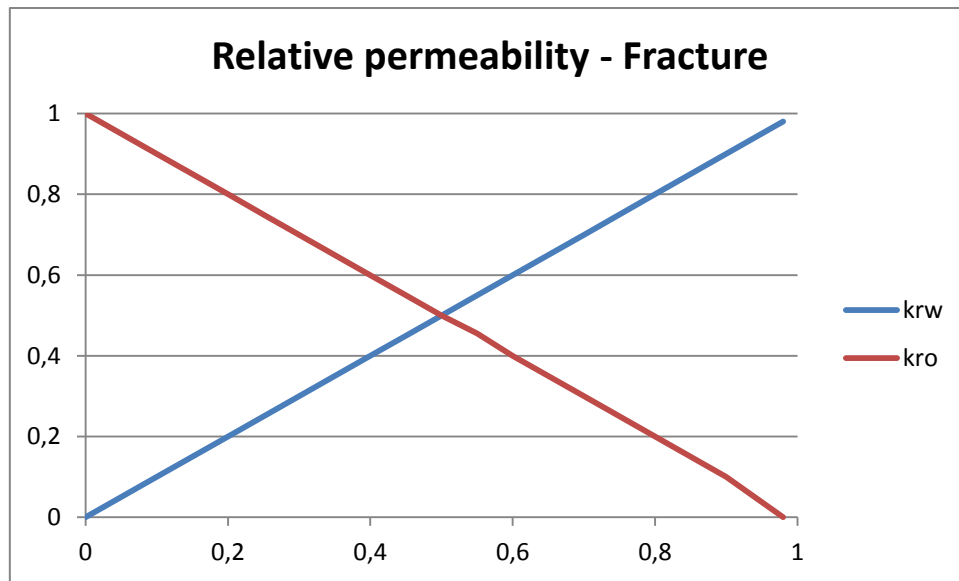


**Figure 8.5:** Relative permeability curves for water and oil in the fracture.

### 8.2.4 Wells

The model contains two wells. The well placement and restrictions are presented in Table 8.5.

**Table 8.5:** Well properties.

| Well type | Max. injection rate<br>[Sm <sup>3</sup> /day] | Max. BHP<br>[bars] | Min. BHP<br>[bars] | Perforations<br>(i,j,k <sub>1</sub> -k <sub>2</sub> ) |
|-----------|---|--------------------|--------------------|---|
| Injector  | 50  | 600                | X                  | (1,10,1-30)   |
| Producer  | X   | X                  | 400                | (20, 10, 1-30)  |

### 8.3 The Surfactant model input data

The surfactant model is developed from the waterflooding model presented in the previous chapter 8.2. The ECLIPSE surfactant keywords that are applied in this model are described in chapter 8.1. The surfactant dataset is taken from Feng et.al (2011) and is presented in table 8.6-8.9. (Feng, et al., 2011)

**Table 8.6:** Interfacial tension between oil and water at different surfactant concentrations.

|   |      |        |         |         |         |         |
|---|------|--------|---------|---------|---------|---------|
| <b>Surfactant concentration [kg/m3]</b> | 0    | 0,1    | 0,5     | 1       | 30      | 100     |
| <b>Interfacial tension [N/m]</b>        | 0,05 | 0,0005 | 1,0E-05 | 1,0E-06 | 1,0E-06 | 1,0E-06 |

**Table 8.7:** Water viscosity at different surfactant concentrations.

|   |      |     |     |
|---|------|-----|-----|
| <b>Surfactant Concentration [kg/m3]</b> | 0    | 30  | 100 |
| <b>Water viscosity [mPa s]</b>          | 0,61 | 0,8 | 1   |

**Table 8.8:** Miscibility condition at different capillary numbers.

|                           |     |      |     |    |   |
|---------------------------|-----|------|-----|----|---|
| <b>Log[Nc]</b>            | -10 | -5,5 | -4  | -3 | 2 |
| <b>Miscibility factor</b> | 0   | 0    | 0,5 | 1  | 1 |

**Table 8.9:** Surfactant adsorption at different surfactant concentrations.

|   |   |        |        |        |
|---|---|--------|--------|--------|
| <b>Surfactant concentration [kg/m3]</b> | 0 | 1      | 30     | 100    |
| <b>Surfactant adsorption [kg/kg]</b>    | 0 | 0,0005 | 0,0005 | 0,0005 |

As explained in the surfactant keyword chapter, when surfactant adsorption is included in the model, then the rock density must be specified in addition. For a Chalk found in Balmoral outcrop in Great Britain, the rock density is 2530kg/m<sup>3</sup> (Manger, 1963). In this model, it is assumed that the rock density is the same as for the Balmoral chalk.

A third saturation table is implemented in the model for the miscibility case, when surfactants have made a microemulsion with oil and water. The relative permeability curves for miscible conditions are calculated using the Corey equation (2.7-2.8) and are given in Figure 8.6. The Corey curve exponent, *n*, was assumed to be 1,5 for miscible conditions. It is assumed that the capillary pressure is reduced to 0.

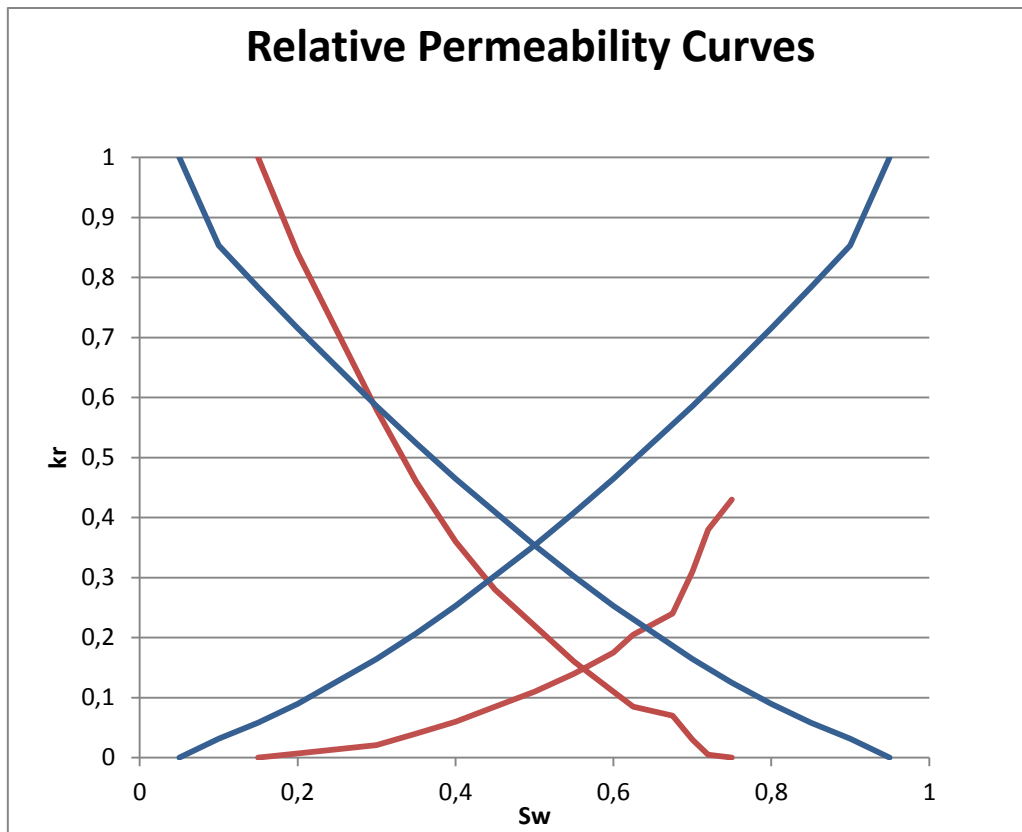


**Figure 8.6:** Relative permeability curves for miscible (blue) and immiscible (orange) conditions.



### 8.4 9Block Model with Four Fractures

A 9 block model with Four Fractures was built for further investigation of surfactants behaviour when they are injected. The model has the same dimensions as the single fracture model and most of the input data is the same. A reduction in the fracture permeability from 90mD to 50mD was done. The fracture permeability was set to 50md after trial and failure method in the model building process. It was tried to maintain the fracture permeability of 90md from the model used for investigation in the earlier chapters, but the simulation run stopped because of convergence problems due to the large permeability differences between fracture and matrix. A finer grid refinement around the fractures was also done to make the layer thickness differences less. These alterations were done to be able to run the model in ECLIPSE. ECLIPSE had problems with the saturation calculations in the intersection between fractures. Because of these problems, also the saturation tables for fracture and miscible conditions had to be changed to avoid convergence problems. It is in this model implemented that the critical water saturation is 0,1 in the fractures, while it is zero for miscible conditions. The model is presented in Figure 8.7.

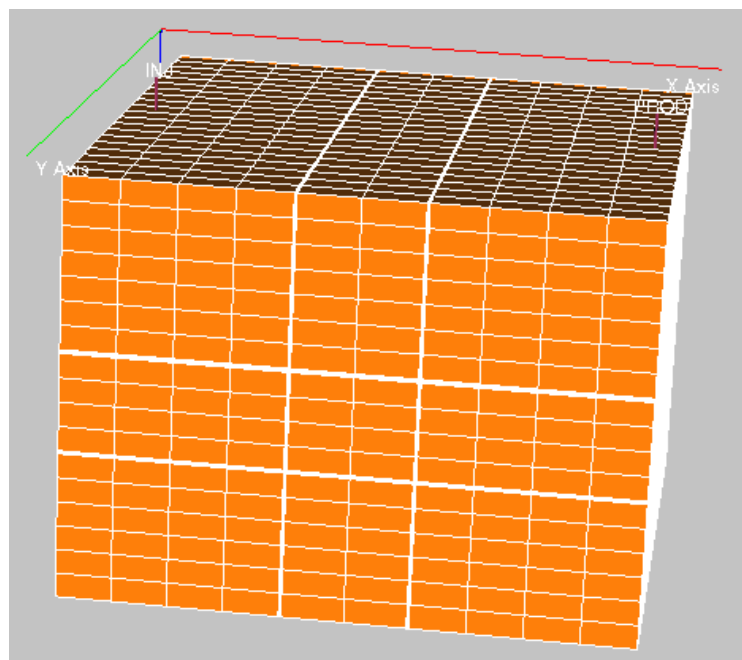


**Figure 8.7:** 9block Model with Four Fractures, initial Oil Saturation.

## 8.5 Polymer Input Data

The Input data for the polymer model was collected from Professors Jon Kleppe's webpage in the EOR folder (Kossack, 2011). Some of the data is modified for this model, as the dead pore space Table 8.11 for example. The polymer injection concentration was set to  $\text{kg}/\text{Sm}^3$ .

**Table 8.10:** Polymer Viscosity for the PLYVISC keyword.

|   |     |     |
|---|-----|-----|
| <b>Polymer Concentration [<math>\text{kg}/\text{Sm}^3</math>]</b> | 0,0 | 7,0 |
| <b>Water Viscosity Multiplier</b>                                 | 1,0 | 3,0 |

**Table 8.11:** Polymer-Rock Properties for PLYROCK keyword.

|  |         |         |         |
|--|---------|---------|---------|
| <b>Dead Pore Space</b>   | 0,04    | 0,16    | 0,16    |
| <b>Residual Resistance factor</b>                                    | 1,5     | 1,5     | 1,5     |
| <b>Mass Density [<math>\text{kg}/\text{m}^3</math>]</b>              | 2530    | 2530    | 2530    |
| <b>Adsorption Index</b>  | 2       | 2       | 2       |
| <b>Maximum Polymer Adsorption [<math>\text{kg}/\text{kg}</math>]</b> | 0,00040 | 0,00040 | 0,00040 |

**Table 8.12:** Polymer Adsorption data for the PLYADS keyword.

|  |     |         |         |
|--|-----|---------|---------|
| <b>Polymer Concentration [<math>\text{kg}/\text{Sm}^3</math>]</b>      | 0,0 | 5,0     | 7,0     |
| <b>Polymer adsorbed by the rock [<math>\text{kg}/\text{kg}</math>]</b> | 0,0 | 0,00010 | 0,00040 |

## 9. Results and Discussion

This chapter presents the simulation results. Table 9.1 gives an overview of the studies that have been done and in which chapter the results for each case are discussed. A complete evaluation of the results is given in chapter 9.13.

**Table 9.1** Overview of case studies

| <b>Case</b>  | <b>Chapter</b> |
|--|----------------|
| Surfactant flow within the model                           | 9.1            |
| Saturation and relative permeability changes               | 9.2            |
| Recovery with and without surfactants                      | 9.3            |
| Capillary pressure sensitivity                             | 9.4            |
| Fracture opening sensitivity                               | 9.5            |
| Surfactant production                                      | 9.6            |
| Surfactant adsorption                                      | 9.7            |
| Changes in input capillary number                          | 9.8            |
| Surfactant concentration in injected solution              | 9.9            |
| 9-block model with four fractures and surfactant injection | 9.10           |
| Surfactant-Polymer injection in 9-block model              | 9.11           |
| Economics  | 9.12           |
| Complete evaluation of results                             | 9.13           |

### 9.1 Surfactant flow within the model

This reservoir model contains a fracture with idealised flow conditions. It is therefore expected that the fluids will flow towards the fracture. A study of the surfactant concentration throughout the reservoir has been done at breakthrough to see how the surfactants flow in the model. All the perforations in injector and producer are open in all 30 layers. Figure 9.1 and Figure 9.2 present how the surfactants flow. Figure 9.1 is a screenshot of the 3D ECLIPSE Floviz result presenter. The figure presents the surfactant concentration in layer five, nine, eleven, fifteen (the fracture), seventeen and twenty-one. From the pictures it is clear that the surfactants move towards the fracture, since the concentration is largest in the fracture and then in the layers closest to the fracture.

Figure 9.2 is a graphic presentation of the surfactant concentration through the reservoir. The figure is a plot of surfactant concentration for seven layers vs. the distance from the injector. Figure 9.2 gives the same results as Figure 9.1, it is clear that surfactants flow towards the fracture and accumulates there and in the surrounding layers.

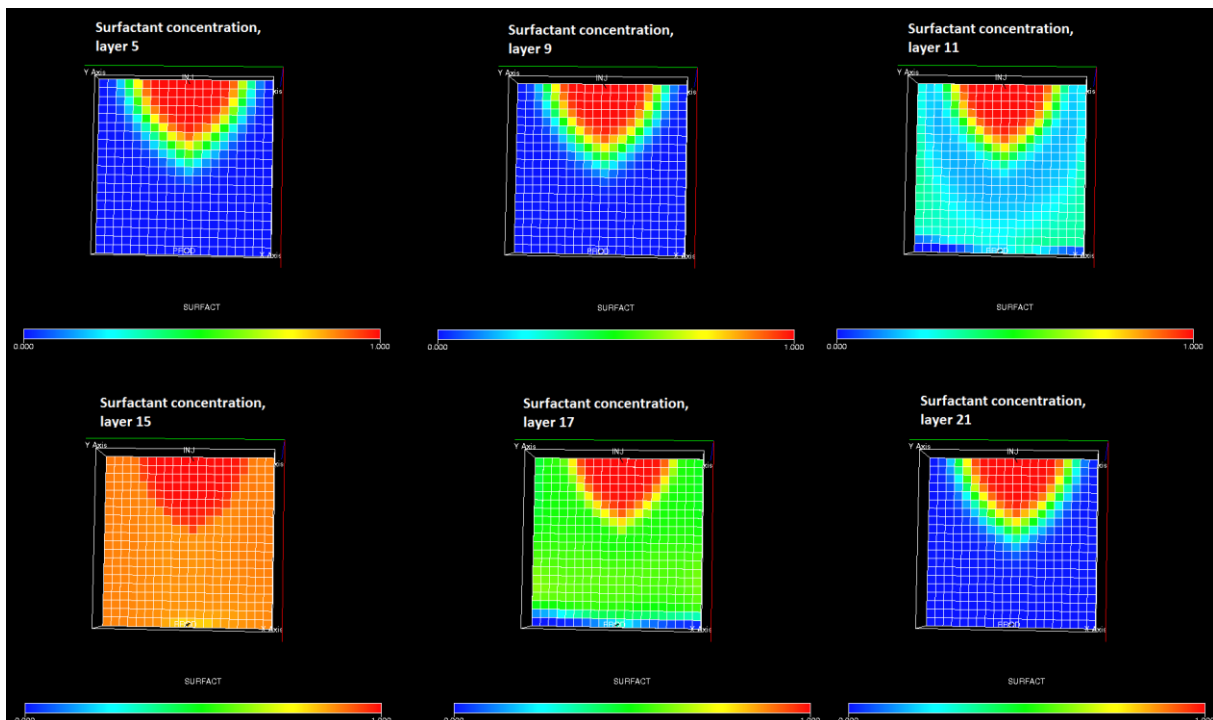


**Figure 9.1:** Surfactant concentration in six layers in various distances from the fracture at breakthrough, where blue is zero and red is  $1 \text{ kg/Sm}^3$ .

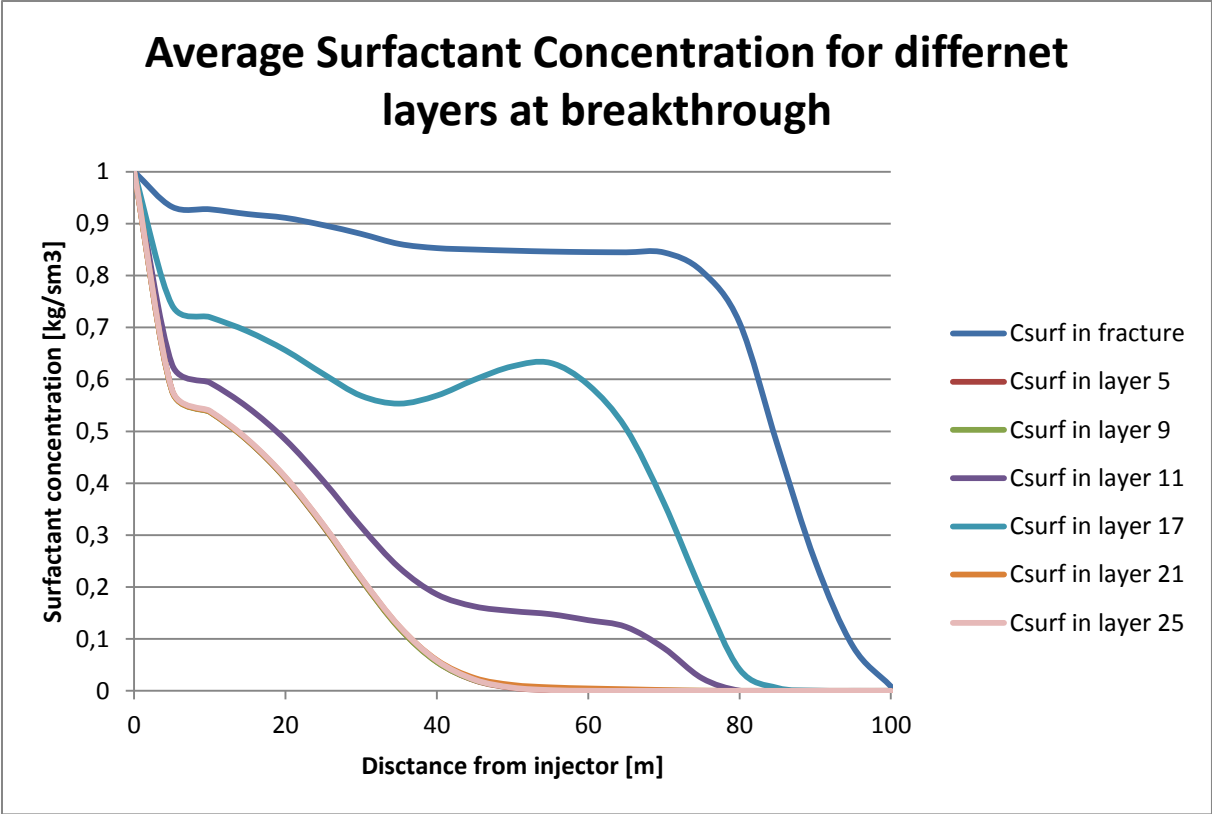
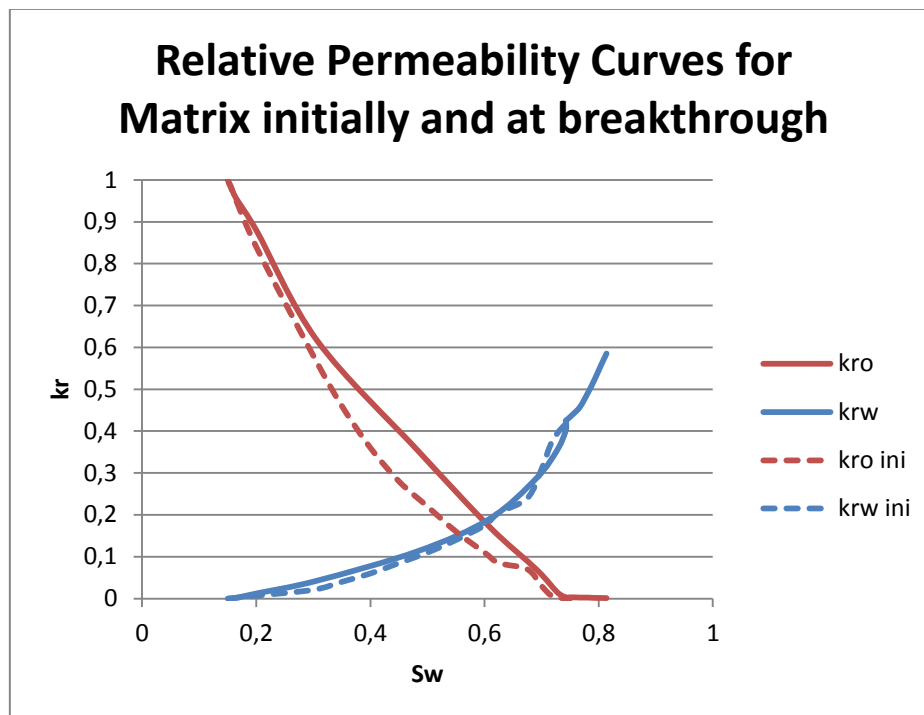


Figure 9.2: Average surfactant concentration for different layers in various distances from the fracture plotted along the length of the reservoir at breakthrough.

## 9.2 Saturation and relative permeability changes

A study of how the saturation and relative permeability curves change throughout the production time has been conducted by plotting the average relative permeability in all the matrix layer for oil and water against the average water saturation for the same layers at surfactant breakthrough time, 2500days. The data is taken for the RPT output file from ECLIPSE. Figure 9.3 shows the curves for the surfactant case, while Figure 9.4 presents the results for the waterflood case. For the waterflood case, the breakthrough is 150 days later, and the plot presented in Figure 9.4 is the relative permeability for the matrix at this timestep.

When a reservoir is flooded with surfactant, the purpose is for the surfactants to act on the fluid and rock surface to reduce the interfacial tension. When IFT is changed, the capillary pressure is also reduced. A more careful explanation on how the surfactants act is carried out in chapter 6. When the capillary pressure is reduced, fluids can more easily enter pores therefore more of the small pores with capillary trapped oil can be flooded. Accordingly will also the saturation change because the residual oil saturation is reduced and the fluid flow can occur at a larger saturation range than initially.



**Figure 9.3:** Average relative permeability curves for matrix for the surfactant flooding case. The blue and orange curves represents the relative permeability for water and oil respectively, initially (dashed) and at breakthrough.

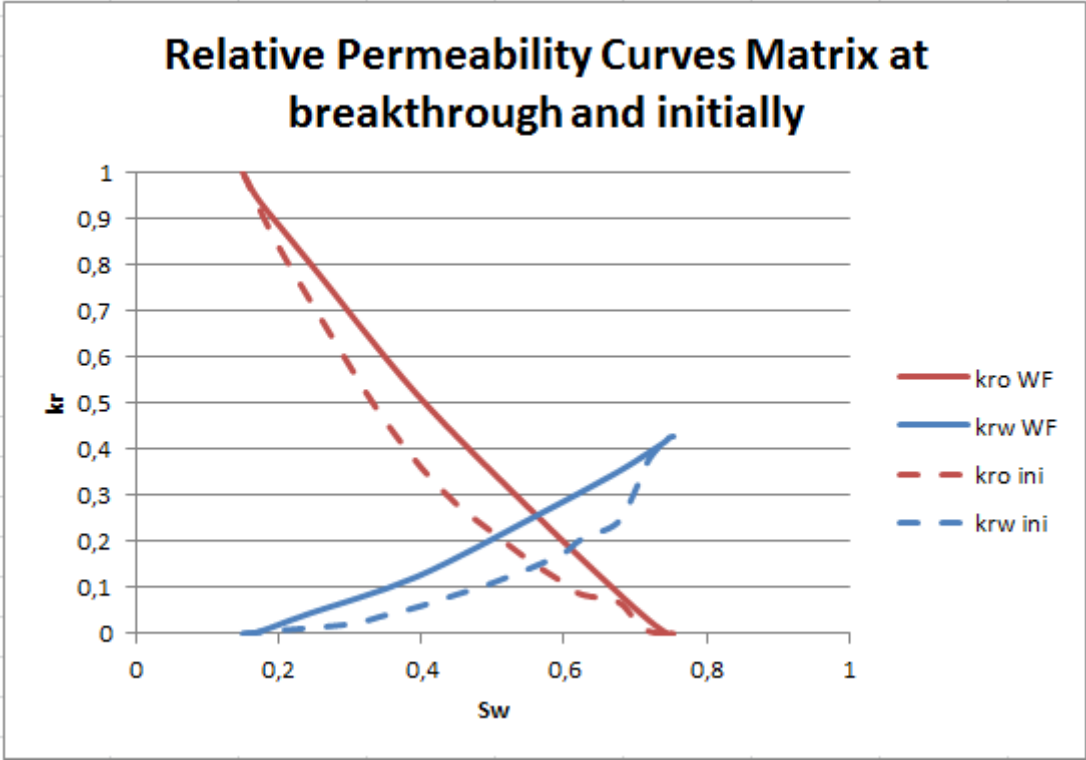


**Figure 9.4:** Average relative permeability curves for matrix for the waterflooding case. The blue and orange curves represents the relative permeability for water and oil respectively, initially (dashed) and at breakthrough.

### 9.3 Recovery with and without surfactants

A comparison of the recovery for the waterflood case and the surfactantflood case was conducted to find out if surfactants improve the recovery in this model, and possibly how much is the recovery is improved.

Figure 9.5 presents the results. The blue lines represent the recovery factor and watercut for the surfactant flood, while the green lines represent the waterflood. The recovery factor is improved with 2,8% for the surfactant case, and the breakthrough occurs sooner. For the surfactant case is breakthrough after 2500 days, while for the water case is the breakthrough is after 2650 days.

Surfactant decreases the IFT and hence the capillary pressure. Therefore can the solution water easier overcome the threshold pressure in the pore openings and flood the pores. Because of this, it is expected that the production will improve with surfactants. However, what is interesting is to see how much it is improved. Whether the improvement is satisfying or not depends on the costs of the chemicals, extra equipment for the implementation of the process etc. An evaluation of benefits and outcomes for this case will be given in chapter 9.12.

A figure of a comparison of the relative permeability curves for surfactant model (surf) and the waterflood model (wf) are given in Figure 9.6. The saturation endpoints for the surfactant model have been moved to more beneficial values, allowing fluid flow to occur at both lower and higher water saturation than for the waterflood case. The relative permeability curves are initially the same for both waterflood and surfactant case. As Figure 9.6 shows, have the endpoints changed only for the surfactant case. This is because the surfactants have reduced the IFT and accordingly pore-entry pressure and hence more of the residual oil is recovered and the fluid flow can occur at a larger saturation range. Figure 6.1 presents a theoretical presentation of how relative permeability and capillary pressure curves may change as a result of IFT reduction.

The dashed lines in Figure 9.5 give the watercut for the two cases. The breakthrough for the surfactants occurs approximately 150 days earlier than for the waterflood. When the relative permeability curves (Figure 9.6) changes, the mobility of the phases changes (equation 3.2). In this case is only the endpoint for the relative permeability to water changed while the relative permeability for oil is constant. The viscosities of oil and water are assumed constant.



Because of these changes is the mobility for water increased, while the oil mobility is constant. Therefore will the injection water flow more easily with surfactants than without and reach the produced sooner.

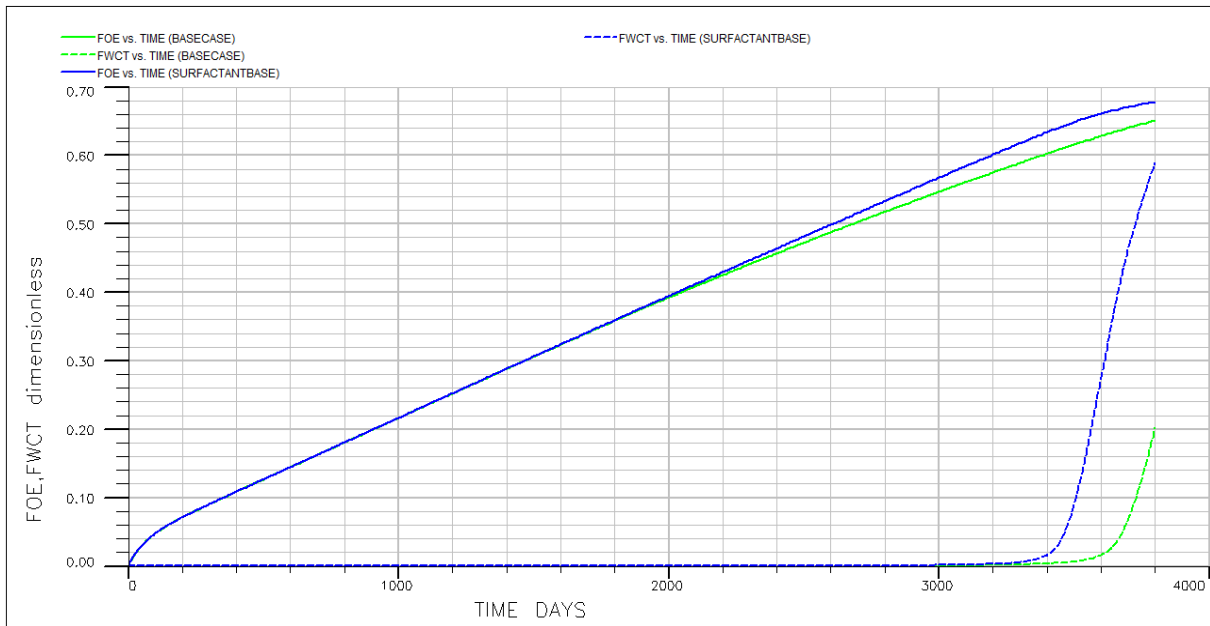


**Figure 9.5:** Recovery factor (FOE) and watercut (FWCT) for surfactant flood (blue) and water flood (green).

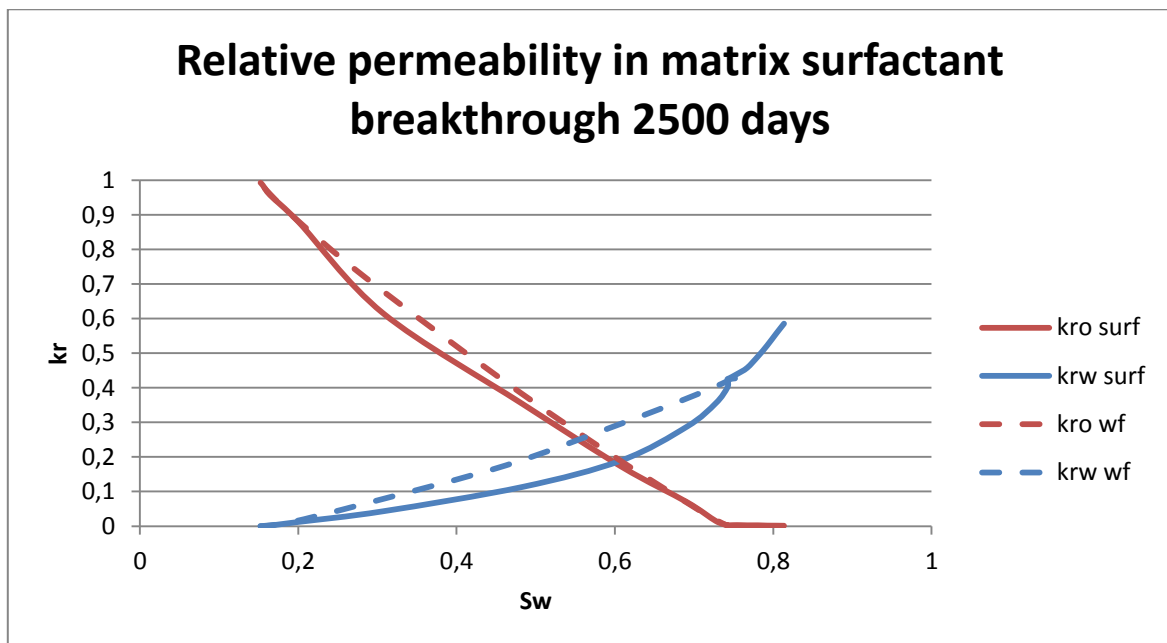


**Figure 9.6:** Average relative permeability for all matrix layers at surfactant breakthrough, for surfactant flood (orange) and waterflood (blue).

### 9.4 Initial Capillary Pressure Sensitivity

A case study to see what impact the initial capillary pressure has on the recovery was conducted. This case is especially interesting, since the surfactants are injected with the purpose to reduce the IFT and capillary pressure. A comparison of surfactant flooding and waterflooding for three cases with different initial capillary pressure was done. Figure 9.7 and Table 9.2 gives the input data for the capillary pressure for the three different cases. The results are given as a plot of recovery for all six cases in Figure 9.8. Because of the small recovery differences, presents the figure the recovery only for the last hundred days.

**Table 9.2:** Capillary pressure input data for the case study.

| Basecase |       |       |        | Pc is 5 times larger in matrix |       |       |        | Pc is 5 times less in matrix |       |       |         |
|----------|-------|-------|--------|--------------------------------|-------|-------|--------|------------------------------|-------|-------|---------|
| Sw       | krw   | kro   | Pcow   | Sw                             | krw   | kro   | Pcow   | Sw                           | krw   | kro   | Pcow    |
| 0,15     | 0     | 1     | 0,138  | 0,15                           | 0     | 1     | 0,69   | 0,15                         | 0     | 1     | 0,0276  |
| 0,2      | 0,007 | 0,84  | 0,062  | 0,2                            | 0,007 | 0,84  | 0,31   | 0,2                          | 0,007 | 0,84  | 0,0124  |
| 0,3      | 0,021 | 0,58  | 0,028  | 0,3                            | 0,021 | 0,58  | 0,14   | 0,3                          | 0,021 | 0,58  | 0,0056  |
| 0,35     | 0,04  | 0,46  | 0,014  | 0,35                           | 0,04  | 0,46  | 0,07   | 0,35                         | 0,04  | 0,46  | 0,0028  |
| 0,4      | 0,06  | 0,36  | 0,007  | 0,4                            | 0,06  | 0,36  | 0,035  | 0,4                          | 0,06  | 0,36  | 0,0014  |
| 0,45     | 0,085 | 0,28  | 0,003  | 0,45                           | 0,085 | 0,28  | 0,015  | 0,45                         | 0,085 | 0,28  | 0,0006  |
| 0,5      | 0,11  | 0,22  | 0,002  | 0,5                            | 0,11  | 0,22  | 0,01   | 0,5                          | 0,11  | 0,22  | 0,0004  |
| 0,55     | 0,14  | 0,16  | 0,001  | 0,55                           | 0,14  | 0,16  | 0,005  | 0,55                         | 0,14  | 0,16  | 0,0002  |
| 0,6      | 0,175 | 0,11  | 0      | 0,6                            | 0,175 | 0,11  | 0      | 0,6                          | 0,175 | 0,11  | 0       |
| 0,625    | 0,205 | 0,085 | -0,003 | 0,625                          | 0,205 | 0,085 | -0,015 | 0,625                        | 0,205 | 0,085 | -0,0006 |
| 0,675    | 0,24  | 0,07  | -0,007 | 0,675                          | 0,24  | 0,07  | -0,035 | 0,675                        | 0,24  | 0,07  | -0,0014 |
| 0,7      | 0,31  | 0,03  | -0,034 | 0,7                            | 0,31  | 0,03  | -0,17  | 0,7                          | 0,31  | 0,03  | -0,0068 |
| 0,72     | 0,38  | 0,005 | -0,069 | 0,72                           | 0,38  | 0,005 | -0,345 | 0,72                         | 0,38  | 0,005 | -0,0138 |
| 0,75     | 0,43  | 0     | -0,207 | 0,75                           | 0,43  | 0     | -1,035 | 0,75                         | 0,43  | 0     | -0,0414 |

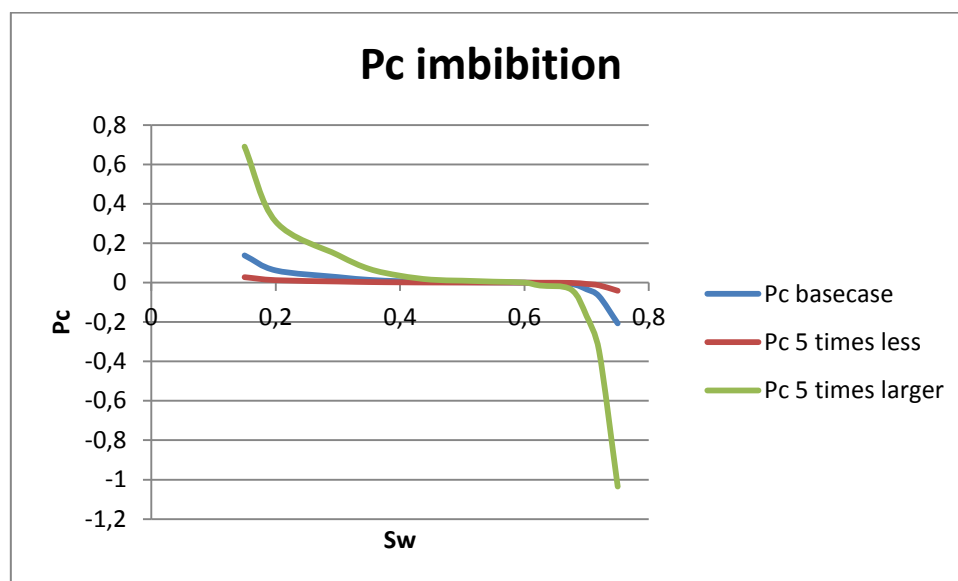


**Figure 9.7:** Three different capillary pressure curves for the Pc sensitivity case study.

The recovery is better for all three surfactant cases compared to the waterflood cases. As Figure 9.8 shows is the recovery approximately the same for all three surfactant cases with various capillary pressures. In the surfactant model is a third saturation table implemented for the miscibility case. When the surfactants are injected and flows through the model, they start to form microemulsion with water and oil. When oil and water are miscible in the microemulsion, ECLIPSE starts to use the miscibility saturation table, and hence change the capillary pressure to zero which is stated in the table (see chapter 8.3 for details). Therefore is it reasonable that the recovery is the same for all three cases.

The recovery for the three different waterflood cases is slightly more different than what is the case for the surfactantflood. For the basecase and the low initial capillary pressure case is the recovery approximately the same, while the recovery is improved with 0,1% for the initial high capillary pressure case.

In chapter 4.4.1 about imbibition in naturally fractured reservoirs is it explained how the capillary forces works in favour of the imbibition. In the waterflood case, the improved recovery for initial high capillary pressure case may be explained by capillary pressure as drive forces for imbibition. Since the rock is water-wet, the capillary forces work in the favour of displacement of oil, such as the rock is surrounded by the preferred fluid.

If the initial capillary pressure was increased or decreased ten times more, the results may be different. Since the capillary pressure is an important drive mechanism to make the imbibition process happen, a very low capillary pressure may not be able to “push” the injected fluid into pores and therefore delay the breakthrough and decrease the recovery. On the other hand, if the initial capillary forces are too strong, they can oppose the pore invasion of the injected fluid and also decrease the recovery.

The saturation table for miscible conditions implemented in the model assumes that there is no capillary pressure in the microemulsion phase. It is not likely that the capillary pressure will become zero. With the purpose to see if this assumption had an impact on the results, was a comparison of the surfactant basecase file done with an equal file but with capillary pressure in miscible conditions. The results presented in Figure 9.9 shows that the oil recovery is the same for the two cases. Therefore is it assumption considered valid for this model.

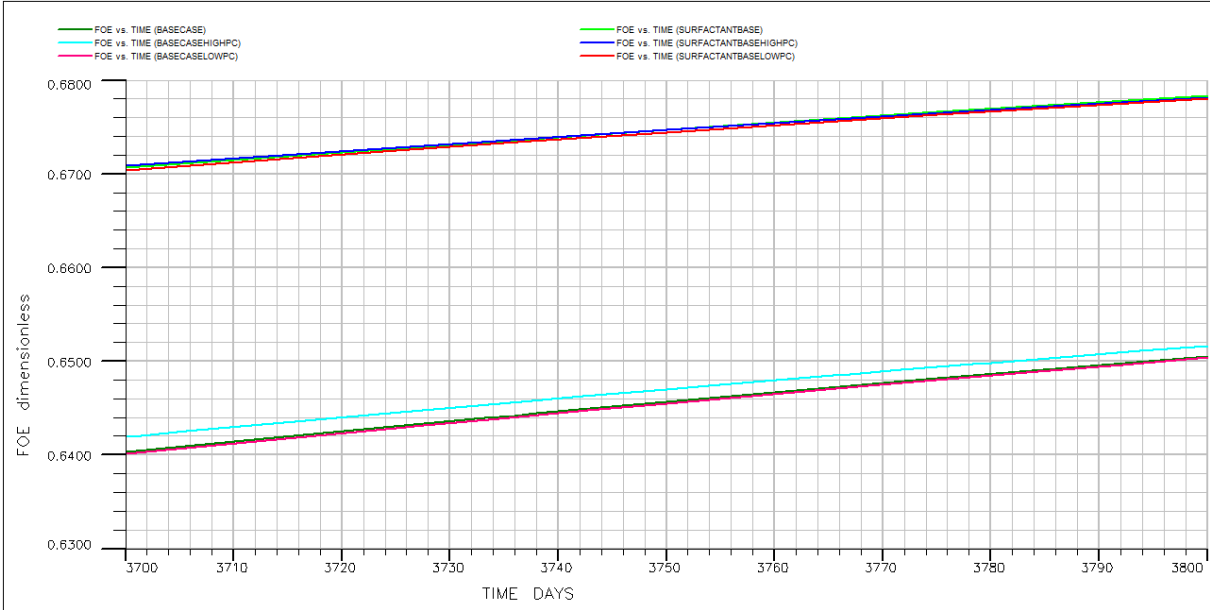


Figure 9.8: Recovery factor (FOE) for three cases of surfactant and waterflooding. Green, blue and red curves for basecase, high Pc and low Pc respectively.

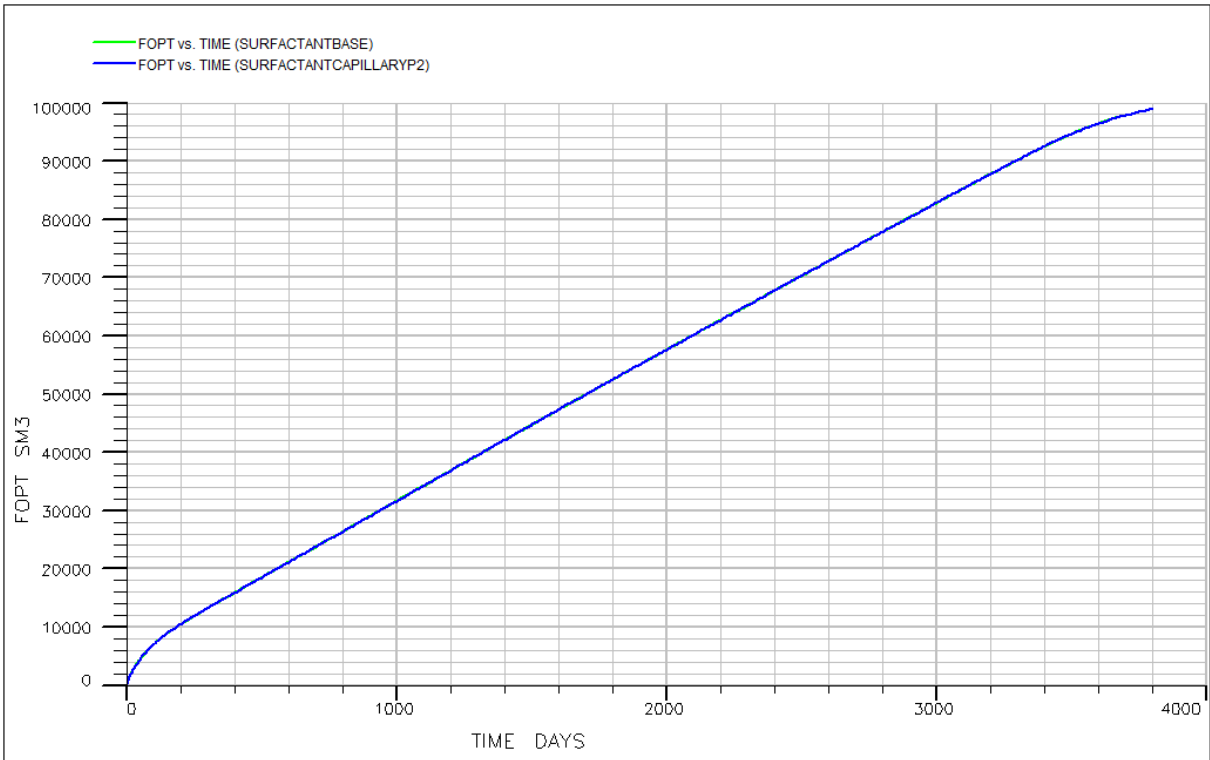


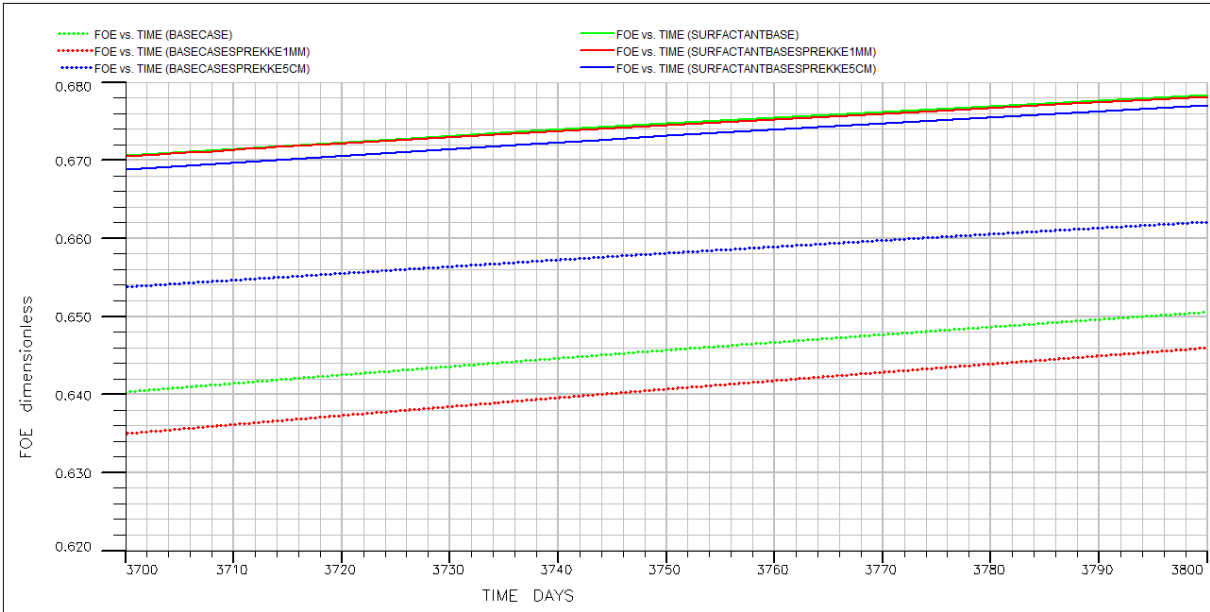
Figure 9.9: Total production for the case with zero capillary pressure in the miscible zones (surfactantbasecase), and for the case where capillary pressure is not zero.

### 9.5 Fracture opening sensitivity

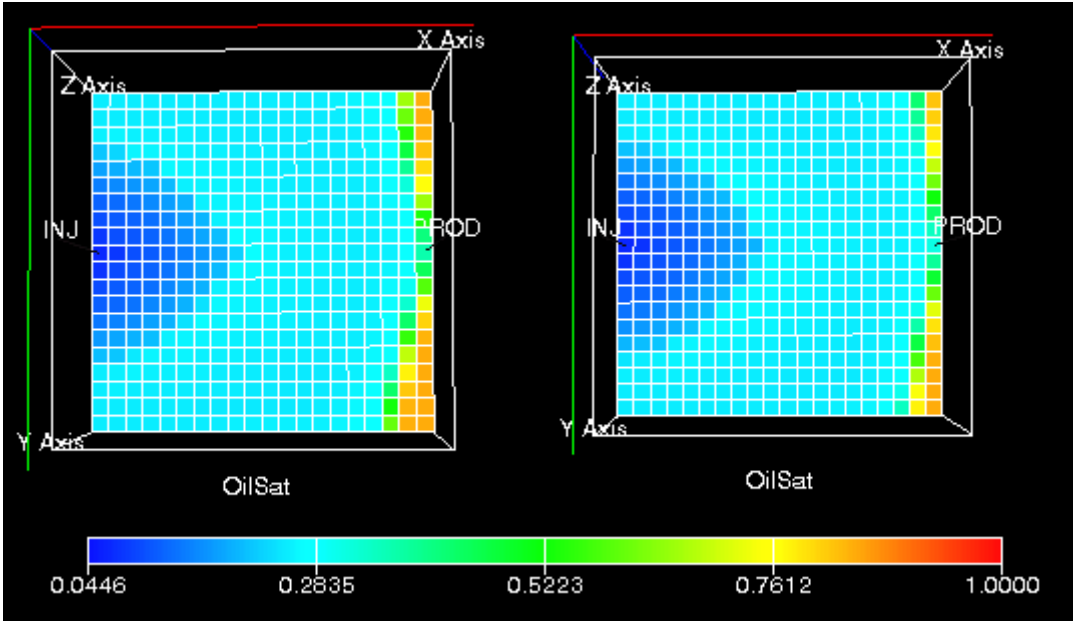
To see what impact the fracture width has on the oil production, this case study compares the recovery for waterflood and surfactant flood at three different fracture widths. The fracture widths that are compared are 1mm, 1cm (basecase) and 5cm. It is expected that the results will be better for the case with the widest fracture, since then the area with idealized flow condition will be larger.

Figure 9.10 gives the recovery results for both waterflood and surfactantflood for the three different fracture widths. For the waterflood case, the results are as expected, where the case with the widest fractures gives best recovery, and the case with only 1 mm fracture produces less. While for the surfactant case are the results unexpected. The case with the widest fracture gives less recovery.

It has to be pointed out that the model is not stable for the case with a fracture width of 1mm. There are several convergence problems due to large differences in permeability an thickness between the layers, and hence the results are inaccurate for this case. However, it is reasonable to assume that the oil production will be less for the 1mm fracture opening case and that the results are a good indication at least. Since the recovery is less for the case with a 5cm wide fracture it may be explained by the poor sweep. It is now more reasonable to call the fracture a high permeable layer with excellent flow conditions. Since most fluids flow toward here, the displacement will be a fingering process. A fingering process leads to poor sweep. Fingering displacement is a large problem for heterogeneous reservoirs with high permeable layers. Polymers are often injected in those layers to slow down the flow and hence increase the sweep throughout the reservoir. As Figure 9.11 shows, the sweep is poorer in layers far from the high permeable layer in the case with a 5cm wide fracture, than for the 1cm wide fracture. This is probably the explanation for the lower recovery in the large fracture case.



**Figure 9.10:** Recovery (FOE) of oil for water and oil at different fracture widths. The red, green and blue curves give the recovery for 1mm, 1cm and 5cm width respectively.



**Figure 9.11:** Oil saturation, end of simulation in the bottom layer for the case with a wide layer (left) and for surfactant basecase (right).

### 9.6 Surfactant Production

Surfactants are expensive chemicals. A high recovery of surfactants may reduce costs by recycling of surfactants for reinjection. This case study was therefore conducted to see how much of the injected surfactants were produced and how much were left in the reservoir model. Contrary from the other case studies, was this study evaluated for 7800 days of production to see if the surfactants followed the waterfront and got produced after the oil production stop.

The results are given in Figure 9.12 where the green line presents total surfactant injection, the red line gives the total adsorption and the blue line is the total surfactant production. The recovery of surfactants is only 0,013%. Most of the surfactants injected in the model are adsorbed by the rock. Almost 70% is adsorbed. The remaining 30% are left in fluid solution in the reservoir. When large amount of surfactants are adsorbed by the rock, the cost of the EOR treatment will be large. Accordingly it is important to consider how much of the surfactants will be adsorbed, and chose a surfactant tailored for the surroundings.

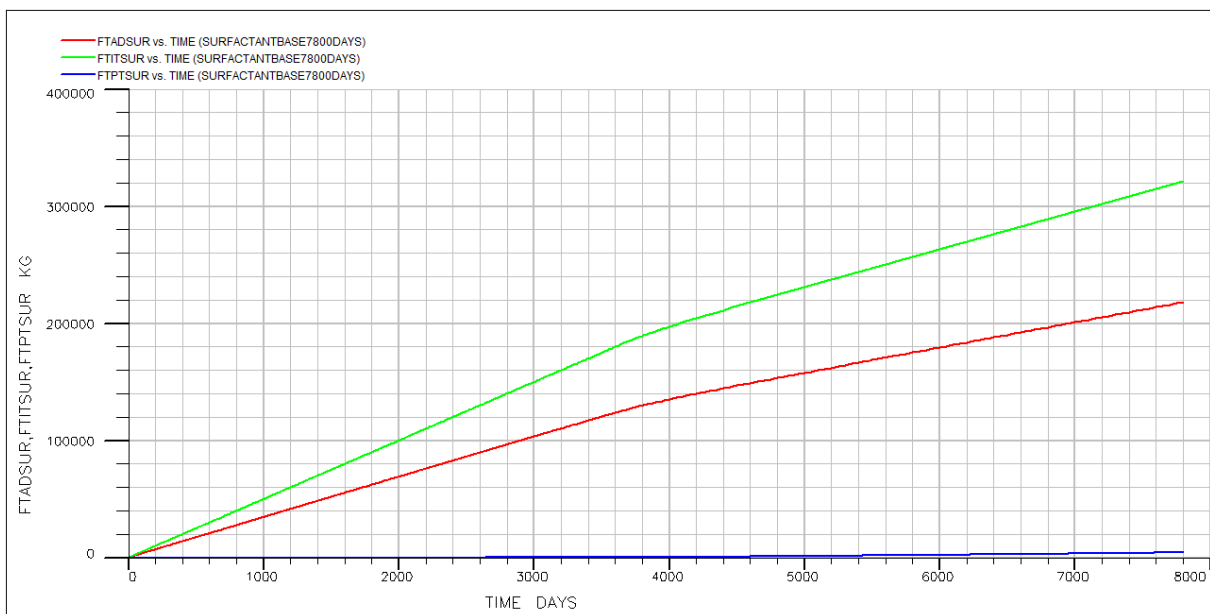


**Figure 9.12:** Total amount of surfactants injected (FTITSUR), adsorbed (FTADSUR) and produced (FTPTSUR).

### 9.7 Surfactant Adsorption case study

A case study with comparison of three different adsorption input data tables was conducted to see what impact the surfactant adsorption has on the recovery. The same amount of surfactants was injected at the same rate for all three cases. Table 9.3 gives the adsorption input data for the three cases. The tables were implanted in the SURFADS keyword in the surfactant model.

Figure 9.13 and Figure 9.14 give the results of the total amount surfactant adsorbed by the rock, and the oil recovery respectively. The recovery changes are very small, therefore the plot is focused only on the last hundred days of production. For the case with less adsorption, the adsorption only changed with 40%, while for the case with more adsorption the adsorption data is exacerbated with 100% compared to the surfactant basecase. The recovery is improved with 0,5% for the less adsorption case and reduced with 0,3% for the case with more adsorption. This shows that the adsorption is not proportional to the oil recovery. The exacerbation of the recovery should be larger than the improvement in the comparison of the two cases with the basecase if adsorption and recovery were proportional related.

That the recovery is better for the case with less surfactant is not surprising since there will be a larger concentration of surfactants available to form microemulsion with oil and water for the case where less of the injected surfactants are adsorbed. In this model the wettability alteration function is not included. In a case where adsorbed surfactants could change the wettability, the results can be quite different. If adsorption results in a more water-wet rock, adsorption could be favourable for the imbibition process and hence might improve the recovery from a basecase with no or less adsorption.

**Table 9.3:** SURFADS keyword input data alteration for the surfactant adsorption case study.

| Basecase                            |                     | Less Adsorption                     |                     | More Adsorption                     |                     |
|-------------------------------------|---------------------|-------------------------------------|---------------------|-------------------------------------|---------------------|
| Local Csurf<br>[kg/m <sup>3</sup> ] | Adsorbed<br>[kg/kg] | Local Csurf<br>[kg/m <sup>3</sup> ] | Adsorbed<br>[kg/kg] | Local Csurf<br>[kg/m <sup>3</sup> ] | Adsorbed<br>[kg/kg] |
| 0                                   | 0                   | 0                                   | 0                   | 0                                   | 0                   |
| 1                                   | 0,0005              | 1                                   | 0,0002              | 1                                   | 0,001               |
| 30                                  | 0,0005              | 30                                  | 0,0002              | 30                                  | 0,001               |
| 100                                 | 0,0005              | 100                                 | 0,0002              | 100                                 | 0,001               |



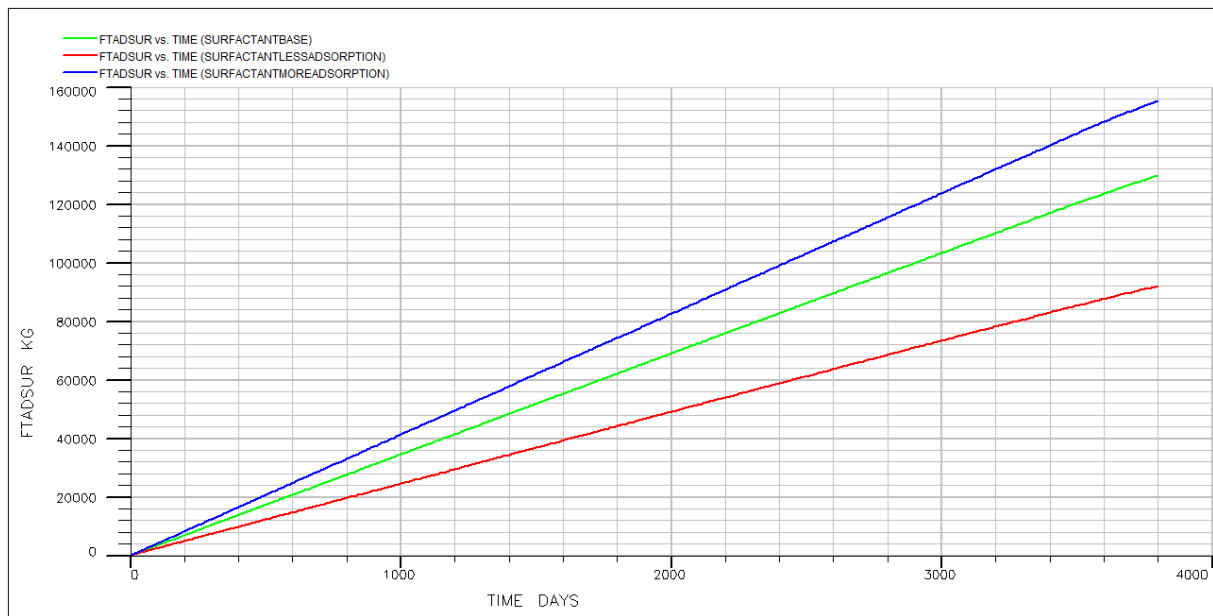


**Figure 9.13:** Surfactant adsorption for the cases with low, intermediate and much adsorption.

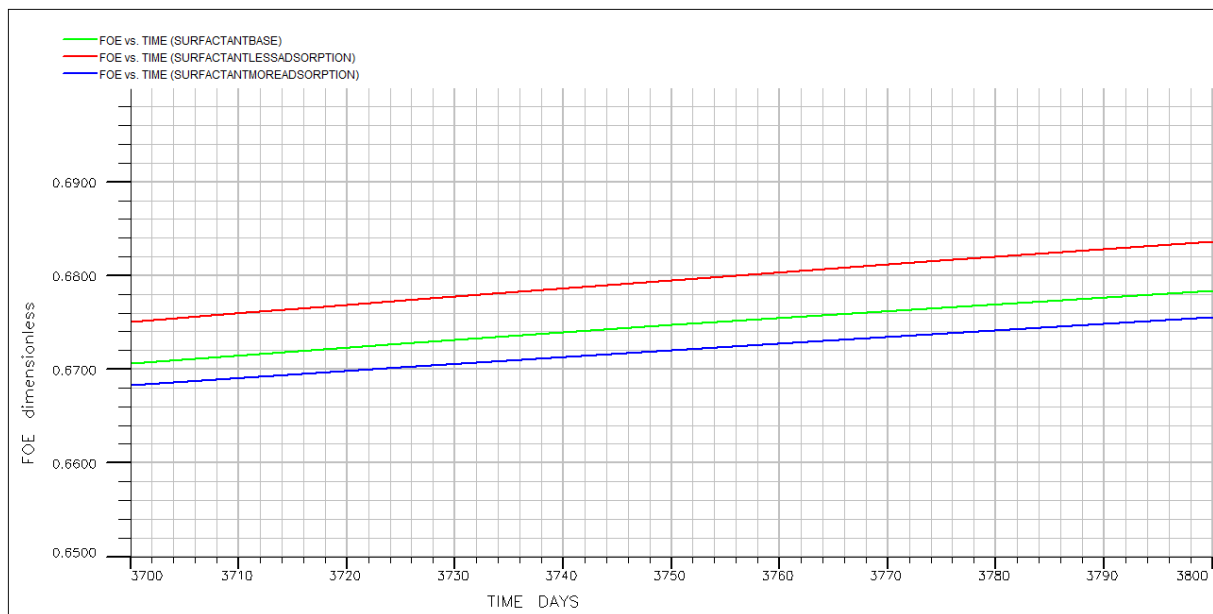


**Figure 9.14:** Recovery comparison of three cases with different surfactant adsorption by rock.

### 9.8 Input Changes in Miscibility Index in the SURFCAPD keyword

For the surfactants to be efficient, should the capillary number be increased with a factor of  $10^4$  (chapter 6). The capillary number is a function of interfacial tension (equation 6.4), and increases when IFT decreases. The IFT between oil and water decreases when surfactants act on the fluid's surfaces and make them miscible in a microemulsion. The SURFCAPD keyword decides when the surfactants can form an emulsion with oil and water and make them partly or fully miscible. This is altered by the miscibility index. Therefore it is interesting to see how changes in the miscibility index impact the recovery. A comparison in recovery for three cases is done in this case study. The surfactant basecase is compared with a case where microemulsion is more likely to occur, and one case where microemulsion is less likely to occur. The input data is given in Table 9.4.

**Table 9.4:** Capillary number alterations for case study

| SurfactantBasecase |          |             | Microemulsion occurs easier case 2 |          |             | Microemulsion occurs more difficult case3 |          |             |
|--------------------|----------|-------------|------------------------------------|----------|-------------|---|----------|-------------|
| Log(Nc)            | Nc       | Miscibility | Log(Nc)                            | Nc       | Miscibility | Log(Nc)                                   | Nc       | Miscibility |
| -10                | 1,00E-10 | 0           | -10                                | 1,00E-10 | 0           | -10                                       | 1,00E-10 | 0           |
| -5,5               | 3,16E-06 | 0           | -5,5                               | 3,16E-06 | 0,3         | -5,5                                      | 3,16E-06 | 0           |
| -4                 | 1,00E-04 | 0,5         | -4                                 | 1,00E-04 | 0,8         | -4  | 1,00E-04 | 0           |
| -3                 | 1,00E-03 | 1           | -3                                 | 1,00E-03 | 1           | -3  | 1,00E-03 | 0,3         |
| 2                  | 1,00E+02 | 1           | 2                                  | 1,00E+02 | 1           | 2   | 1,00E+02 | 0,5         |
| 5                  | 1,00E+05 | 1           | 5                                  | 1,00E+05 | 1           | 5   | 1,00E+05 | 1           |
| 10                 | 1,00E+10 | 1           | 10                                 | 1,00E+10 | 1           | 10  | 1,00E+10 | 1           |

The result of the study is presented in Figure 9.15. The changes are small and as expected. For the case where microemulsion can occur easier is the recovery improved with 1,6%, while the recovery is 1% less for the case where microemulsion does not occur as easily. The IFT reduction required to make oil and water miscible, is not as big for case 2 as for the two other cases. However this improvement is caused by “removing” boundaries for microemulsion to occur. Therefore must this case be probability evaluated. It is assumed that the initial capillary number is approximately  $10^{-9}$  since the initial IFT between oil and water is 0,05N/m (Table 8.6) and the initial production rate is 120Sm<sup>3</sup>/day. As mentioned, the capillary number should be increased by a factor of  $10^4$  for the surfactant flood to be efficient. To simulate this, a miscibility index larger than zero should not be implemented in the model before the capillary

number is in the range of  $10^{-5}$ . In case 2, partly miscibility can occur for a capillary number of  $10^{-6}$ . Therefore can the results for this case be slightly unrealistic.

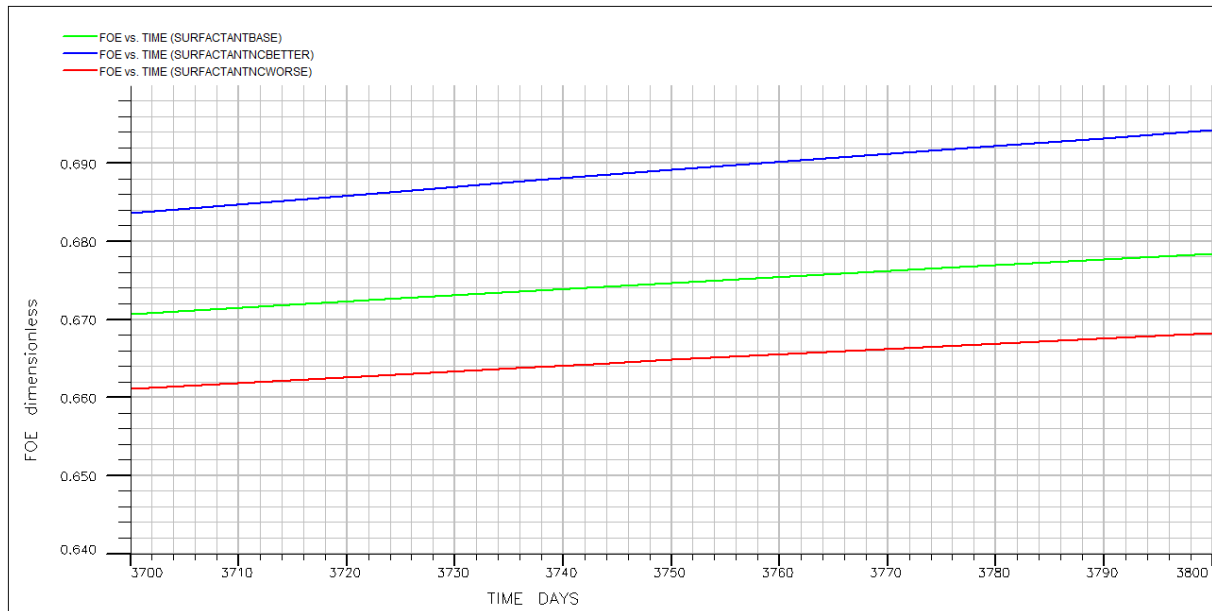


**Figure 9.15:** Recovery (FOE) for case study with miscibility index alteration. Surfactant basecase, case 2 and case 3 are presented with green, blue and red curves respectively.

### 9.9 Surfactant concentration in injected solution

A case study of the impact the surfactant concentration of the injected solution has on the production was conducted. The surfactant concentration in the surfactant base case is  $1\text{kg}/\text{Sm}^3$ . The concentration was changed to a case with low concentration of  $0,1\text{kg}/\text{Sm}^3$ , and a case with high concentration of  $30\text{kg}/\text{Sm}^3$ .

Figure 9.16 shows the results from changes in the surfactant concentration in the injected solution. The results show that the recovery is increased with surfactants with concentrations of  $1\text{kg}/\text{Sm}^3$  and  $30\text{kg}/\text{Sm}^3$ . For the case with low surfactant concentration is the recovery the same as for the waterflood. The injection rate decreases after 1825 days, because the bottom hole pressure in the injection well becomes too high, so the injection constrains changes from injection rate to bottom hole pressure. The bottom hole pressure increases, because the flow rate out of the reservoir is less than the flow rate into the reservoir.

Because of the earlier discussed principal of critical micelle concentration, an expected result would have been that the oil production would be the same for surfactant base case and the case with a higher surfactant concentration. This hypothesis is assumed because Table 8.6 shows that IFT is not further reduced even if the surfactant concentration is increased thirty times. After CMC is reached, a further increase in surfactant concentration will not increase the micelle concentration, therefore the surfactants will not be able to reduce the interfacial tension any further.

However, another reasonable explanation to the increase in total oil production could be that the water viscosity also increases. From Table 8.7, it can be seen that the water viscosity increases with approximately 30% when the surfactant concentration is  $30\text{kg}/\text{Sm}^3$ . The higher water viscosity explains why the breakthrough happens later for the high surfactant concentration case. It may also explain the higher recovery. A high water viscosity improves the sweep efficiency. Polymers are often included in surfactant flood with the purpose to increase the sweep efficiency by increasing the water viscosity. In this case is the water viscosity higher than the oil viscosity and the water sweeps the reservoir well. Figure 9.17 shows the IFT changes in the model. The IFT changes when surfactants are present to make a microemulsion. For the case with a high surfactant concentration, the IFT is changed in much larger areas than for the Surfactant base case. This can indicate that the high surfactant

concentrated solution sweeps the reservoir model better, and hence the recovery will also improve.

On the other hand, Figure 9.18, shows that the recovery factor is only improved with 3,5% at breakthrough, while the surfactant concentration is increased with 3000%. This increase will not be conventional. An estimate of the costs is presented in chapter 9.12.

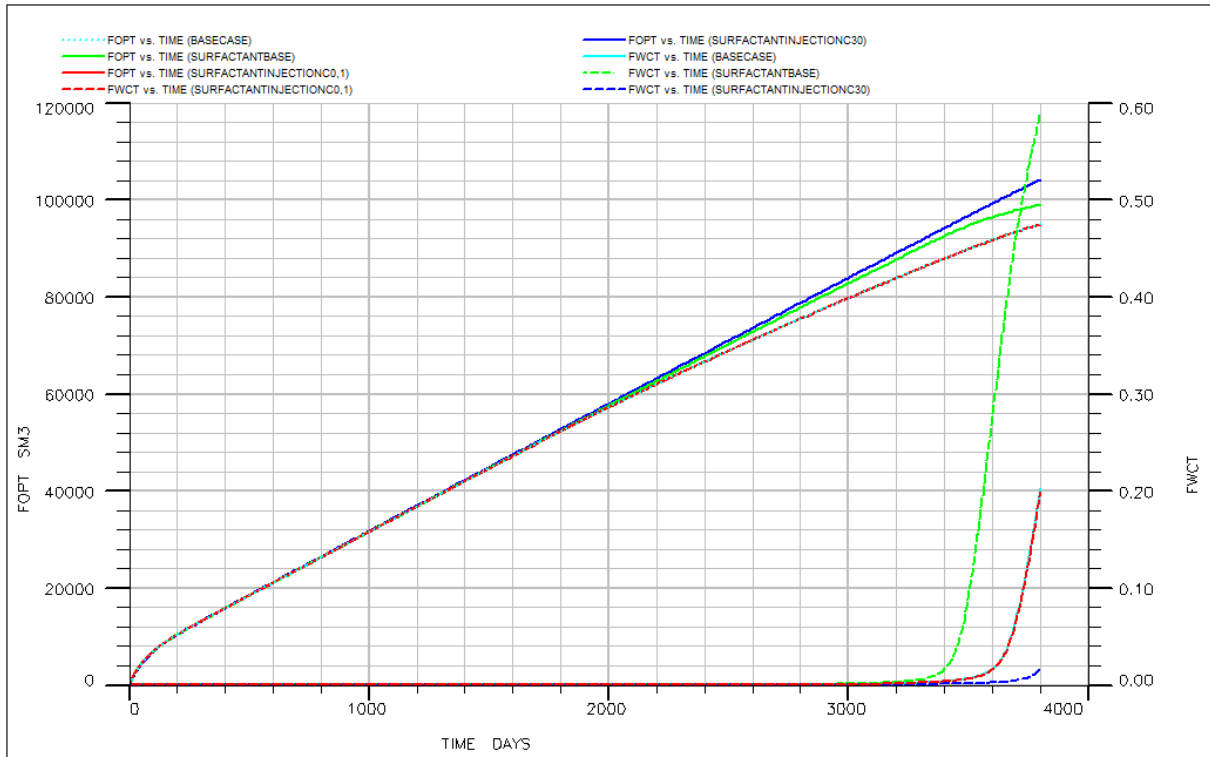


**Figure 9.16:** Plot of total oil production and watercut at breakthrough for the three different surfactant concentrations in the injection fluid. The green line is for the surfactantbasecase with a concentration of  $1\text{kg}/\text{Sm}^3$ , the blue line is for high concentration,  $30\text{kg}/\text{Sm}^3$ , and the red line is for low concentration,  $0,1\text{kg}/\text{Sm}^3$ . The light blue line is for waterflood.

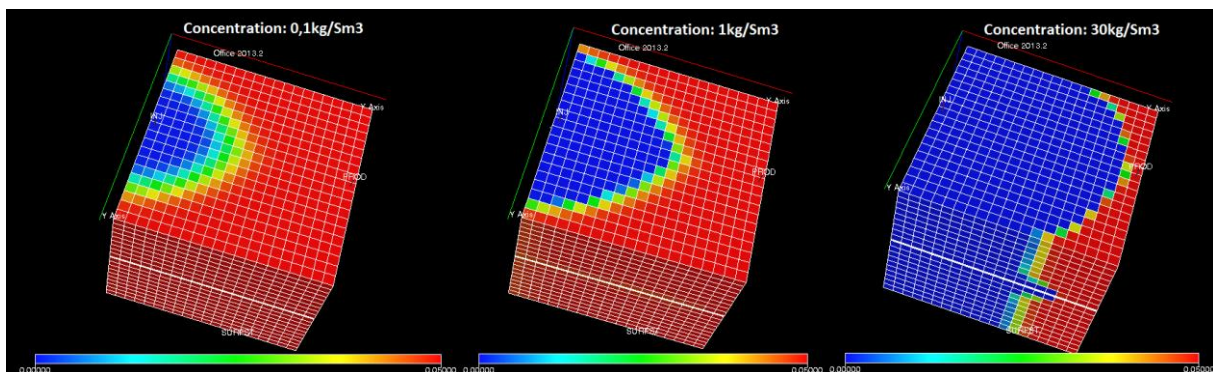


**Figure 9.17:** IFT distribution in the reservoir model at breakthrough for the three cases with increasing surfactant concentration to the right.

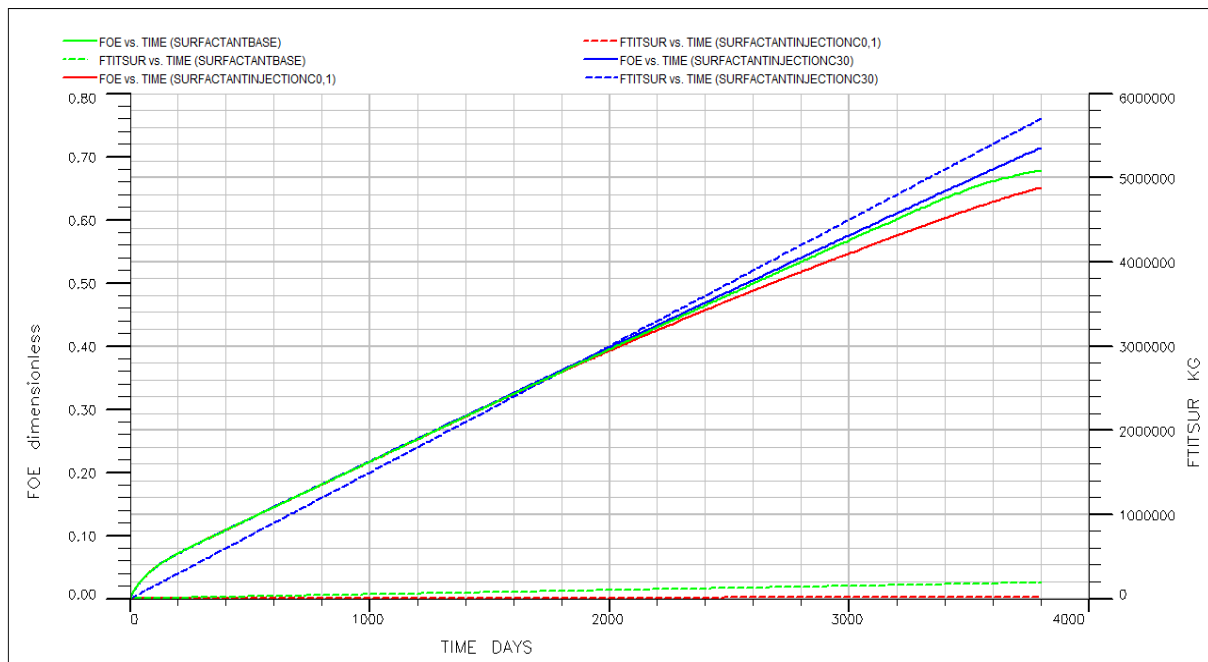


**Figure 9.18:** Recovery factor (FOE, solid lines) and total amount of surfactant injected (FTITSUR, dashed lines) for the three different surfactant concentrations in the injection fluid. The green line is for the surfactantbasecase with a concentration of  $1\text{kg}/\text{Sm}^3$ , the blue line is for high concentration,  $30\text{kg}/\text{Sm}^3$ , and the red line is for low concentration,  $0,1\text{kg}/\text{Sm}^3$ .

## 9.10 9-block model with four fractures and surfactant injection

With the purpose to investigate the flow pattern of the injection fluid solution further, a 9-block model was built with four fractures. Two of the fractures were placed in the x-direction (the seventh and fourteenth row) and with an intersection with two fractures in z-direction (the eleventh and twenty-first layers).

Figure 9.19 shows how the injected surfactants flow toward fractures. The fractures in x-direction that intersect with the layers presented in figure 9.19, transports fluids from the bottom and the top towards the fractured layers in flow direction. The sweep is very poor, and most of the fluids flow toward the middle of the model in the middle of all the fractures, with the fractured layers as the “highway”.

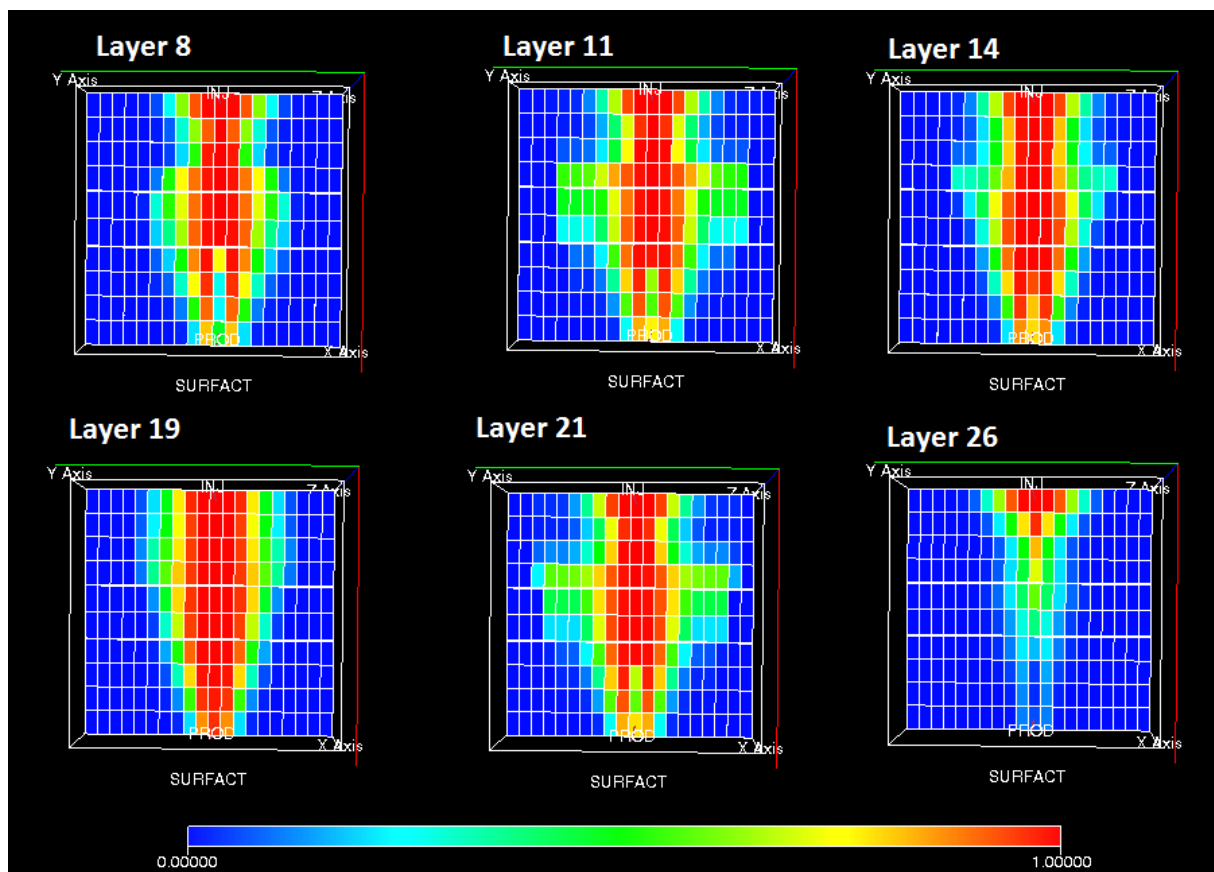


**Figure 9.19:** Surfactant concentration in various layers. Layer 11 and layer 21 are fractures.

### 9.11 9-block model with Surfactant-Polymer injection

As Figure 9.19 presented in the previous subchapter, is the sweep efficiency very poor. Because of the poor sweep is polymers injected with the purpose to investigate what is most profitable of pure surfactant injection and surfactant polymer injection.

In the SP-flood, are surfactants injected the first 900 days, then polymers for the next 900 days followed by chase water for the ultimate 800 days. In the surfactant injection model, are the surfactants injected continuously.

Figure 9.22 presents the recovery for the surfactant and SP-flood. The recovery is 3% better for the polymer-surfactant flood. The improved recovery is because of the increased sweep caused by the polymers. Figure 9.20 and Figure 9.21 present the oil saturation in various layers for the surfactant flood model and the surfactant-polymer flood respectively at the end of the flood, 2600 days. It is clear that the SP- model is better swept than the pure surfactant model, especially in the top and bottom layers. The surfactants reach breakthrough after only 126 days. The surfactant production rate is very low as for the single block model presented in earlier subchapters. However, the early breakthrough indicates that the surfactants are present throughout the length of the reservoir. As presented in the previous subchapter, flow the surfactants to the fractures and concentrate in the fractured layers and the layers close to the fractures. Because of this, it is clear that there is a large concentration of surfactants in the reservoir model prior to the polymer injection. The surfactants make a low interfacial tension solution in the middle layers, where they are mostly concentrated. When the polymers arrive they lower the viscosity of the solution water and spread the solution with now surfactants and polymers out to a larger area where the surfactants can form microemulsion and a low tension solution. When the chase water is injected, the remaining surfactants and polymers are displaced by the water front. In the pure surfactant injection model is the surfactant concentration maintained, but since the sweep is poor, is most of the surfactants concentrated in the good flow condition areas, in the fractures and in between the fractures (Figure 9.19).

A polymer flood with chase water was also studied. Polymers were injected for 1800 days, followed by 600 days of chase water. Figure 9.23 presents a comparison of the oil recovery for surfactant flood, SP-flood and polymer flood. The recovery is increased with 0,36% for the polymer injection compared to the surfactant flood.



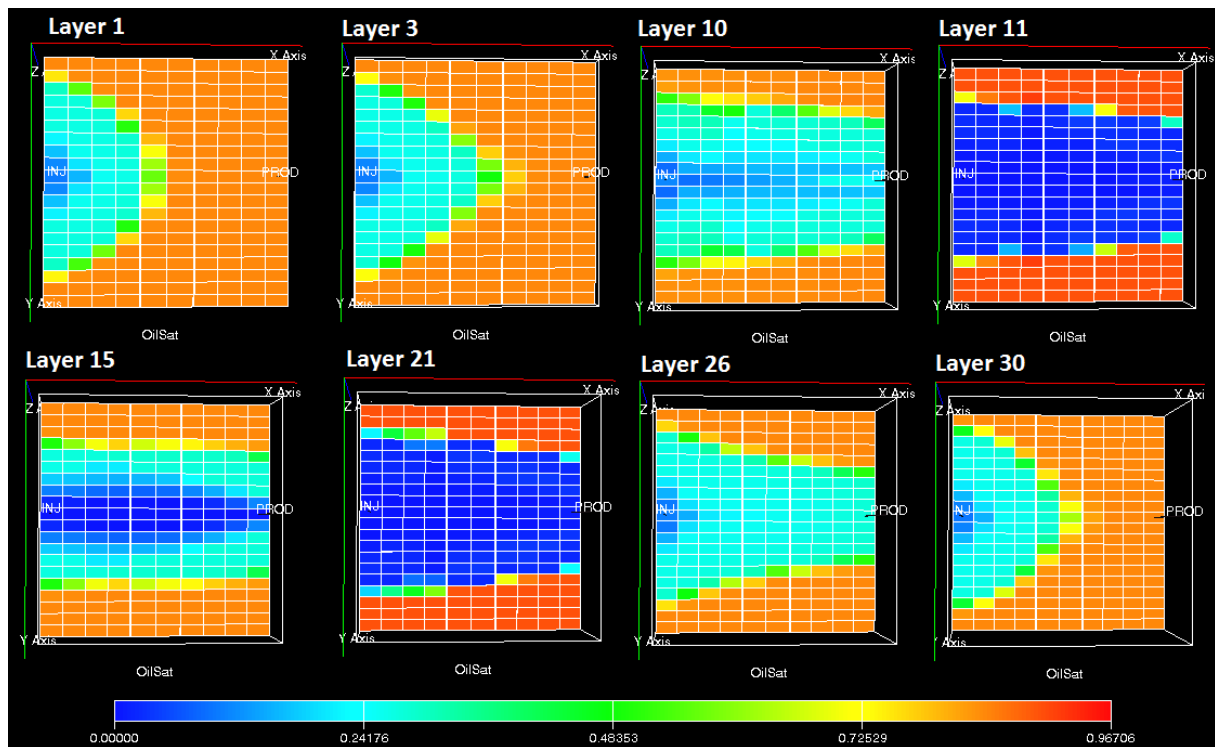


Figure 9.20: Oil Saturation in various layers for the surfactant flood model.

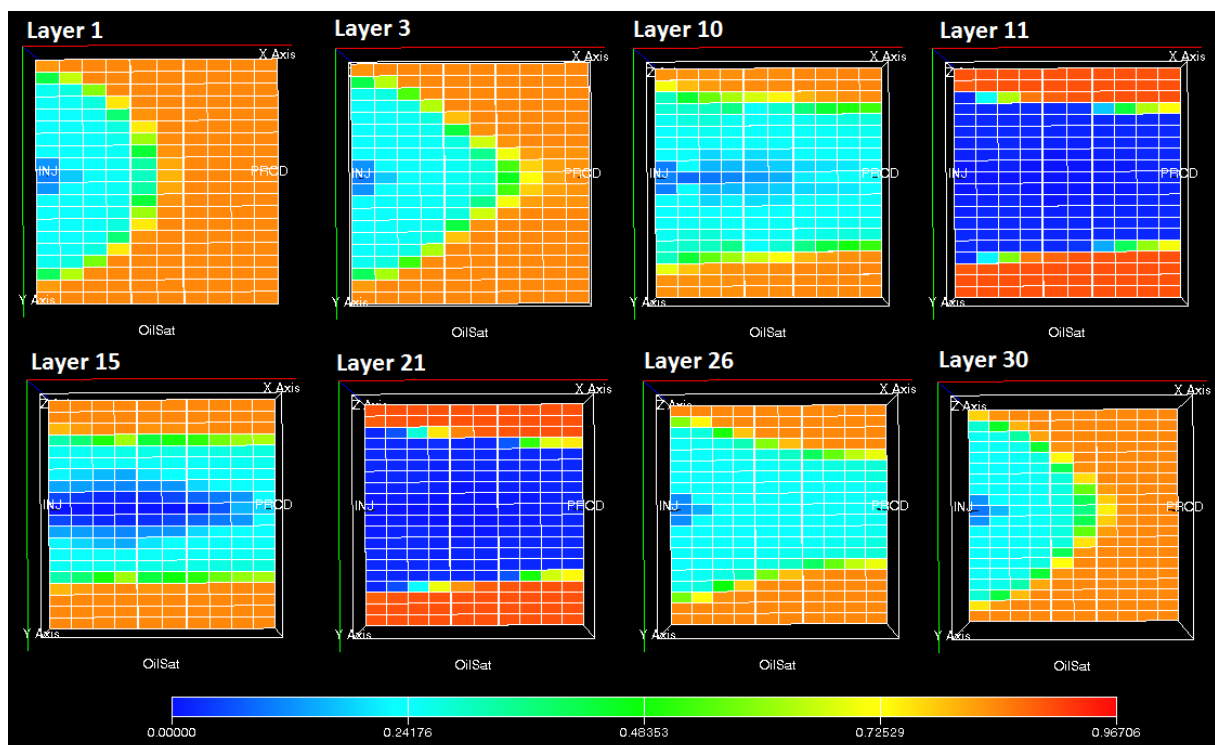
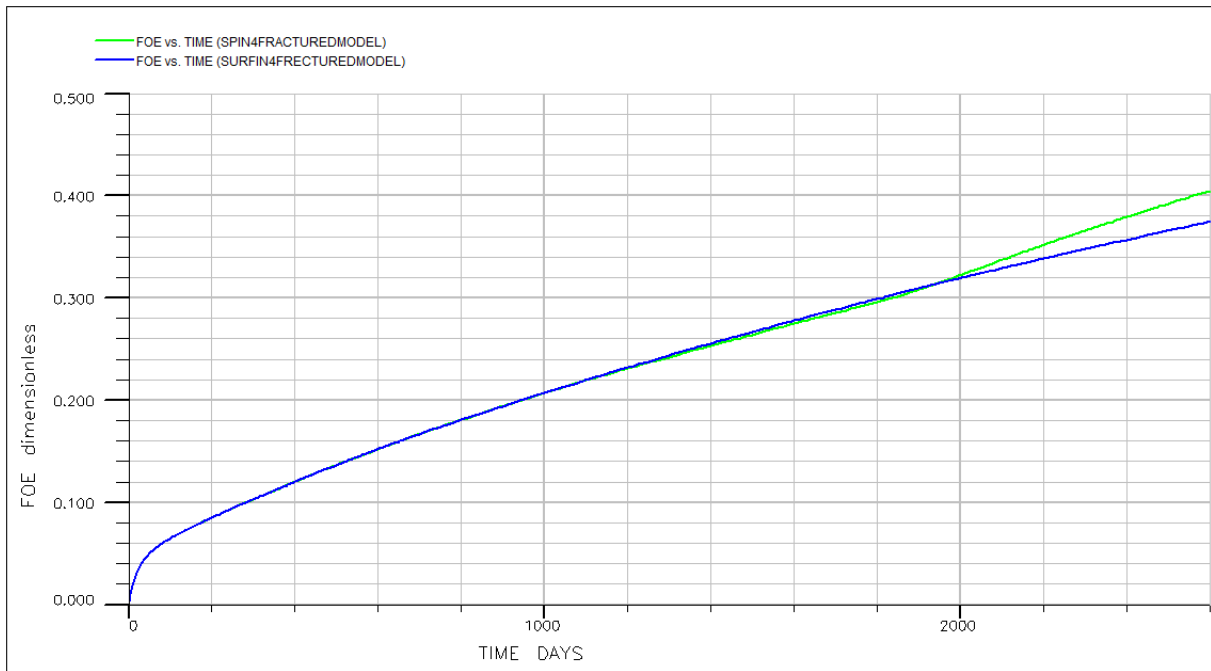
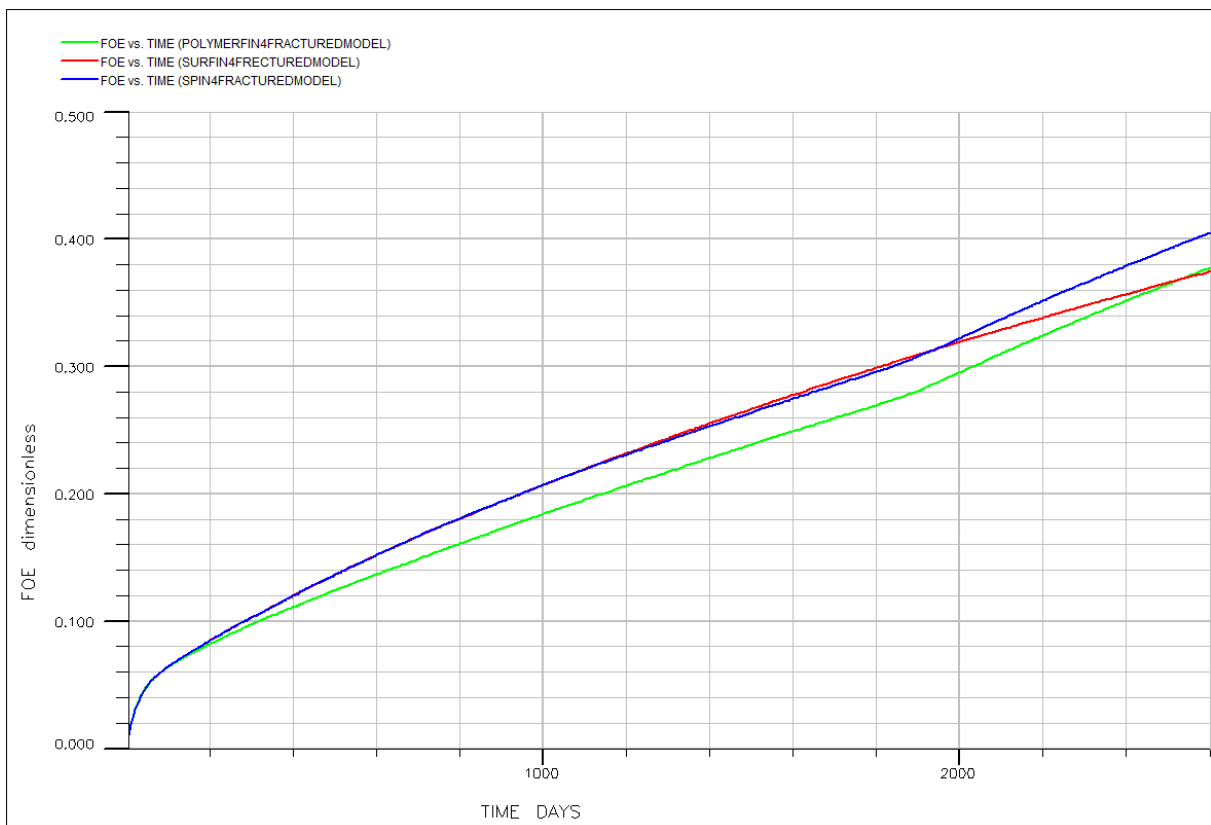


Figure 9.21: Oil Saturation in various layers for the surfactant-polymer model.



**Figure 9.22:** Recovery factor (FOE) for the SP- flood (green) and surfactantflood (blue).



**Figure 9.23:** Oil recovery (FOE) for Surfactant injection (red), SP injection (blue) and polymer injection (green).

### 9.12 Economic Evaluation

An economical evaluation has been done to see if surfactant injection is conventional in the reservoir models presented in this chapter. For calculation of the net present value, NPV, equation (9.1) has been used. The net present value formulation considers the future revenue and converts it till today's value. The discount rate,  $r$ , is assumed to be 0,08 (Abadli, 2012). And the inflation rate for US dollars is 0,02 (TradingEconomics, 2014). NPV is used to evaluate if a project is conventional. A positive NPV is a profitable project.

In this case it is assumed that all revenue is from selling oil, while the only expenses are the costs of chemicals. The production is for 3800 days for the single fracture model, while it is for 2600 days for the four fractures model. The total oil production for each year is taken from Eclipse Office result viewer. Chemical prices are taken from (Wyatt, et al., 2008) and are assumed to be constant throughout the production years. The oil price is taken from (Oil-Price.net, 2014) and is for Brent crude oil. The results are presented in Table 9.6-9.10.

**Table 9.5:** Oil and surfactant price.

|                          |       |        |       |       |
|--------------------------|-------|--------|-------|-------|
| <b>Oil Price (Brent)</b> | 109,7 | \$/bbl | 691,7 | \$/kg |
| <b>Surfactant Price</b>  | 1,85  | \$/lb  | 4,08  | \$/kg |
| <b>Polymer Price</b>     | 1,20  | \$/lb  | 2,65  | \$/kg |

(9.1)

$$NPV = \sum_{t=0}^n \frac{Revenue - Expenses}{(1 + r)^t}$$

$$Discount\ factor = \frac{1}{(1 + r)^t}$$

## 9.12.1 NPV-Results for Single Block Model

**Table 9.6:** Results NPV calculations, incremental revenue for the surfactant flood.

| Days of production | Project year | Base case oil prod Sm <sup>3</sup> | Oil prod with surf Sm <sup>3</sup> | Incremental oil prod Sm <sup>3</sup> | Oil price \$/Sm <sup>3</sup> | Incremental Revenue from oil prod | Surfactant injected kg | Surfactant Expenses \$ | Net cash flow \$ | Discount factor | Present Value \$ | Net Present Value \$ |
|--------------------|--------------|------------------------------------|------------------------------------|--------------------------------------|------------------------------|-----------------------------------|------------------------|------------------------|------------------|-----------------|------------------|----------------------|
| 365                | 0            | 1,50E+04                           | 1,50E+04                           | -1,46E+01                            | 6,92E+02                     | -1,01E+04                         | 1,83E+04               | 7,44E+04               | -8,45E+04        | 1,00E+00        | -8,45E+04        | -8,45E+04            |
| 730                | 1            | 2,45E+04                           | 2,46E+04                           | 5,77E+01                             | 7,06E+02                     | 4,07E+04                          | 1,83E+04               | 7,44E+04               | -3,37E+04        | 9,26E-01        | -3,12E+04        | -1,16E+05            |
| 1095               | 2            | 3,41E+04                           | 3,42E+04                           | 1,15E+02                             | 7,20E+02                     | 8,27E+04                          | 1,83E+04               | 7,44E+04               | 8,27E+03         | 8,57E-01        | 7,09E+03         | -1,09E+05            |
| 1460               | 3            | 4,36E+04                           | 4,37E+04                           | 1,51E+02                             | 7,34E+02                     | 1,11E+05                          | 1,83E+04               | 7,44E+04               | 3,65E+04         | 7,94E-01        | 2,90E+04         | -7,97E+04            |
| 1825               | 4            | 5,30E+04                           | 5,32E+04                           | 2,00E+02                             | 7,49E+02                     | 1,50E+05                          | 1,83E+04               | 7,44E+04               | 7,51E+04         | 7,35E-01        | 5,52E+04         | -2,45E+04            |
| 2190               | 5            | 6,18E+04                           | 6,24E+04                           | 5,94E+02                             | 7,64E+02                     | 4,54E+05                          | 1,83E+04               | 7,44E+04               | 3,79E+05         | 6,81E-01        | 2,58E+05         | 2,34E+05             |
| 2555               | 6            | 7,02E+04                           | 7,17E+04                           | 1,49E+03                             | 7,79E+02                     | 1,16E+06                          | 1,83E+04               | 7,44E+04               | 1,09E+06         | 6,30E-01        | 6,85E+05         | 9,19E+05             |
| 2920               | 7            | 7,81E+04                           | 8,07E+04                           | 2,65E+03                             | 7,95E+02                     | 2,10E+06                          | 1,83E+04               | 7,44E+04               | 2,03E+06         | 5,83E-01        | 1,18E+06         | 2,10E+06             |
| 3285               | 8            | 8,36E+04                           | 8,99E+04                           | 6,24E+03                             | 8,10E+02                     | 5,06E+06                          | 1,83E+04               | 7,44E+04               | 4,98E+06         | 5,40E-01        | 2,69E+06         | 4,79E+06             |
| 3650               | 9            | 9,26E+04                           | 9,72E+04                           | 4,61E+03                             | 8,27E+02                     | 3,81E+06                          | 1,83E+04               | 7,44E+04               | 3,74E+06         | 5,00E-01        | 1,87E+06         | 6,66E+06             |
| 3800               | 9,4          | 9,49E+04                           | 9,90E+04                           | 4,06E+03                             | 8,43E+02                     | 3,43E+06                          | 6,94E+03               | 2,83E+04               | 3,40E+06         | 4,85E-01        | 1,65E+06         | 8,31E+06             |

As Table 9.6 shows, is the cumulative incremental NPV 4,34E+06\$. Injection of surfactants is conventional for this reservoir model. However, as discussed in chapter 7 are there large extra costs for a chemical EOR project. The costs are related to logistics including transport and storage of chemicals, separation facilities, recycling and deposit challenges etc. These costs are not included in these NPV calculations.

In the previous section (9.9), a comparison on the recovery for injection of surfactants at various concentrations was conducted. Figure 9.16 showed that the case with highest surfactant concentration gave best recovery. However, this increase is not conventional because of the tremendous amounts of surfactants required. Table 9.7 shows the NPV value for the incremental revenue for high concentration surfactant flooding compared with waterflood. The NPV is negative with a value of 3,45E+06. In addition for a more detailed budget must also the additional storage requirement be included. For the case with low surfactant concentration is a few cubic meters less produced than for the waterflood case. Therefore it is naturally not conventional, as Table 9.8 shows.

**Table 9.7:** Results NPV calculations, incremental revenue for the surfactant flood with a surfactant concentration of 30kg/Sm<sup>3</sup>.

| Days of production | Project year | Base case oil prod Sm <sup>3</sup> | Oil prod with surf Sm <sup>3</sup> | Incremental oil prod Sm <sup>3</sup> | Oil price \$/Sm <sup>3</sup> | Incremental Revenue from oil prod | Surfactant injected kg | Surfactant Expenses \$ | Net cash flow \$ | Discount factor | Present Value \$ | Net Present Value \$ |
|--------------------|--------------|------------------------------------|------------------------------------|--------------------------------------|------------------------------|-----------------------------------|------------------------|------------------------|------------------|-----------------|------------------|----------------------|
| 365                | 0            | 1,50E+04                           | 1,50E+04                           | 1,12E+01                             | 6,92E+02                     | 7,76E+03                          | 5,48E+05               | 2,23E+06               | -2,23E+06        | 1,00E+00        | -2,23E+06        | -2,23E+06            |
| 730                | 1            | 2,45E+04                           | 2,48E+04                           | 2,57E+02                             | 7,06E+02                     | 1,81E+05                          | 5,48E+05               | 2,23E+06               | -2,05E+06        | 9,26E-01        | -1,90E+06        | -4,12E+06            |
| 1095               | 2            | 3,41E+04                           | 3,44E+04                           | 3,45E+02                             | 7,20E+02                     | 2,48E+05                          | 5,48E+05               | 2,23E+06               | -1,99E+06        | 8,57E-01        | -1,70E+06        | -5,83E+06            |
| 1460               | 3            | 4,36E+04                           | 4,40E+04                           | 4,34E+02                             | 7,34E+02                     | 3,19E+05                          | 5,48E+05               | 2,23E+06               | -1,91E+06        | 7,94E-01        | -1,52E+06        | -7,35E+06            |
| 1825               | 4            | 5,30E+04                           | 5,34E+04                           | 4,53E+02                             | 7,49E+02                     | 3,39E+05                          | 5,48E+05               | 2,23E+06               | -1,89E+06        | 7,35E-01        | -1,39E+06        | -8,74E+06            |
| 2190               | 5            | 6,18E+04                           | 6,32E+04                           | 1,41E+03                             | 7,64E+02                     | 1,08E+06                          | 5,48E+05               | 2,23E+06               | -1,16E+06        | 6,81E-01        | -7,87E+05        | -9,53E+06            |
| 2555               | 6            | 7,02E+04                           | 7,23E+04                           | 2,15E+03                             | 7,79E+02                     | 1,67E+06                          | 5,48E+05               | 2,23E+06               | -5,58E+05        | 6,30E-01        | -3,52E+05        | -9,88E+06            |
| 2920               | 7            | 7,81E+04                           | 8,20E+04                           | 3,86E+03                             | 7,95E+02                     | 3,07E+06                          | 5,48E+05               | 2,23E+06               | 8,33E+05         | 5,83E-01        | 4,86E+05         | -9,39E+06            |
| 3285               | 8            | 8,36E+04                           | 8,87E+04                           | 5,08E+03                             | 8,10E+02                     | 4,12E+06                          | 5,48E+05               | 2,23E+06               | 1,89E+06         | 5,40E-01        | 1,02E+06         | -8,37E+06            |
| 3650               | 9            | 9,26E+04                           | 1,00E+05                           | 7,90E+03                             | 8,27E+02                     | 6,53E+06                          | 5,48E+05               | 2,23E+06               | 4,30E+06         | 5,00E-01        | 2,15E+06         | -6,22E+06            |
| 3800               | 9,4          | 9,49E+04                           | 1,04E+05                           | 9,22E+03                             | 8,43E+02                     | 7,77E+06                          | 5,48E+05               | 2,23E+06               | 5,54E+06         | 4,85E-01        | 2,68E+06         | -3,54E+06            |

**Table 9.8:** Results NPV calculations, for the surfactant flood with low surfactant concentration.

| Days of production | Project year | Base case oil prod Sm <sup>3</sup> | Oil prod with surf Sm <sup>3</sup> | Incremental oil prod Sm <sup>3</sup> | Oil price \$/Sm <sup>3</sup> | Incremental Revenue from oil prod | Surfactant injected kg | Surfactant Expenses \$ | Net cash flow \$ | Discount factor | Present Value \$ | Net Present Value \$ |
|--------------------|--------------|------------------------------------|------------------------------------|--------------------------------------|------------------------------|-----------------------------------|------------------------|------------------------|------------------|-----------------|------------------|----------------------|
| 365                | 0            | 1,50E+04                           | 1,50E+04                           | 6,67E+00                             | 6,92E+02                     | 4,61E+03                          | 1,83E+03               | 7,44E+03               | -2,83E+03        | 1,00E+00        | -2,83E+03        | -2,83E+03            |
| 730                | 1            | 2,45E+04                           | 2,45E+04                           | -3,14E+01                            | 7,06E+02                     | -2,22E+04                         | 1,83E+03               | 7,44E+03               | -2,96E+04        | 9,26E-01        | -2,74E+04        | -3,02E+04            |
| 1095               | 2            | 3,41E+04                           | 3,40E+04                           | -4,48E+00                            | 7,20E+02                     | -3,22E+03                         | 1,83E+03               | 7,44E+03               | -1,07E+04        | 8,57E-01        | -9,15E+03        | -3,94E+04            |
| 1460               | 3            | 4,36E+04                           | 4,36E+04                           | -3,12E+01                            | 7,34E+02                     | -2,29E+04                         | 1,83E+03               | 7,44E+03               | -3,04E+04        | 7,94E-01        | -2,41E+04        | -6,35E+04            |
| 1825               | 4            | 5,30E+04                           | 5,30E+04                           | -3,90E+01                            | 7,49E+02                     | -2,92E+04                         | 1,57E+03               | 6,40E+03               | -3,56E+04        | 7,35E-01        | -2,61E+04        | -8,96E+04            |
| 2190               | 5            | 6,18E+04                           | 6,18E+04                           | -1,46E+01                            | 7,64E+02                     | -1,11E+04                         | 1,57E+03               | 6,40E+03               | -1,75E+04        | 6,81E-01        | -1,19E+04        | -1,02E+05            |
| 2555               | 6            | 7,02E+04                           | 6,33E+04                           | -6,91E+03                            | 7,79E+02                     | -5,38E+06                         | 1,57E+03               | 6,40E+03               | -5,39E+06        | 6,30E-01        | -3,39E+06        | -3,50E+06            |
| 2920               | 7            | 7,81E+04                           | 7,81E+04                           | -2,01E+01                            | 7,95E+02                     | -1,60E+04                         | 1,57E+03               | 6,40E+03               | -2,24E+04        | 5,83E-01        | -1,31E+04        | -3,51E+06            |
| 3285               | 8            | 8,36E+04                           | 8,56E+04                           | 1,99E+03                             | 8,10E+02                     | 1,61E+06                          | 1,57E+03               | 6,40E+03               | 1,60E+06         | 5,40E-01        | 8,67E+05         | -2,64E+06            |
| 3650               | 9            | 9,26E+04                           | 9,26E+04                           | -2,86E+01                            | 8,27E+02                     | -2,36E+04                         | 1,57E+03               | 6,40E+03               | -3,00E+04        | 5,00E-01        | -1,50E+04        | -2,66E+06            |
| 3800               | 9,4          | 9,49E+04                           | 9,49E+04                           | -2,10E+01                            | 8,43E+02                     | -1,77E+04                         | 1,57E+03               | 6,40E+03               | -2,41E+04        | 4,85E-01        | -1,17E+04        | -2,67E+06            |

### 9.12.2 NPV-Results for Four-Fractures Model

An economical evaluation of chemical floods in the 9-block model with four fractures was conducted. In chapter 9.11 was the recovery for a case with surfactant-polymer flood compared with a surfactant flood. In addition a polymer flood was conducted with a slightly increased oil recovery compared to the surfactant flood. The results of the NPV calculations are presented in Table 9.9 and Table 9.10 for SP and polymer flood respectively.

The SP-flood is conventional and should be preferred instead of surfactant flood. However, these calculations only consider the chemical costs as expenses. As discussed in chapter 6.7, can polymer injection with surfactants lead to a decrease in CMC, so that less surfactant are required to obtain the same results. In this case was surfactants injected with the same concentration as for the pure surfactant flood. Surfactant expenses could therefore might be reduced. On the other hand, should also extra facility costs for storage of polymers be included, while the storage requirement for surfactant could be reduced in the case where surfactant concentration can be reduced when they are injected with polymers.

A polymer flood instead of a surfactant flood is not conventional. This is because a high concentration of polymers is required to obtain a high water viscosity for better sweep. However, from Figure 9.23 it can be seen that the recovery for the pure polymer injection is still increasing at the end of the simulation run. For a simulation run of another two years, is it conceivable that the recovery for polymers would be larger, and it could be conventional.

**Table 9.9:** Incremental NPV calculations for SP-flood compared with surfactant flood.

| Project Year | Oil prod with surf Sm <sup>3</sup> | Oil prod with SP Sm <sup>3</sup> | Incremental oil prod Sm <sup>3</sup> | Oil price \$/Sm <sup>3</sup> | Incremental Revenue from oil prod | Surfactant injected kg | Surfactant injected in SE kg | Polymers Injected kg | Surfactant Expenses \$ | SP Expenses \$ | Net cash flow \$ | Discount factor | Present Value \$ | NPV \$    |
|--------------|------------------------------------|----------------------------------|--------------------------------------|------------------------------|-----------------------------------|------------------------|------------------------------|----------------------|------------------------|----------------|------------------|-----------------|------------------|-----------|
| 0            | 1,47E+04                           | 1,47E+04                         | -3,20E+01                            | 6,92E+02                     | -2,21E+04                         | 1,83E+04               | 1,83E+04                     | 0,00E+00             | 7,44E+04               | 7,44E+04       | -2,21E+04        | 1,00E+00        | -2,21E+04        | -2,21E+04 |
| 1            | 2,21E+04                           | 2,20E+04                         | -5,38E+01                            | 7,06E+02                     | -3,79E+04                         | 1,83E+04               | 1,83E+04                     | 0,00E+00             | 7,44E+04               | 7,44E+04       | -3,79E+04        | 9,26E-01        | -3,51E+04        | -5,72E+04 |
| 2            | 2,82E+04                           | 2,82E+04                         | -5,93E+01                            | 7,20E+02                     | -4,26E+04                         | 1,83E+04               | 8,50E+03                     | 6,30E+04             | 7,44E+04               | 2,01E+05       | -1,69E+05        | 8,57E-01        | -1,45E+05        | -2,03E+05 |
| 3            | 3,39E+04                           | 3,35E+04                         | -3,81E+02                            | 7,34E+02                     | -2,80E+05                         | 1,83E+04               | 0,00E+00                     | 9,63E+04             | 7,44E+04               | 2,55E+05       | -4,60E+05        | 7,94E-01        | -3,65E+05        | -5,68E+05 |
| 4            | 3,89E+04                           | 3,85E+04                         | -4,42E+02                            | 7,49E+02                     | -3,31E+05                         | 1,83E+04               | 0,00E+00                     | 8,01E+04             | 7,44E+04               | 2,12E+05       | -4,69E+05        | 7,35E-01        | -3,44E+05        | -9,12E+05 |
| 5            | 4,35E+04                           | 4,52E+04                         | 1,69E+03                             | 7,64E+02                     | 1,29E+06                          | 1,83E+04               | 0,00E+00                     | 0,00E+00             | 7,44E+04               | 0,00E+00       | 1,36E+06         | 6,81E-01        | 9,27E+05         | 1,46E+04  |
| 6            | 4,78E+04                           | 5,15E+04                         | 3,63E+03                             | 7,79E+02                     | 2,83E+06                          | 1,83E+04               | 0,00E+00                     | 0,00E+00             | 7,44E+04               | 0,00E+00       | 2,91E+06         | 6,30E-01        | 1,83E+06         | 1,85E+06  |
| 7            | 4,83E+04                           | 5,22E+04                         | 3,92E+03                             | 7,95E+02                     | 3,12E+06                          | 1,83E+04               | 0,00E+00                     | 0,00E+00             | 7,44E+04               | 0,00E+00       | 3,19E+06         | 5,83E-01        | 1,86E+06         | 3,71E+06  |

**Table 9.10:** Incremental NPV calculation for polymer-flood compared with surfactant flood.

| Project Year | Oil prod with surf Sm <sup>3</sup> | Oil prod with SP Sm <sup>3</sup> | Incremental oil prod Sm <sup>3</sup> | Oil price \$/Sm <sup>3</sup> | Incremental Revenue from oil prod | Surfactant injected kg | Polymers Injected kg | Surfactant Expenses \$ | Polymer Expenses \$ | Net cash flow \$ | Discount factor | Present Value \$ | NPV \$    |
|--------------|------------------------------------|----------------------------------|--------------------------------------|------------------------------|-----------------------------------|------------------------|----------------------|------------------------|---------------------|------------------|-----------------|------------------|-----------|
| 0            | 1,47E+04                           | 1,38E+04                         | -9,36E+02                            | 6,92E+02                     | -6,47E+05                         | 1,83E+04               | 1,10E+05             | 7,44E+04               | 4,50E+05            | -1,10E+06        | 1,00E+00        | -1,10E+06        | -1,10E+06 |
| 1            | 2,21E+04                           | 1,96E+04                         | -2,48E+03                            | 7,06E+02                     | -1,75E+06                         | 1,83E+04               | 8,91E+04             | 7,44E+04               | 3,63E+05            | -2,11E+06        | 9,26E-01        | -1,95E+06        | -3,05E+06 |
| 2            | 2,82E+04                           | 2,52E+04                         | -3,08E+03                            | 7,20E+02                     | -2,21E+06                         | 1,83E+04               | 8,54E+04             | 7,44E+04               | 3,48E+05            | -2,56E+06        | 8,57E-01        | -2,20E+06        | -5,25E+06 |
| 3            | 3,39E+04                           | 3,03E+04                         | -3,63E+03                            | 7,34E+02                     | -2,66E+06                         | 1,83E+04               | 8,11E+04             | 7,44E+04               | 3,31E+05            | -2,99E+06        | 7,94E-01        | -2,38E+06        | -7,63E+06 |
| 4            | 3,89E+04                           | 3,51E+04                         | -3,82E+03                            | 7,49E+02                     | -2,86E+06                         | 1,83E+04               | 7,33E+04             | 7,44E+04               | 2,99E+05            | -3,16E+06        | 7,35E-01        | -2,32E+06        | -9,94E+06 |
| 5            | 4,35E+04                           | 4,16E+04                         | -1,85E+03                            | 7,64E+02                     | -1,41E+06                         | 1,83E+04               | 0,00E+00             | 7,44E+04               | 0,00E+00            | -1,41E+06        | 6,81E-01        | -9,62E+05        | -1,09E+07 |
| 6            | 4,78E+04                           | 4,79E+04                         | 1,02E+02                             | 7,79E+02                     | 7,94E+04                          | 1,83E+04               | 0,00E+00             | 7,44E+04               | 0,00E+00            | 7,94E+04         | 6,30E-01        | 5,00E+04         | -1,09E+07 |
| 7            | 4,83E+04                           | 4,86E+04                         | 3,57E+02                             | 7,95E+02                     | 2,83E+05                          | 1,83E+04               | 0,00E+00             | 7,44E+04               | 0,00E+00            | 2,83E+05         | 5,83E-01        | 1,65E+05         | -1,07E+07 |

### 9.13 Complete Evaluation of the Results

Two mechanistic models were built with more or less the same input data. The first model with a single fractured was built with the purpose to investigate how different input parameters affected the recovery performance. While the second model with nine matrix blocks and four fractures was built with the purpose to further investigate how the injected surfactants flow in the reservoir and to study the polymer's effect on sweep efficiency and recovery. In the next two subchapters is a complete evaluation of the two models done, while the conclusions are presented in chapter 10.

#### 9.13.1 Single Fracture Model Evaluation

The model is built on many assumptions, such as there is only one continuous fracture throughout the reservoir. The fracture is also many times wider than a natural fracture. The thought is that this only fracture represents the sum of fluid flow in several fractures in the same area. The problem with simulation of fractures in Eclipse is that there will be large convergence problems because of the enormous differences in permeability and layer thickness between fracture and matrix. Very small timesteps could maybe handle these problems. In this study was the problem solved by increasing the fracture width to 1 cm and decreasing the fracture permeability to 90mD. In addition some grid refinement around the fracture was also done to reduce the large layer thickness differences.

Other assumption that is made for this study is related to the surfactant flooding case. The wettability alteration function is not included in the model. This is done because the rock in this case is water-wet. The initial relative permeability curves implemented in the model are for a typical water-wet rock (Figure 8.3). For typical oil-wet rocks is the endpoint relative permeability for water much higher. And the intersection of the relative permeability curves for oil and water will also occur at lower water saturation.

In the model is a third saturation table implemented for the case where surfactants make oil and water miscible in a microemulsion. The capillary pressure is assumed to be zero and the relative permeability curves are calculated using the Corey equations, which are assumed to be reasonable. The capillary pressure is not likely to become zero which means that the IFT will become zero in case of no capillary pressure. Therefore a table with capillary pressure



should be considered to be included. However, a simulation run was done for comparison of the performance of the surfactant flood with and without capillary pressure in the case of miscible conditions. The results were equal and are presented in Figure 9.9.

All the results, except the fracture width study, are reasonable and as expected based on the theory presented in chapter 1 to 7; this is a good indication for the model to be reliable.

Not many studies on this topic has been done in the past, therefore was it difficult to obtain surfactant data suited for carbonates. The most uncertain data implemented is the adsorption data, which are for a low permeable sandstone with clay layers. The rock surface is very different for carbonates and rocks with clay. Clay has a negative charged surface and adsorbs cationic surfactants easily, while the calcite,  $\text{Ca}^+$ , in carbonates adsorb anionic surfactants very easily. Since no chemical properties of surfactants are included in the Eclipse 100 surfactant model, it is hard to define the type of surfactant. However, an anionic surfactant is most widely used. Anionic surfactants have low adsorption on sandstones, and it is therefore possible that the adsorption data for this model is too low, if the data is initially designed for an anionic surfactant flood in sandstone with clay layers. Anyway, the results in this case showed that the recovery did not vary that much with the various adsorption data implemented.

In this case, where the basecase is built with Ekofisk data, an anionic surfactant should be injected with the purpose to lower the IFT and not alter the wettability. The surfactant should be injected with  $\text{Na}_2\text{CO}_2$  to reduce the adsorption. The surface charge for carbonates is determined by the potential of  $\text{Ca}^+$ ,  $\text{CO}_3^{2-}$  and  $\text{HCO}^-$  ions. By injecting  $\text{Na}_2\text{CO}_2$  with anionic surfactants, there will be an overload of  $\text{CO}_3^{2-}$  and  $\text{HCO}^-$  ions on the carbonate surface that will make it negatively charge, and hence the anionic surfactants will not be adsorbed because of the electrostatic forces (Hirasaki & Zhang, 2004). The anionic surfactant concentration will be maintained and can work to lower the IFT. The simulation results show that the IFT is reduced in the areas that are flooded by surfactants (Figure 9.17) and is the cause of the improved recovery obtained for the surfactant case.

Even though there are uncertainties about the adsorption data, the results show that about 70% of the injected surfactant is adsorbed by the rock. Only 0,013% surfactants are produced, the rest is left in pores in the reservoir. These data are interesting from an economical point of view. When only a few percent are produced, the expenses of recycling for reinjection will be unprofitable.

As the first results presented shows, the surfactants will move towards the fracture when they are injected into the model. The surfactant concentration in the fracture and in the closest layers, are by far most affected by surfactants. It is also in these layers the sweep efficiency is best. Figure 9.1 presents the sweep of several layers in various differences from the fracture. The sweep is quite poor in the layers that are far from the fracture. As explained in chapter 9.3 will the mobility for water increase when there are surfactants present. Therefore will the surfactant water move faster and finger through the reservoir where the best conductivity is. Figure 9.17 shows how the sweep efficiency is improved for the case with high surfactant concentration. As discussed in chapter 9.9 is the sweep efficiency improved in this case because the water viscosity is increased because of the high concentration. The high surfactant concentration flood is not conventional, but an injection of polymers together with surfactants will result in high water viscosity and better sweep efficiency. Polymers are cheaper than surfactants and a lower concentration of surfactants is required for a Surfactant-Polymer flood (Wyatt, et al., 2008).

As discussed in chapter 9.4 where a study of effect of different initial capillary pressure values was done, the recovery hardly differs for the three cases. Also as discussed earlier in this chapter the recovery does not differ when there is capillary pressure present in the miscible phase, and when the capillary pressure is zero. These results are a bit odd and should be considered more carefully.

Capillary pressure is the main drive mechanism in the imbibition process. Without capillary pressure to force water into pores for displacement of oil, there would be large amount of residual oil left in the reservoir. However, if the forces get too strong, no fluids will be able to overcome the entry pressure in many of the small pores. By reducing the IFT and hence capillary pressure by applying surfactants, a desirable “capillary pressure value” can be obtained, that is large enough to govern imbibition, but low enough so it will not oppose imbibition in the smallest pores. Since the results shows that initial capillary pressure and the capillary pressure in the model after it is swept by surfactant roughly do not affect the results another force must be present to govern the displacement process. Hirasaki and Zhang suggested that the buoyance forces will take over, when the capillary forces are reduced.

Initial capillary pressure, fracture opening, surfactant adsorption, surfactant concentration and capillary number input data are all parameters that have different effect on the surfactant performance. Most of the recovery changes are very small, less than 1%. However, for the surfactant concentration study was the performance more varied for the three cases. Until the

CMC concentration which was in this case for the surfactant basecase, does not the surfactants reduce IFT any further. A higher concentration may only lead to a more viscous injection fluid front that sweeps the reservoir more efficiently. However, surfactants are expensive, and polymers should be preferred when the purpose is to increase the viscosity of the displacing fluid.

### 9.13.2 Nine-Block Model Evaluation

To be able to run the simulation of the 9-block model with four fractures, the fracture permeability and fracture and miscibility saturation tables had to be changed. The changes in the saturation tables were small (2%) and have probably little impact on the results. The permeability changes in the fractures made the difference in the fractures and matrix less. Because of these changes, Eclipse was able to run the simulation. These changes are a bit more dramatic.

Because of the little variation between fracture and matrix permeability are also the variation in flow conditions little. Therefore is it conceivable that the results only show tendencies of the surfactant flow in the model. Such as the degree of surfactants concentrated in the areas in the fractures and around the fractures is less than the reality with large permeability differences. However, the results from the investigation of the surfactant's flow pattern are still a clear tendency and it is reasonable to think that in a reservoir model with larger permeability differences will it be clearer that the surfactants flow towards good flowing conditions such as high permeable fractures.

In the SP-flood case may the results be poorer because of the low permeability heterogeneity. In a case where the fractures have a much higher and realistic permeability, would probably also the sweep be poorer, when it is assumed that the tendency of surfactant flow towards fractures is valid. For very high permeable fractures, will the injection fluid flow to the fractures and the injection front will finger through the reservoir, leading to a very poor sweep. Polymers are often used in heterogeneous reservoirs to reduce the flow conductivity in layers with very good permeability to reduce the fingering in the displacement process and improve the sweep (chapter 6.7). Therefore could the improved recovery factor be greater for the case with SP flood compared to the surfactant flood. Because the SP flood would have a more even displacing front, while the front in the surfactant flood would finger through the reservoir, leading to a good recovery for the SP flood compared to the surfactant flood.

The selection of polymer input data has been somewhat uncritical. As mentioned in chapter 8, are the input data taken from Charles Kossack's EOR folder on Professor Jon Kleppe's homepage. There is no information of which rock type the adsorption data is for, therefore may the adsorption data be wrong. The initial water viscosity is much lower and the oil viscosity is higher in Kossack's file than for this model. Which means that for Kossack's case is a larger polymer concentration required to increase the water viscosity for the desired

sweep effect. Therefore may the polymer concentration used in this case be too high. The polymer concentration determines the water viscosity multiplier. In this model, a lower water viscosity multiplier is chosen to avoid a too viscous injection front. This means, that the concentration of polymers is maybe too high compared to the effect it gives, which means that the polymer used in this 9-block model is inefficient. The sweep efficiency results would be the same, for a case where only the polymer concentration is changed in all input keyword, but the other data remain constant. But the NPV calculation results would be different. SP flood would be even more conventional, because of lower polymer costs if the concentration can be reduced and give the same results.

The results for the polymer flood compared to the surfactant flood show a recovery increase of only 0, 36%, and a negative NPV of  $-1,07E07$ . However, for a simulation run for another 1000 days or more, could the results maybe be different, because of the late and rapid increase in recovery of polymers would most conceivable continue.



## 10. Conclusion

1. Based on the study of the simulation results obtained in this thesis, an injection of surfactants in Ekofisk can be successful and a further evaluation should be done.
2. The low surfactant production and high surfactant adsorption results show that a great loss of surfactants in terms of adsorption must be expected, and research on adsorption reduction should be done with purpose to minimise costs and increasing recovery of oil and surfactants.
3. Injected surfactants in fractured reservoirs will flow towards the fracture(s), and polymers should be injected with the surfactants for better sweep efficiency.
4. Surfactant concentration is the parameter that affects the surfactant performance the most in terms of recovery.
5. The oil recovery increases with 2,8% and related NPV increases with 8,31E+06\$ when surfactants are injected in the single fracture reservoir model compared with recovery by waterflood.
6. A surfactant-polymer flood with chase water increases the oil recovery with 3% and related NPV with 3,71E+06\$ in the fracture network model compared with a surfactant flood.





## 11. Future Recommendations

- Build a more complex model with heterogeneity and a fracture network to have a more realistic model for investigation of surfactant flow behaviour.
- Include the Eclipse tracer tracking function to follow the movement of the injected fluid
- Include the wettability alteration function (SURFACTW), to see the differences in recovery when the relative permeability curves are changed to more water-wet or in the case where the surfactant alters the wettability to mixed-wet or even oil-wet.
- Investigate the recovery mechanism for the case with very low to no capillary pressure in the miscibility zones.
- Flood the models with water first, and follow with various chemical flood patterns to obtain the most profitable flood.

## Nomenclature

|                |   |
|----------------|---|
| $A$            | Cross-section area  |
| $ACN$          | Alkane Carbon Number  |
| $ASP$          | Alkane-Surfactant-Polymer   |
| $b$            | Fracture opening  |
| $C$            | Empirical constant in IFT calculations                              |
| $CA(C_{surf})$ | Adsorption isotherm as a function of local surfactant concentration |
| $C_i$          | Compressibility to substance $i$                                    |
| $C_{surf}$     | Surfactant Concentration  |
| $EACN$         | Equivalent Alkane Carbon Number                                     |
| $EO$           | Ethylene oxide group  |
| $EOR$          | Enhanced Oil Recovery   |
| $FAWAG$        | Foam Assisted water alternating gas                                 |
| $FINT$         | Fracture intensity  |
| $FOE$          | Recovery factor   |
| $FTADSUR$      | Total surfactant adsorption   |
| $FTITSUR$      | Total amount of surfactants injected                                |
| $FTPTSUR$      | Total amount of surfactants produced                                |
| $FWCT$         | Field Water Cut   |
| $G$            | Gravity forces  |
| $g$            | gravity   |
| $HC$           | Miscible gas  |
| $h_c$          | capillary height  |
| $H_w$          | Water height  |
| $IFT$          | Interfacial tension   |
| $k$            | absolute permeability   |
| $k_i$          | Effective permeability of fluid $i$                                 |
| $k_{ri}$       | Relative permeability of fluid $i$                                  |
| $k_{ri}^0$     | End-point relative permeability of phase $i$ .                      |
| $L$            | Length  |
| $LFD$          | Linear fracture density   |
| $LFDH$         | Linear fracture density in horizontal direction                     |
| $LFDV$         | Linear fracture density in vertical direction                       |
| $LNG$          | Liquefied Natural Gas   |
| $LPG$          | Liquefied Petroleum Gas   |
| $M$            | Mobility ratio  |
| $MD$           | Mass density of rock  |
| $MEOR$         | Microbial Enhanced Oil Recovery                                     |
| $M_i$          | Mobility to fluid phase $i$   |
| $n$            | Corey exponent  |

|               |  |
|---------------|--|
| $N_c$         | Capillary number                                 |
| $n_f$         | Number of fractures                              |
| $NPV$         | Net Present Value                                |
| $p$           | Pressure   |
| $P_c$         | Capillary pressure                               |
| $PLYADS$      | Polymer Adsorption Data                          |
| $PLYROCK$     | Polymer-rock properties                          |
| $PLYVISC$     | Polymer Viscosity                                |
| $PO$          | Propylene oxide group                            |
| $PORV$        | Pore Volume of a cell                            |
| $q$           | Volumetric flow rate                             |
| $r$           | radius   |
| $r$           | discount rate                                    |
| $SAGD$        | Steam Applied Gravity Drainage                   |
| $S_i$         | Saturation of fluid $i$                          |
| $SP$          | Solubilisation Parameter                         |
| $SP$          | Surfactant-Polymer                               |
| $SURFACT$     | Model initialisation                             |
| $SURFACTW$    | Wettability alteration with surfactants          |
| $SURFADS$     | Surfactant adsorption                            |
| $SURFCAPD$    | Capillary de-saturation                          |
| $SURFNUM$     | Grid region specification                        |
| $SURFROCK$    | Rock properties                                  |
| $SURFST$      | IFT data   |
| $SURFVISC$    | Viscosity modifier                               |
| $SWAG$        | Simultaneous water and gas                       |
| $u$           | Displacement front velocity                      |
| $v$           | velocity   |
| $V_b$         | Bulk volume                                      |
| $V_p$         | Pore volume                                      |
| $V_{ptot}$    | Total pore volume                                |
| $WAG$         | Water alternating gas                            |
| $WF$          | Waterflood                                       |
| $WSURFACT$    | Injected surfactant concentration                |
| $Z$           | Displacement front distance                      |
| $Z_{bl}$      | Height of fracture system                        |
| $\theta$      | Contact angle                                    |
| $\lambda$     | Dimensionless fracture-matrix interflow capacity |
| $\mu_i$       | viscosity of fluid phase $i$                     |
| $\rho_i$      | Density of fluid $i$                             |
| $\sigma_{ij}$ | Interfacial tension between phase $i$ and $j$    |
| $\varphi$     | Porosity   |
| $\omega$      | Dimensionless fracture storage capacity          |

## Bibliography

Abadli, F., 2012. *Simulation Study of Enhanced Oil Recovery by ASP Flooding for Norne Field C-Segment. MS thesis.* Trondheim: Norwegian University of Science and Technology, Department of Petroleum Engineering and Applied Geophysics.

Al-Yousef, A., Han, M., Al-Saleh, S. & Company, S. A. O., 2013. *Oil recovery process for carbonate reservoirs.* Saudia Arabia, Patent No. US8550164 B2.

Austad, T., Fjelde, I., Veggeland, K. & Taugbøl, K., 1994. Physicochemical principles of low tension polymer flood. *Journal of Petroleum Science and Engineering*, pp. 255-269.

Austad, T. & Standnes, D., 2003. Spontaneous imbibition of water into oil-wet carbonates. *Journal of Petroleum Science and Engineering*, 39(3-4), pp. 363-376.

Cayias, J., Schechter, R. & Wade, W., 1977. "The Utilization of Petroleum Sulfonates for Producing Low Interfacial Tensions Between Hydrocarbons and Water. *Journal of Colloid and Interface Science*, 15 3, 59(1), pp. 31-38.

Chilingarian, G., Mazzullo, S. & Rieke, H., 1996. *Carbonate Reservoir Characterization: A Geologic Engineering Analysis, Part II.* s.l.:Elsevier.

Feng, X. et al., 2011. *Case Study: Numerical Simulation of Surfactant Flooding in Low Permeability Oil Field. SPE 145036.* Kuala Lumpur, Malaysia: Society of Petroleum Engineers.

Fuseni, A., Han, M. & Al-Mobith, A., 2013. *Phase Behaviour and Interfacial Tension Properties of an Amphoteric Surfactant for EOR Application. SPE-168104-MS.* Khobar, Saudia Arabia, Society of Petroleum Engineers.

Ghahfarokhi, A., 2012. *Reservoir Property Determination by Core Analysis and Well Testing, Lecture TPG4115, Well Testing of Naturally Fractured Reservoirs,* Trondheim: Norwegian University of Science and Technology, Department of Petroleum Engineering and Applied Geophysics.

Green, D. & Willhite, P., 1998. *Enhanced Oil Recovery.* Texas: Society of Petroleum Engineers Textbook Series.

Hirasaki, G., Miller, C. & Puerto, M., 2008. *Recent Advances in Surfactant EOR. SPE-115386-MS.* Denver, Colorado, USA, Society of Petroleum Engineers.

Hirasaki, G., van Domselaar, H. & Nelson, R., 1983. *Evaluation of the Salinity Gradient Concept in Surfactant Flooding. SPE-8825-PA,* s.l.: Society of Petroleum Engineers.

Hirasaki, G. & Zhang, D., 2004. Surface Chemistry of Oil Recovery From Fractured, Oil-Wet, Carbonate Formations. SPE-88365-PA. *SPE Journal*, 01 06.

Holter, K., 2012. *Simulation of Low Salinity Waterflooding in a Synthetic Reservoir Model and Frøy Field Reservoir Model. MS thesis.* Trondheim: Norwegian University of Science and Technology, Department of Science and Technology.

Huh, C., 1979. Interfacial Tensions and Solubilisation Ability of a Microemulsion Phase that Coexist with Oil and Brine. *Journal of Colloid and Interface Science*, 71(2), pp. 408-426.

Kossack, C., 2011. *Professor Jon Kleppes homepage*. [Online] Available at: <http://www.ipt.ntnu.no/~kleppe/pub/kossack-files-2011/EOR%20Datasets%20for%20Distribution%20at%20NTNU/> [Accessed 01 06 2014].

Lake, L., 1989. *Enhanced Oil Recovery*. Upper Saddle River(New Jersey): Prentice Hall Incorporated.

Levitt, D. et al., 2009. Identification and Evaluation of High-Performance EOR Surfactants, SPE 100089-PA. *SPE Res Eval & Eng*, 04.

Lu, J. et al., 2012. *Surfactant Enhanced Oil Recovery from Naturally Fractured Reservoirs, SPE159979*. San Antonio, Texas, Society of Petroleum Engineers.

Manger, G., 1963. *Porosity and Bulk Density of Sedimentary Rocks*, Washington: United States Government Printing Office.

Manrique, E. et al., 2010. *EOR: Current Status and Opportunities, SPE-130113-MS*. Tulsa, Oklahoma, Society of Petroleum Engineers.

Norwegian Petroleum Departemet, N., 2011. *Norwegian Petroleum Department*. [Online] Available at: <http://www.npd.no/en/Publications/Facts/Facts-2011/Chapter-10/Ekofisk/> [Accessed 30 05 2014].

Norwegian Petroleum Department, N., 2008. *Norwegian Petroleum Department*. [Online] Available at: <http://www.npd.no/en/Publications/Norwegian-Continental-Shelf/No2-2008/Recovering-progress-on-IOR/> [Accessed 30 05 2014].

Oil-Price.net, 2014. *Oil-price.net*. [Online] Available at: <http://www.oil-price.net> [Accessed 30 05 2014].

Raney, K., Ayirala, S., Chin, R. & Verbeek, P., 2012. Surface and Subsurface Requirements for Successful Implementation of Offshore Chemical Enhanced Oil Recovery. SPE-155116-PA. *SPE Prod & Oper*, 08.

Riise, L., 2005. *Evaluation of the Second Depletion on the Ekofisk Field. MS thesis*, Trondheim/Stavanger: Norwegian University of Science and Technology, Department of Petroleum Engineering and Applied Geophysics and ConocoPhillips.

Roshanfekar, M. & Johns, R., 2011. Prediction of optimum salinity and solubilization ratio for microemulsion phase behavior with live crude at reservoir pressure. *Fluid Phase Equilibria*, 15 5, 304(1-2), pp. 52-60.

Schlumberger, 1998a. *Schlumberger Oilfield Glossary*. [Online] Available at: <http://www.glossary.oilfield.slb.com/en/Terms.aspx?LookIn=term%20name&filter=effective%20permeability> [Accessed 04 06 2014].

## Bibliography

---

Schlumberger, 1998b. *Schlumberger Oilfield Glossary*. [Online] Available at: <http://www.glossary.oilfield.slb.com/en/Terms.aspx?LookIn=term%20name&filter=fracture+permeability> [Accessed 04 06 2014].

Schlumberger, 1998c. *Schlumberger Oilfield Glossary*. [Online] Available at: <http://www.glossary.oilfield.slb.com/en/Terms.aspx?LookIn=term%20name&filter=mobility>

Schlumberger, 1998d. *Oilfield Glossary*. [Online] Available at: <http://www.glossary.oilfield.slb.com/en/Terms.aspx?LookIn=term%20name&filter=primary%20recovery> [Accessed 04 06 2014].

Schlumberger, 1998e. *Oilfield Glossary*. [Online] Available at: [http://www.glossary.oilfield.slb.com/en/Terms/s/secondary\\_recovery.aspx](http://www.glossary.oilfield.slb.com/en/Terms/s/secondary_recovery.aspx) [Accessed 04 06 2014].

Schlumberger, 1998f. *Oilfield Glossary*. [Online] Available at: <http://www.glossary.oilfield.slb.com/en/Terms.aspx?LookIn=term%20name&filter=enhanced+oil+recovery> [Accessed 04 06 2014].

Schlumberger, 2011a. *Eclipse Technical Description*, s.l.: Schlumberger.

Schlumberger, 2011b. *Eclipse Reference Manual*, s.l.: Schlumberger.

Schramm, L., 1992. *Petroleum Emulsions, Basic Principles*. Calgary, Alberta, Canada: American Chemical Society.

Sheng, J., 2010. Optimum phase type and optimum salinity profile in surfactant flooding. *Journal of Petroleum Science and Engineering*, 75(1-2), pp. 143-153.

Sheng, J., 2011. *Modern Chemical Enhanced Oil Recovery: Theory and Practice*. s.l.: Elsevier Inc. .

Sheng, J., 2013. Surfactant-Polymer Flooding. In: *Enhanced Oil Recovery Field Case Studies*. Boston: Gulf Professional Publishing, pp. 117-142.

Skauge, A. & Fotland, P., 1990. Effect of Pressure and Temperature on the Phase Behavior of Microemulsions. SPE-14932-PA. *SPE-Journal*, 1 11.

Skår, H., 2013. *Surfactants and Spinning Drop Interfacial Tension Measurements*, Trondheim : Norwegian University of Science and Technology, Department of Petroleum Engineering and Applied Geophysics.

Statoil, 2008. *Statoil*. [Online] Available at: <http://www.statoil.com/en/technologyinnovation/optimizingreservoirrecovery/recoverymetho>

<ds/waterassistedmethodsImprovedOilRecoveryior/pages/chemicalflooding.aspx>

[Accessed 04 06 2014].

Teigland, R. & Kleppe, J., 2006. *EOR Survey in the North Sea*, SPE-99546-MS. Tulsa, Oklahoma, U.S.A, Society of Petroleum Engineers.

Torsæter, O., 2011. *Flow in Porous Media TPG4112 , Course Lecture, Relative Permeability*. Trondheim(Trondheim): Norwegian University of Science and Technology, Department of Petroleum Engineering and Applied Geophysics.

Torsæter, O., 2013. *Unconventional Reservoirs, Course compendium*, Trondheim: Norwegian University of Science and Technology, Department of Petroleum Engineering and Applied Geophysics.

Torsæter, O., 2014a. *Naturally Fractured Reservoir Course Compendium, First Part: Fractured Reservoir Description and Geometry..* Trondheim: Norwegian University of Science and Technology.

Torsæter, O., 2014b. *Naturally Fractured Reservoirs, course compendium: Third Part*, Trondheim: Norwegian University of Science and Technology, Department of Petroleum Engineering and Applied Geophysics.

Torsæter, O., 2014c. *Naturally Fractured Reservoirs, course lecture: Fracture fluid exchange*. Trondheim: Norwegian University of Science and Technology, Department of Petroleum Engineering and Applied Geophysics.

Torsæter, O. & Abtahi, M., 2003. *Experimental Reservoir Engineering Laboratory Work Book*. Trondheim: Department of Petroleum Engineering and Applied Geophysics, Norwegian University of Science and Technology.

TradingEconomics, 2014. *Trading Economics*. [Online] Available at: <http://www.tradingeconomics.com/united-states/inflation-cpi> [Accessed 30 05 2014].

Warren, J. & Root, P., 1963. The Behaviour of Naturally Fractured Reservoirs, SPE-426-PA. *SPE Journal*, 09.

Wyatt, K., Pitts, M. & Surkalo, H., 2008. *Economics of Field Proven Chemical Flooding Technologies*, SPE-113126-MS. Tulsa, Oklahoma, Society of Petroleum Engineers.

Zolutukhin, A. & Ursin, J., 2000. *Introduction to Petroleum Reservoir Engineering*. Stavanger: Høyskoleforlaget.